UNIVERSIDAD DE CHILE
FACULTAD DE CIENCIAS FÍSICAS Y MATEMÁTICAS
DEPARTAMENTO DE INGENIERÍA ELÉCTRICA

DESIGN AND EVALUATION OF ADAPTIVE BEACONING ALGORITHMS FOR COOPERATIVE VEHICULAR SAFETY SYSTEMS

TESIS PARA OPTAR AL GRADO DE
DOCTOR EN INGENIERÍA ELÉCTRICA

SANDY BOLUFÉ AGUILA

PROFESOR GUÍA:
DR. CESAR A. AZURDIA MEZA

PROFESORES CO-GUÍAS:
DRA. SANDRA CÉSPEDES UMAÑA
DR. SAMUEL MONTEJO SÁNCHEZ

MIEMBROS DE LA COMISIÓN:
DR. MARCOS EDUARDO ORCHARD CONCHA
DR. JUAN FELIPE BOTERO VEGA
DR. CARLOS A. GUTIÉRREZ DÍAZ DE LEÓN

SANTIAGO DE CHILE
2021

SUMMARY OF THE THESIS SUBMITTED
FOR THE DEGREE OF DOCTOR IN ELECTRICAL ENGINEERING
BY: SANDY BOLUFÉ AGUILA
DATE: 2021
ADVISOR: PROF. CESAR A. AZURDIA MEZA
CO-ADVISOR: PROF. SANDRA CÉSPEDES UMAÑA
CO-ADVISOR: PROF. SAMUEL MONTEJO SÁNCHEZ

DESIGN AND EVALUATION OF ADAPTIVE BEACONING ALGORITHMS FOR COOPERATIVE VEHICULAR SAFETY SYSTEMS

In cooperative vehicular safety systems, the beaconing process is essential for tracking neighboring vehicles and supporting safety applications. Although different congestion and awareness control approaches have been proposed, to date, little attention has been paid on whether these approaches are adequate or not to support safety applications. This thesis addresses the challenge of guaranteeing the proper performance of safety applications by designing and evaluating distributed beaconing algorithms based on adaptive control of transmission parameters. Specifically, I propose and evaluate a POSition-ACCuracy (POSACC) based adaptive beaconing algorithm which prioritizes the position error and communication reliability maintaining the warning distance, channel load, and end-to-end latency into the operative range of safety applications. I also evaluate other relevant adaptive approaches to understand their benefits and limitations regarding road safety. In addition, I assess the incident detection capability of the overtaking application in autonomous driving when it is running with messages gathered from the addressed approaches, considering packet losses due to channel fading. Simulation results show that POSACC not only is more effective than the addressed approaches for guaranteeing the operational requirements of safety applications in a wider range of traffic situations but also for detecting unsafe overtaking maneuvers in different operating conditions.

RESUMEN DE LA TESIS PARA OPTAR
AL GRADO DE DOCTOR EN INGENIERÍA ELÉCTRICA
POR: SANDY BOLUFÉ AGUILA
FECHA: 2021
PROF. GUÍA: CESAR A. AZURDIA MEZA
PROF. CO-GUÍA: SANDRA CÉSPEDES UMAÑA
PROF. CO-GUÍA: SAMUEL MONTEJO SÁNCHEZ

DISEÑO Y EVALUACIÓN DE ALGORITMOS DE BEACONING ADAPTATIVOS PARA SISTEMAS COOPERATIVOS DE SEGURIDAD VEHICULAR

En los sistemas vehiculares cooperativos, el proceso de beaconing es esencial para proveer soporte a las aplicaciones de seguridad. Esta tesis aborda el desafío de garantizar el correcto desempeño de las aplicaciones de seguridad mediante el diseño y evaluación de algoritmos de beaconing basados en el control adaptativo de los parámetros de transmisión. Específicamente, propongo y evalúo un algoritmo de beaconing adaptativo basado en la exactitud de posición (POSACC) que prioriza el error de posición y confiabilidad de la comunicación manteniendo la distancia de advertencia, carga del canal y latencia de extremo a extremo en el rango operativo de las aplicaciones de seguridad. También evalúo otros enfoques adaptativos relevantes para comprender sus beneficios y limitaciones respecto a la seguridad vial. Además, evalúo la capacidad de detección de incidentes de la aplicación de adelantamiento para vehículos autónomos cuando esta se ejecuta con mensajes obtenidos de los enfoques objetivos, considerando pérdidas de paquetes debido al desvanecimiento del canal. Los resultados muestran que POSACC no solo es más efectivo que los enfoques abordados en garantizar los requerimientos operacionales de las aplicaciones de seguridad en una gama más amplia de situaciones de tráfico, sino también en detectar maniobras inseguras en diferentes condiciones de operación.

Acknowledgements

I want to acknowledge CONICYT for supporting me with the Doctoral Grant No. 21171722, as well as the Department of Electrical Engineering, Universidad de Chile, for the opportunity of undertaking my studies in its excellent Ph.D program. This work received support from the Program ERANeT-LAC Project RETRACT ELAC2015/T10-0761 and ANID Basal Project FB0008.

I would like to express my sincere gratitude to my esteemed advisor, Cesar A. Azurdia Meza, for receiving me with open arms as well as for his unconditional support, invaluable advice, and patience during my Ph.D study. Thank you very much for sharing with me your immense knowledge and plentiful experience and for encouraging me throughout my academic research and my daily life.

This accomplishment would not have been possible either without the support of my co-advisors, Sandra Céspedes and Samuel Montejo. I am deeply grateful to both for their unwavering support, insightful comments and suggestions, as well as their assistance at every stage of the research project.

I would like to express my gratitude to my parents, my wife, and my brother. Without their tremendous understanding and encouragement in the past few years, it would be impossible for me to complete my study.

Finally, I also would like to thank my research teams, colleagues, lab mates, and friends for the kind help, treasured support, and the cherished time that we spent together.

Sandy Bolufé Aguila

Contents

List of Tables

List of Figures

List of Acronyms

AC	Access Category
ADS	Autonomous Driven System
AIFS	Arbitration Inter-Frame Space
AIMD	Additive Increase Multiplicative Decrease
AVs	Autonomous Vehicles
BSM	Basic Safety Messages
BSS	Basic Service Set
CAM	Cooperative Awareness Messages
CBR	Channel Busy Ratio
CCH	Control Channel
CMDI	Channel Monitoring and Decision Interval
CR	Communication Range
CSMA/CA	Carrier Sense Multiple Access with Collision Avoidance
C-V2X	Cellular Vehicle-to-Everything
CW	Contention Window
DC-BTP	Dynamic Control of Beacon Transmission Power
DC-BTR	Dynamic Control of Beacon Transmission Rate
DC-BTR&P	Dynamic Control of Beacon Transmission Rate and Power
DCC	Decentralized Congestion Control
DCF	Distributed Coordination Function
DENMs	Decentralized Environmental Notification Messages
DMG	Dynamic Message Generation
DSRC	Dedicated Short-Range Communication
ETSI	European Telecommunication Standards Institute
FABRIC	Fair Adaptive Beaconing Rate for Intervehicular Communication
FB	Fixed Beaconing
GPS	Global Positioning System
HCF	Hybrid Coordination Function
ICRW	Intersection Collision Risk Warning
IDR	Incident Detection Rate

IEEE	Institute of Electrical and Electronics Engineers
INTERN	Integration
ITS	Intelligent Transportation Systems
IVTRC	InterVehicle Transmit Rate Control
IVTRC-Th	InterVehicle Transmit Rate Control - Threshold
KFs	Kalman Filters
LCRW	Longitudinal Collision Risk Warning
LDM	Local Dynamic Map
LIMERIC	Linear Message Rate Integrated Control
LTE-V2X	Long-Term Evolution-V2X
MAC	Medium Access Control
NGV	Next Generation V2X
NORAC	Non-cooperative beacon Rate and Awareness Control
NR-V2X	New Radio-V2X
OBUs	On-Board Units
OCB	Outside the Context of a Basic Service Set
OMNeT++	Objective Modular Network Testbed in C++
PDFs	Probability Density Functions
PDR	Packet Delivery Ratio
PER	Packet Error Ratio
PHY	Physical
POSACC	POSition-ACCuracy
PULSAR	Periodically Update Load Sensitive Adaptive Rate
QPSK	Quadrature Phase Shift Keying
RSU	Road-Side Unit
SAE	Society of Automotive Engineers
SMDI	Status Monitoring and Decision Interval
SNR	Signal-to-Noise Ratio
SPS	Semi-Persistent Scheduling
SUMO	Simulation of Urban MObility
TTCC	Time-To-Collision Congestion Control
Veins	Vehicles in network simulation
VSCC	Vehicle Safety Communication Consortium
V2I	Vehicle-to-Infrastructure
V2V	Vehicle-to-Vehicle
V2X	Vehicle-to-Everything
WAVE	Wireless Access in Vehicular Environments
WSMP	WAVE Short Message Protocol

Chapter 1

Introduction

Cooperative vehicular safety systems are gaining increasing momentum: automotive manufacturers are equipping new vehicles with wireless communication devices, and applications with different use cases are being designed for road safety. Cooperative safety applications aim to detect potential crashes on the road and to notify vehicles in advance [1]. To increase vehicles' knowledge about the surrounding environment, they are equipped with devices such as On-Board Units (OBUs), global positioning system (GPS) receivers, on-board sensors producing vehicle-state measurements, and antennas [2]. This technology enables the exchange of information among vehicles, as well as executing cooperative safety applications (e.g., cooperative collision warning, lane change assistance, overtaking assistance, and emergency electronic brake light) to detect and mitigate potential crashes in real-time. If an imminent danger is identified, the cooperative safety application provides visual and/or audible warnings to drivers in human-driven vehicles and takes collision avoidance actions in the case of autonomous driving. The Dedicated Short-Range Communication (DSRC) is a short-range wireless access technology released in the US that operates in the 5.9 GHz frequency band [3], providing communication support for cooperative vehicular safety systems. In the US, DSRC usually refers to spectrum or technologies in which vehicular systems operate, including the suite of standards defined by the IEEE 1609 Working Group; 1609.4 for Channel Switching [4], 1609.3 for Network Services (including the WAVE Short Message Protocol - WSMP) [5], 1609.2 for Security Services [6], as well as the standard created by the IEEE 802.11 Working Group; IEEE 802.11p [7] (currently known as IEEE 802.11-OCB [8]) which defines the physical (PHY) and medium access control (MAC) layers for Wireless Access in Vehicular Environments (WAVE) [9].

Cooperative vehicular safety systems rely on the continuous exchange of status information between neighboring vehicles on a common control channel (CCH). To make neighbors aware of its presence, each vehicle regularly transmits one-hop broadcast messages, called beacons. The beacons are formally known as Basic Safety Messages (BSM) [10] in the US or Cooperative Awareness Messages (CAM) [11] in Europe. These messages include information about the status of the transmitting vehicle; such as its position, speed, acceleration, and heading. The beaconing process allows the receiving vehicle to create a Local Dynamic Map (LDM) based on the status information of its neighborhood [11]. Then, the status information is used by cooperative safety applications to detect and mitigate potentially dangerous

traffic situations in real-time (e.g., the crash risk can be estimated by analyzing the movement status of vehicles) [11].

1.1 Motivation

The proper performance of cooperative safety applications requires a correct, reliable and time-critical exchange of information between vehicles in different traffic conditions. In this context, the European Telecommunication Standards Institute (ETSI) has specified the operational requirements in terms of position accuracy, warning distance, and end-to-end latency for cooperative safety applications such as Longitudinal Collision Risk Warning (LCRW) and Intersection Collision Risk Warning (ICRW) [12], [13]. According to ETSI, LCRW (e.g., safety-relevant lane change and safety-relevant vehicle overtaking) and ICRW (e.g., turning collision risk warning and merging collision risk warning) applications demand a position accuracy equal or less than 1 and 2 m (respectively) with a confidence interval equal to 95 %, a communication range of 300 m when the channel load is at a relaxed state, and end-to-end latency equal or less than 300 ms [12], [13].

However, meeting such high requirements on different vehicular scenarios remains an open challenge due to vehicular environment characteristics and limitations of IEEE 802.11p based wireless communication technology. Vehicles may require a high beacon rate to guarantee the position accuracy requirements of cooperative safety applications [14], [15]. For instance, in highways, which usually have a high number of vehicles moving at different speeds and incurring on lane changes, or in urban roads, where vehicles are characterized by low or medium speeds, frequent heading and lane changes, sudden braking, and overtaking. On the other hand, limitations related to the wireless communication technology based on the IEEE 802.11p standard lead to a degradation of the communication reliability in vehicular scenarios with a high beaconing load. Examples of these limitations are: *a*) in both the US and Europe, the existence of a single 10 MHz shared control channel is considered for transmitting beacons and dissemination messages [16], [17]; *b*) due to cost issues, most wireless communication devices for vehicular networks can only tune one radio channel at a time [18]; *c*) the MAC mechanism of the IEEE 802.11p protocol is an asynchronous approach that cannot efficiently utilize the wireless medium, especially in scenarios where nodes transmit in broadcast mode [19]; d) the physical data-rates provided by the IEEE 802.11p protocol range from 3 to 27 Mbps, where low data-rates can tolerate poor channel conditions but introduce severe interferences [20]; and e) safety-related messages are relatively large, i.e., between 250 and 800 bytes, due to security-related overhead (e.g., digital signatures and certificates) [21], where a higher message size leads to a degradation of communication reliability caused by packet collisions.

Several works have shown the challenge of providing robust and timely communications in vehicular environments. For instance, the work in [22] evaluated the static beaconing with a beacon rate of 10 beacon/s on an unobstructed intersection with a Road-Side Unit (RSU). The simulation results demonstrated that vehicle dynamics and channel congestion reduces position accuracy. In this scenario, the position error achieved by the static beaconing of 10 beacon/s is high, exceeding 5 and 10 m for approximately 60 % of the simulation time. In [15], it is shown that the static beaconing of 10 Hz only provides a position accuracy

of 2 m for velocities lower than 70 km/h. The Vehicle Safety Communication Consortium (VSCC) specified that 10 beacon/s is the minimum beacon rate required for cooperative safety applications [14]. However, the static beaconing of 10 Hz affects negatively communication reliability especially in scenarios with a high vehicular density. Measurements of 71.1 % packet error ratio (PER), with 360 nodes transmitting at 10 beacon/s have been reported in [23]. Such high PER levels significantly impair a vehicle's ability to identify potential collision threats in a timely manner. Simply reducing the beacon rate is not a suitable solution because it reduces the position accuracy perceived by neighboring vehicles. In [15], it is shown that the static beaconing of 2 Hz provides a position error equal to or higher than 10 m for velocities higher than 70 km/h. According to [24], at a fixed message broadcast rate every 100 ms (10 beacon/s) per vehicle, it is expected that the DSRC channel congestion would be severe resulting in message loss probabilities that may be over 20 %. At an average message broadcast rate every 500 ms (2 beacon/s) per vehicle, the DSRC channel would be relatively less congested resulting in message loss probabilities that may be between 4 and 5 %. In [25], it is shown that 120 vehicles beaconing at 25 Hz will result in very low reception rates (less than 20 %). The simulation results reported in [26] show that severe packet loss can occur in vehicular networks. The reliable transmission range can be reduced by up to 90 %. The main reason for this degradation is the interference caused by transmissions of other vehicles within the traffic jam. The works in [26], [27] show that the packet collision probability is high (up to 95 %) for a low contention window (equal to 3), even if only 10 vehicles exist in the communication range.

The varying conditions of the wireless channel and vehicular traffic impose the necessity of considering adaptive approaches. Although congestion and awareness control approaches with diverse goals have been proposed in the literature [28], [29], to date, little attention has been paid on whether the proposed approaches are adequate or not to support cooperative safety applications. Congestion control approaches [30]-[33] aim at keeping the channel load below a certain target threshold and to achieve local/global fairness. However, these approaches usually do not consider the operational requirements of safety-related applications or vehicle dynamics. In contrast, awareness control approaches [11], [34]-[38] can consider road safety or vehicle dynamics, but they usually are not designed to simultaneously satisfy the operational requirements of cooperative safety applications. Furthermore, channel busy ratio (CBR) is generally used as a priority metric; however other critical metrics directly related to road safety, such as position error, packet collision rate, packet delivery ratio (PDR), and end-to-end latency are not considered. In this context, the design and evaluation of adaptive beaconing algorithms oriented to provide the quality of service required by cooperative safety applications are vital for the proper deployment of the next-generation cooperative vehicular safety systems.

1.2 Problem Statement

I am interested in providing the operational requirements of cooperative safety applications in a wide range of traffic situations. Therefore, the underlying trade-off between the beacon transmission parameters should be further investigated. A high beacon rate is required to improve position accuracy but it could lead to a congested channel, especially, in scenarios with a high vehicular density. Channel congestion leads to a degradation of communication reliability caused by packet collisions [39], [40]. Even if the channel is not congested, a high

beacon rate can still cause severe interferences due to the hidden terminal problem and the Distributed Coordination Function (DCF) procedure of IEEE 802.11p [41], [26]. At the same time, packet collisions have a negative impact on position accuracy. Furthermore, increasing the beacon transmission power cannot be done in an uncontrolled manner. On the one hand, the probability of successful reception of a single transmission decreases but, on the other hand, if all vehicles increase their beacon transmission power it might result in a saturated wireless channel with a high packet collision probability [42]. In addition, increasing the size of the minimum contention window of IEEE 802.11p can reduce packet collisions, but it increases the end-to-end latency.

To explain how the position accuracy, communication reliability, and end-to-end latency impact on collision avoidance capability of cooperative safety applications in both human-driven and autonomous vehicles, let's consider the LCRW and ICRW applications. The LCRW [12] application focuses on detecting potential collisions between vehicles at any part on the front or rear side. If a longitudinal crash risk is detected, the vehicle must issue a crash risk warning to the driver or take emergency actions (e.g., in autonomous driving). On the other hand, the ICRW [13] application focuses on detecting potential crash risks between two or more vehicles in an intersection area. In the crossing crash case, the crash risk is detected between vehicles whose trajectories may cross in the conflict zone. To detect a potential crash, these applications should use the received CAMs in a certain time window for tracking or predicting the future positions of vehicles [11]. This means that, if the vehicles receive a low number of CAMs (i.e., low reliability) or not updated status data (i.e., low position accuracy), the safety application will be impaired in detecting the dangerous situation on time or accurately predicting the trajectory of vehicles. In this work, communication reliability is quantified by using a well-established performance metric such as the packet delivery ratio, whereas the position accuracy is evaluated by using the average position error, which is a novel performance metric introduced in [15] to evaluate the position accuracy provided by a certain beacon rate. Note that, end-to-end latency not only affects position accuracy but also communication reliability. Therefore, providing the operational requirements of cooperative safety applications in different traffic situations is not a trivial problem and imposes a challenge in vehicular networks.

1.3 General Objective

Design and evaluate adaptive beaconing algorithms to provide the operational requirements, in terms of position accuracy, communication reliability, and end-to-end latency, of cooperative safety applications in a wide range of traffic situations.

1.4 Specific Objectives

1. Propose, model, and validate beacon transmission rate control strategies depending on vehicle movement status to limit the position error perceived by neighboring vehicles and to control the channel load.
2. Propose, model, and validate complementary beaconing strategies based on the adaptive control of transmission power and/or contention window size to control interferences and end-to-end latency, considering vehicular traffic dynamics and density.

3. Design, model, and validate adaptive beaconing algorithms by integrating the proposed control strategies, considering the complexity and trade-off between the required design goals.
4. Evaluate the performance of the proposed adaptive beaconing algorithms by using realistic simulation frameworks, considering metrics related to design goals and a comparison with other relevant beaconing algorithms.
5. Evaluate the performance of safety applications via realistic simulation frameworks, using the cooperative awareness generated by proposed and addressed beaconing algorithms.

1.5 Hypotheses

The operational requirements of cooperative safety applications in terms of average position error, packet delivery ratio, and end-to-end latency, can be provided for a wide range of traffic situations through the adaptive control of beaconing transmission parameters outperforming other relevant beaconing approaches.

1.6 Contributions

This thesis contributes to the current state of knowledge by adopting position accuracy and communication reliability as the highest priority metrics due to their direct impact on the decision-making process, in real-time, of road safety applications. I have provided a control mechanism that adapts the beacon rate depending on vehicle movement status to achieve the required position accuracy and a control mechanism that adapts the transmission power according to channel load and beacon rate to reduce packet collisions. I have introduced a dynamic joint power/rate control distributed algorithm that limits the position error computed by surrounding vehicles while reducing packet collisions. To overcome the limitations of the dynamic joint power/rate control approach, I have provided a control mechanism that computes the vehicle's transmission power to maximize the probability of successful reception at the target warning distance, as well as a control mechanism that computes the size of the minimum contention window to minimize the probability of packet collisions. Accordingly, I have devised a POSition-ACCuracy (POSACC) based adaptive beaconing algorithm oriented to provide the operational requirements of road safety applications. I have evaluated the performance of the proposed and other relevant beaconing algorithms in different traffic conditions using a realistic simulation framework and highlighting their benefits and limitations related to road safety. Finally, I also have assessed the impact of awareness control on the overtaking application in autonomous driving by considering different operative situations.

1.7 Thesis Organization and Papers Published

This doctoral thesis is organized according to "Format 2: New optional doctoral thesis format based on 2 accepted/published ISI journal papers." https://www.die.cl/sitio/proceso-de-doctorado/.

Therefore, Chapter 1, the Introduction, contains the following sections: the research motivation, the problem statement, the general and specific objectives, the hypotheses, the contributions, the thesis organization and papers published.

As a result of this doctoral thesis, two journal papers (WoS) were published, and also two papers were published at international conferences. As Format 2 requires, the contents of Chapters 2 through 5 are the published papers in chronological order.

Chapter 2 [43] contains a published international conference paper, presented at the 33rd Annual ACM Symposium on Applied Computing (SAC'18), Pau, France, April 9-13, 2018. In this research, I designed a beacon rate control mechanism oriented to limit the position error perceived by neighboring vehicles, as well as a beacon transmission power control mechanism oriented to mitigate packet collisions. These control mechanisms were integrated into a dynamic joint power/rate control distributed algorithm, which was evaluated with a realistic simulation framework in an urban scenario considering different traffic densities. The proposed algorithm demonstrated its effectiveness to set a good trade-off between position accuracy, packet collisions, and warning range, by outperforming other combinations of fixed and adaptive beaconing addressed in the paper. However, it achieves such benefits at the cost of decreasing the warning range of vehicles with higher dynamics, which is a drawback for road safety. Accordingly, I continued investigating other alternatives to provide a high position accuracy without compromising the communication range of vehicles. Therefore, in [44], I investigated the beaconing based on probability density functions to better understand its benefits and limitations regarding road safety.

Chapter 3 [44] contains a published international conference paper, presented at the 4th International Conference on Vehicle Technology and Intelligent Transport Systems (VEHITS 2018) - Special Session on Resilient Smart city Transportation (RESIST), Funchal, Madeira, Portugal, March 16-18, 2018. In this research, I evaluated the performance of a dynamic beaconing strategy where both beacon rate and transmit power are assigned by means of probability density functions (PDFs). I investigated four types of PDFs (e.g., Constant, Uniform, Normal, and Triangular), attending to four different performance metrics, in four distinct vehicular scenarios, using a realistic simulation framework. As a baseline, I used the beaconing algorithm introduced by Kloiber et al. in [34], which proposes to mitigate recurring interferences by randomly selecting the transmit power of vehicles. Simulation results allowed me to set a relationship between the use of a certain distribution and the traffic characteristics of the vehicular scenario. I observed that although the uniform PDF is effective to mitigate packet collisions, it also has drawbacks for road safety. The main one is that vehicles can set a low beacon transmission rate and power when a high position accuracy or warning range is required to mitigate a critical situation. On the contrary, vehicles with low dynamics can set a high beacon transmission rate and power when a high position accuracy or warning range is not required.

Chapter 4 [45] contains the first journal paper, published in IEEE Access, 2020. In this research, I focused on designing a beaconing algorithm oriented to provide the operational requirements of cooperative safety applications in a wide range of traffic situations. To accomplish this goal, I proposed a control mechanism that computes the beacon transmission power according to vehicle dynamics to maximize the probability of successful reception at the

target warning distance. I also proposed a control mechanism that computes the size of the minimum contention window according to the number of surrounding neighbors to minimize the probability of packet collisions. These two control mechanisms and the beacon rate control mechanism proposed in [43] were integrated into a POSition-ACCuracy (POSACC) based adaptive beaconing algorithm. POSACC overcomes the limitations of my previous work [43], assigning a higher warning range to vehicles with higher dynamics. POSACC adopts position accuracy and communication reliability as the highest priority metrics, and it focuses on guaranteeing these metrics, maintaining the vehicle's warning distance, channel load, and end-to-end latency into the operative range of cooperative safety applications. POSACC was compared with three different state-of-the-art adaptive beaconing algorithms; ETSI DMG [11] which is the awareness control approach specified by European standards, LIMERIC [31] which is one of the most important congestion control approaches available in the literature, and DC-BTR&P [43] which is my previous approach. Simulation results demonstrated that POSACC is more effective than the benchmark algorithms for providing the operational requirements of cooperative safety applications in a wider range of traffic situations.

Chapter 5 [46] contains the second journal paper, published in IEEE Communications Letters, 2021. This research was oriented to evaluate a cooperative safety application and awareness control approaches working together, as well as to highlight the benefits and limitations of the addressed approaches for road safety. Specifically, I evaluated the effectiveness of relevant awareness control approaches, such as ETSI DMG [11], IVTRC [35], IVTRC-Th [47], and POSACC [45], for supporting the V2V-based overtaking application in autonomous driving. In the comparison, I also included a fixed beaconing approach of 10 Hz which is the higher message frequency specified by ETSI in [11]. I designed an operation mode for the overtaking application in autonomous vehicles. Then, I assessed the incident detection capability of the overtaking application when it is running with messages gathered from these approaches, taking into account motion state sensors' errors and packet losses due to channel fading. Simulation results demonstrated that POSACC is more effective than the remaining beaconing approaches for detecting unsafe overtaking maneuvers in different operating conditions.

Finally, Chapter 6 contains the general conclusions of this thesis as well as the future work.

Appendix A contains the published papers on journals (WoS) and conferences that contributed to the development of this thesis.

1.8 Other Publications

This doctoral thesis is composed of two papers published in journals (WoS) and two papers published at international conferences. However, there are nine more published papers; two in journals (WoS) and seven at conferences, which are directly related to the topic addressed in this thesis and therefore are additional contributions. In the following, the published papers are presented in chronological order.

The work in [48] is a published conference paper, presented at the III Spring School on Networks (SSN 2017), Pucón, Chile, 2017. This paper introduces an adaptive beaconing algorithm based on dynamic control of beacon rate oriented to limit the position error computed by surrounding vehicles. The work in [49] is a published conference paper, presented at the 2017 CHILEAN Conference on Electrical, Electronics Engineering, Information and Communication Technologies (IEEE CHILECON 2017), Pucón, Chile, 2017. This work proposes two novel channel hopping sequence approaches to rendezvous, in order to allow vehicular applications to use unlicensed channels. The work in [50] is a published conference paper, presented at the 6th International Workshop on ADVANCEs in ICT infrastructures and Services (ADVANCE 2018), Santiago, Chile, 2018. This work develops an experimental setup to evaluate an adaptive beaconing algorithm that helps to maintain cooperative knowledge in vehicular communication networks. The work in [51] is a published conference paper, presented at the 4th International Conference on Vehicle Technology and Intelligent Transport Systems (VEHITS 2018) - Special Session on Resilient Smart city Transportation (RESIST), Funchal, Madeira, Portugal, 2018. This work presents a genetic-based approach to determine optimal values of frequency and transmission power in beacon-based vehicular ad-hoc networks. The work in [52] is a published conference paper, presented at the School on Systems and Networks (SSN 2018), Valdivia, Chile, 2018. This work analyzes how an RSU improves connectivity in scenarios where vehicles are approaching over perpendicular roads on an intersection with obstructing buildings.

The work in [53] is a published conference paper, presented at the IEEE 39th Central America and Panama Convention (IEEE CONCAPAN 2019), Guatemala City, Guatemala, 2019. This work describes the IEEE 1609 and IEEE 802.11p standards, which define the DSRC and WAVE technologies. Emphasis is made on the physical and data link layers. The work in [54] is a published conference paper, presented at the IEEE Latin-American Conference on Communications (LATINCOM 2020), Santo Domingo, Dominican Republic, 2020. This manuscript presents a beamforming scheme for V2V communications in the context of urban intersections. The work in [55] is a journal paper (WoS), published in Electronics, 2021. This work introduces a new channel estimation and equalization technique based on a Semi-supervised Extreme Learning Machine (SS-ELM) in order to address the harsh characteristics of the vehicular channel and improve the performance of the communication link. The work in [56] is a journal paper (WoS), published in Sensors, 2021. This work proposes a neuroevolution of augmenting topologies-based adaptive beamforming scheme to control the radiation pattern of an antenna array and thus mitigate the effects generated by shadowing in urban V2V communication at intersection scenarios. The published papers that contributed to the development of this thesis are shown in Appendix A.

Chapter 2

Dynamic Control of Beacon Transmission Rate and Power with Position Error Constraint in Cooperative Vehicular Networks

Cooperative vehicular networks require the continuous exchange of beacon messages between neighboring vehicles to support cooperative awareness applications. The position error computed by surrounding vehicles impacts on applications' capability to detect and mitigate potentially dangerous traffic situations in real-time. A challenge in cooperative safety systems is to maintain a high position accuracy while controlling the communication channel load. In this paper, we propose a novel joint power/rate control distributed algorithm to meet the position accuracy requirements of cooperative safety applications. The beacon transmission rate is adjusted dynamically as a function of the vehicle movement status, to constrain position error computed by surrounding vehicles. Then, the transmit power is adjusted according to the channel load and the preset beacon transmission rate, to decrease packet collisions. This algorithm has been evaluated in a realistic simulation framework, considering different traffic densities for an urban scenario. The simulation results demonstrate that the proposed algorithm outperforms other basic beaconing algorithms addressed in this paper, in terms of trade-off between position accuracy, packet collisions, and warning range.

2.1 Introduction

Intelligent Transportation Systems (ITS), based on Vehicle-to-Vehicle (V2V) and Vehicle-to-Infrastructure (V2I) communications, are technologies designed to support road safety and traffic efficiency applications [1]. In these systems, the vehicles are equipped with On-Board Units (OBUs), global positioning system (GPS) receivers, air interfaces, and sensors which record the vehicle status. This technology allows the information exchange between vehicles and infrastructure devices such as Road-Side Units (RSUs), as well as processing and display information to drivers and passengers. The Dedicated Short-Range Communication (DSRC) is a short-range wireless access technology that operates in the 5.9 GHz frequency

band, providing communication support for road safety and traffic efficiency applications in vehicular networks. In the US, DSRC usually refers to spectrum or technologies in which vehicular systems operate, including IEEE 802.11p [7] (currently known as IEEE 802.11-OCB[1] [8]) which defines physical (PHY) and medium access control (MAC) layers for Wireless Access in Vehicular Environments (WAVE) [57].

Cooperative vehicular networks have been identified as a promising technology to enable ITS. These networks require the continuous exchange of status information between neighboring vehicles to support cooperative awareness applications. For the surrounding vehicles to be aware of its presence, each vehicle regularly transmits one-hop broadcast messages, called beacons. The beacons include information about the status of the vehicle, such as its position, speed, acceleration, and heading [58]. This process, known as beaconing, allows the receiver vehicles to create a Local Dynamic Map (LDM) based on surrounding environment information, which is essential for the proper performance of cooperative awareness applications. For instance, safety applications such as intersection collision warning and lane change assistance use the beaconing information to detect and mitigate potentially dangerous situations in real-time.

The highly dynamic mobility of vehicles in these networks leads to a rapid expiration of the beacons information. Consequently, the position errors can impact the proper performance of cooperative safety applications, which rely on real-time accurate information. Beacon transmission rate directly translates into accuracy of cooperative awareness. In traffic jams scenarios, a beacon transmission rate of 1 beacon/s could be enough to provide the position accuracy needed for the proper performance of cooperative safety applications. However, this beacon rate is not enough to achieve the required cooperative awareness level on a multi-lane high speed highway with frequent lane changes. In this context, the technical report of the Vehicle Safety Communication Consortium (VSCC) [14] specifies that 10 beacon/s is the minimum beacon rate required to meet the position accuracy of several cooperative safety applications, while some cooperative safety-critical applications can demand a beacon rate up to 50 beacon/s. Therefore, finding the appropriate beacon transmission rate for each scenario is essential for the proper performance of the system.

A high beacon rate could lead to a congested channel, especially, in scenarios with high vehicle density, resulting in more packet collisions. Consequently, the increase in position error according to the number of packet collisions may lead to not meet the accuracy requirements of cooperative safety applications. Different strategies have been proposed to control the load generated by beaconing in the control channel (CCH), and at the same time to guarantee the communication requirements of safety applications [29]. The algorithm proposed by Zemouri et al. [59] adapts the transmit rate to meet the channel requirements in terms of collision rate and busy ratio. Then, the transmit power is adjusted to guarantee a certain level of awareness for closer neighbors. In the algorithm proposed by Sepulcre et al. [36], the packet transmission rate of each vehicle is configured taking into consideration the minimum required by the application, plus a certain margin. Then, the transmit power is set to the minimum power level needed to ensure the demanded packet reception rate at the application warning distance. In the proposal of Aigun et al. [60], the algorithm adapts the transmit power in order to reach a desired awareness ratio at the target distance, while

[1]OCB - Outside the Context of a Basic Service Set (BSS) in IEEE 802.11-2016.

adjusting the beacon rate to keep the current channel busy ratio below a certain threshold. These approaches have been focused on the channel load and specific communication requirements, combining the control of beacon rate and transmit power, but do not consider the vehicle movement status and the vehicular traffic dynamics, as well as its impact on the position error computed by surrounding vehicles.

The communication requirements of cooperative safety applications can be defined in terms of warning range [61] and packet inter-reception time [62]. These requirements can be different according to the application type [63] and the vehicular context [64]. Therefore, meeting the communication requirements of all applications in each scenario is a very complex task. The responsibility for meeting the requirements of a specific performance metric in the worst case (more demanding applications) can lead to not meeting the requirements of these and other applications, in different metrics. Therefore, in beaconing-based systems, it is essential to define the metric with the greatest impact for safety-critical applications. We believe that the precision and freshness of the beaconing information is indispensable for the decision-making process, in real-time, of cooperative safety applications [15]. For this reason, we propose the position error as a priority metric, due to its impact on the vehicle's systems capability to detect and mitigate potentially dangerous situations on time. In this context, we propose and evaluate a novel joint power/rate control distributed algorithm that adjusts the beacon rate and transmit power to meet a target position error according to the accuracy requirements of cooperative safety applications. The algorithm dynamically adjusts the beacon rate based on vehicle movement status and then adjusts the transmit power according to the channel load and the preset beacon rate to decrease packet collisions.

The main contributions of this paper are: ***i)*** to model the position error as a priority metric due to its high impact on the performance of position-based real-time applications in vehicular systems; ***ii)*** to propose a dynamic joint power/rate control distributed method that limits the position error computed by surrounding vehicles while reducing packet collisions; and ***iii)*** to define an algorithm able to adapt to the vehicular environments considering the movement status of vehicles and the local-global beaconing load condition. The proposed algorithm has the best trade-off among the studied performance metrics. It reduces the number of harmful position errors and the average packet collisions below 50 % in comparison to the dynamic beacon rate control algorithms that use the maximum transmit power. Further, the proposed algorithm achieves a position accuracy close to that obtained by the dynamic beacon transmission power control algorithms that use the maximum beacon rate, but with less than 15 % of packet collisions and a higher warning range, registering more than three times the average number of vehicles in the LDM database.

2.2 Proposed Algorithm

In this section, we present a novel joint power/rate control distributed algorithm that uses the dynamic adjustment of beacon rate and transmit power to meet the position accuracy requirements of cooperative safety applications. The proposed algorithm is the integration of two control algorithms; the first one focuses on the dynamic adjustment of beacon transmission rate, whereas the second one focuses on the dynamic adjustment of beacon transmission power.

2.2.1 Dynamic Control of Beacon Transmission Rate

Dynamic Control of Beacon Transmission Rate (DC-BTR) computes the beacon transmission rate required by the i-th vehicle (denoted as n_{i}) as a function of its movement status, to limit in real-time the position error computed by surrounding vehicles. DC-BTR avoids the use of high beacon transmission rates all the time. Instead, each vehicle uses an adaptive beacon transmission rate according to the traffic dynamics of each scenario. The communication channel load is implicitly regulated by the flow dynamics of vehicular traffic [15], where a high speed generally leads to low vehicle densities, whereas a low speed typically leads to high vehicle densities, especially in urban scenarios.

We denote the average position error ($\overline{E}$) as in [15], which expresses the mean error assuming that the event of looking up the position in the LDM database is uniformly distributed between the minimum and maximum time difference to the transmission event of the beacon,

$$\overline{E} = \frac{\lfloor E \rfloor + \lceil E \rceil}{2}, \tag{2.1}$$

where $\lfloor E \rfloor$ denotes the lower error boundary resulting from the transmission delay (t_D), and $\lceil E \rceil$ is the upper boundary that occurs when the position of a vehicle is looked up right before receiving the next beacon.

By using kinematic equations, $\overline{E}$ can be expressed as a function of the velocity[2] (v_{i}) and acceleration (a_{i}) of n_{i},

$$2\overline{E_{\mathrm{i}}} = v_{\mathrm{i}} t_D + I_{b_{\mathrm{i}}} \left(v_{\mathrm{i}} + \frac{a_{\mathrm{i}} I_{b_{\mathrm{i}}}}{2} \right) + t_D (a_{\mathrm{i}} I_{b_{\mathrm{i}}} + v_{\mathrm{i}}), \tag{2.2}$$

where $I_{b_{\mathrm{i}}}$ is the beacon interval of n_{i} (equivalent to the inverse of beacon transmission rate, $R_{b_{\mathrm{i}}}$). We assume beacon messages of the same size (b_z) and equal data-rate (R_D), so t_D is the same for all vehicles, $t_D = b_z / R_D$.

From (2.2), a second degree polynomial of the form $P(I_{b_{\mathrm{i}}}) = A I_{b_{\mathrm{i}}}^2 + B I_{b_{\mathrm{i}}} + C$ is obtained as,

$$a_{\mathrm{i}} I_{b_{\mathrm{i}}}^2 + 2(v_{\mathrm{i}} + a_{\mathrm{i}} t_D) I_{b_{\mathrm{i}}} + 4(v_{\mathrm{i}} t_D - \overline{E_{\mathrm{i}}}) = 0. \tag{2.3}$$

In the general case of $a_{\mathrm{i}} \neq 0$, the polynomial solutions ($I_{b_{\mathrm{i}\{1,2\}}}$) can be computed as follows,

$$I_{b_{\mathrm{i}\{1,2\}}} = \frac{-B \pm \sqrt{D}}{2A}, \tag{2.4}$$

where $D = B^2 - 4AC$ with $A = a_{\mathrm{i}}$, $B = 2(v_{\mathrm{i}} + a_{\mathrm{i}} t_D)$, and $C = 4(v_{\mathrm{i}} t_D - \overline{E_{\mathrm{i}}})$. On the other hand, if $a_{\mathrm{i}} = 0$, the solution ($I_{b_{\mathrm{i}}}$) is,

$$I_{b_{\mathrm{i}}} = \frac{2(\overline{E_{\mathrm{i}}} - v_{\mathrm{i}} t_D)}{v_{\mathrm{i}}}. \tag{2.5}$$

[2]The velocity vector is not used since position error considers the movement in a straight line between the last received position and the current position of the vehicle. Therefore, in order to reduce the complexity, it is assumed that the vehicle moves in a single dimension (direction of longitudinal displacement).

Fig. 2.1a shows the beacon transmission rate required to achieve a target average position error of 0.5 m and 1 m. Note that the impact of velocity on beacon transmission rate is greater than the impact of acceleration. Further, and as expected, the target average position error decreases when the beacon transmission rate increases. This cost directly impacts on the communication channel load. Fig. 2.1b shows the average position error as a function of the acceleration and velocity for an I_{b_i} equal to 1 s. Note that the average position error increases when the vehicle acceleration increases. This increment on average position error is significant when a high position accuracy is required. In this context, it should be considered that the maximum position error computed by the cooperative safety-critical application is twice the average position error, see (2.1).

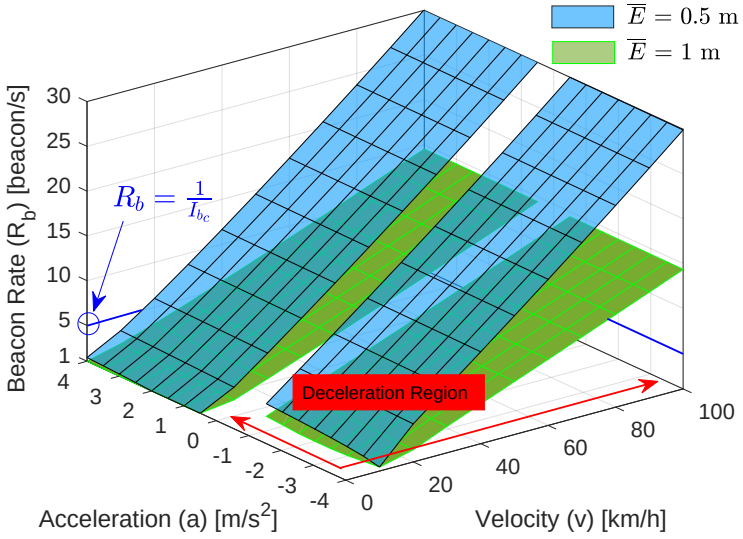

(a)

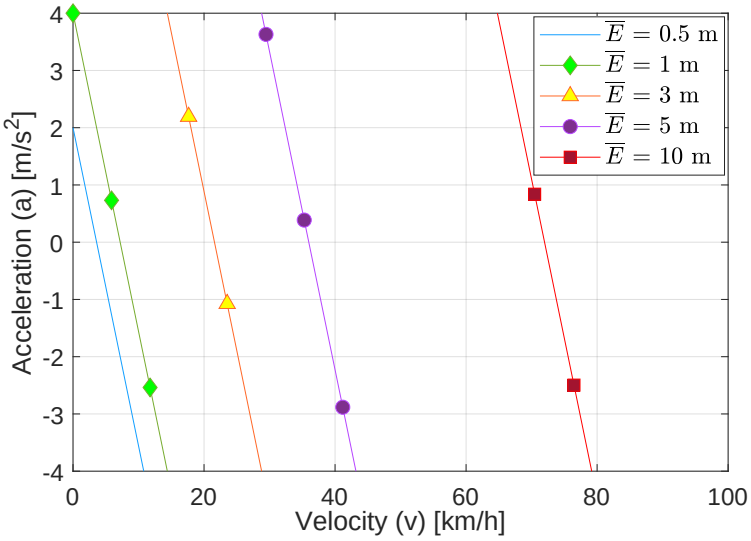

(b)

Figure 2.1: (a) R_{b_i} as a function of v_i and a_i for $\overline{E_i}$ = 0.5 m and $\overline{E_i}$ = 1 m with b_z = 250 bytes and R_D = 6 Mbps, (b) Acceleration vs velocity for different values of $\overline{E_i}$ with I_{b_i} = 1 s.

Algorithm 1 describes the steps followed by DC-BTR to compute the beacon transmission rate in real-time according to the movement status of the vehicle n_{i} and the target position error. The next beacon interval is computed by n_{i} at each beacon transmission. Lines 1-20 involve the decisions associated according to the movement status of n_{i}: repose (Line 1-2), the beacon transmission rate is set to 1 beacon/s equivalent to the minimum value required for the proper performance of the less demanding vehicular applications [58]; accelerated movement (Line 3-7), the beacon transmission rate is computed using (2.4); uniform movement (Line 8-11), the beacon transmission rate is computed according to (2.5); deceleration (Line 12-20) in order to notify with immediacy to surrounding vehicles a possible braking, it is set a critical beacon interval (I_{b_c}). It should be noted that if two valid solutions are found, the solution that generates the lowest channel load is selected (see Line 5 and Line 16).

Algorithm 1: DC-BTR

Data: $\{v_{\mathrm{i}}, a_{\mathrm{i}}, t_D, I_{b_c}, \overline{E_{\mathrm{i}}}\}$
Result: $\{R_{b_{\mathrm{i}}}\}$

Tx: *Algorithm to execute on each beacon transmission*:
Begin

```
1   if (v_i == 0 && a_i == 0) then
2       I_{b_i} ← 1;
    end
3   else if (v_i >= 0 && a_i > 0) then
4       Compute I_{b_{i{1,2}}} using (2.4);
5       I_{b_i} ← maximum{I_{b_{i{1}}}, I_{b_{i{2}}}};
6       if (I_{b_i} > 1) then
7           I_{b_i} ← 1;
        end
    end
8   else if (v_i > 0 && a_i == 0) then
9       Compute I_{b_i} using (2.5);
10      if (I_{b_i} > 1) then
11          I_{b_i} ← 1;
        end
    end
12  else if (v_i > 0 && a_i < 0) then
13      Compute D;
14      if (D > 0) then
15          Compute I_{b_{i{1,2}}} using (2.4);
16          I_{b_i} ← maximum{I_{b_{i{1}}}, I_{b_{i{2}}}};
17          if (I_{b_i} > I_{b_c}) then
18              I_{b_i} ← I_{b_c};
            end
        end
19      else if (D <= 0) then
20          I_{b_i} ← I_{b_c};
        end
    end
21  R_{b_i} ← ceil(1/I_{b_i});
22  return R_{b_i};
end
```

2.2.2 Dynamic Control of Beacon Transmission Power

Dynamic Control of Beacon Transmission Power (DC-BTP) adapts the transmit power according to the relative communication channel load and the preset beacon transmission rate, in order to decrease packet collisions. In scenarios with high vehicle density or high traffic dynamics, the generated beaconing load could lead to a congested channel, increasing significantly the packet collisions. As a consequence, the increase in position error due to beacon message loss impacts negatively the vehicular systems' capability to detect and mitigate potentially dangerous traffic situations in real-time.

The normalized relative channel load (L_{i}) on n_{i} is estimated according to the load offered by n_{i} and the load perceived from all vehicles registered in its LDM database, normalized with respect to the data-rate,

$$L_{\mathrm{i}} = \frac{b_z \left(R_{b_{\mathrm{i}}} + \sum_{\substack{k=1 \\ k \neq \mathrm{i}}}^{N_{\mathrm{i}}} R_{b_k} P_{S_k} P_{R_k} \right)}{R_D}, \tag{2.6}$$

where P_{R_k} is the probability of successful message reception at n_{i} as a function of the distance to n_k and P_{S_k} is the probability of successful transmission of the k-th vehicle in presence of multiple transmitters.

P_{R_k} is computed using the analytic model proposed by Killat et al. in [65], which depends on the distance between the sender (n_k) and receiver (n_{i}), the communication range of n_k, the carrier frequency, and the antenna heights. While P_{S_k} is modeled according to Van Eenennaam et al. [25], where P_{S_k} is the probability that neither shared receivers choose to transmit in the same time slot used by n_{i} and that the hidden nodes do not transmit in the same time slot of n_{i}, or in the previous time slot. Fig. 2.2a shows P_{R_k} for different communication ranges (CR) and distances (d) between the transmitter and receiver, over a crossover distance of 556 m. Fig. 2.2b illustrates P_{S_k} for a beacon rate of up to 40 beacon/s and a maximum number of 150 vehicles in the carrier-sense-range, considering that all vehicles use the same beacon size and transmission rate. Note that, when more than 15 beacon/s are transmitted and 60 or more vehicles converge, P_{S_k} drops below 0.6.

The transmit power ($P_{T_{\mathrm{i}}}$) is adjusted by the vehicle n_{i} before each beacon transmission as follows,

$$P_{T_{\mathrm{i}}} = P_{T_{\min}} + (P_{T_{\max}} - P_{T_{\min}})(1 - \frac{L_{\mathrm{i}}}{L_o}) R_{b_{\mathrm{i}}}^{-\beta}, \tag{2.7}$$

where $P_{T_{\min}}$ is the transmit power required by n_{i} to generate a minimum warning range, $P_{T_{\max}}$ is the allowed maximum transmit power, L_o is the normalized critical channel load, and β is a weight factor which controls the impact of the beacon rate on the transmit power. It should be noted that (2.7) controls the beacon transmission power between minimum and maximum transmit power values, being $P_{T_{\mathrm{i}}} = P_{T_{\min}}$ for $L_{\mathrm{i}} = L_o$, and $P_{T_{\mathrm{i}}} = P_{T_{\max}}$ for $L_{\mathrm{i}} \approx 0$ and $R_{b_{\mathrm{i}}} = 1$ beacon/s. Fig. 2.3 shows the transmit power according to the normalized relative channel load and beacon transmission rate, with $P_{T_{\min}} = 7$ dBm, $P_{T_{\max}} = 20$ dBm, $L_o = 0.4$, and $\beta = 2$. Note that the transmit power decreases when the normalized relative channel load or/and the beacon rate increases, while a minimum warning range is guaranteed.

Algorithm 2 describes the steps followed by DC-BTP to compute the beacon transmission power used by n_{i} in real-time. This algorithm is composed by two subroutines, one of them is executed on each beacon reception and the other is executed before each beacon transmission. In the first subroutine (Line 1-5), the relative beaconing load (L_{b_k}) of each sender vehicle n_k is computed and registered in the LDM database. In the second subroutine (Line 1-10), the beaconing load ($L_{b_{\mathrm{i}}}$) of n_{i} and the total relative beaconing load (L_K) of all sender vehicles is computed. Finally, the transmit power is computed as a function of the normalized critical channel load, the normalized relative load, and the beacon transmission rate.

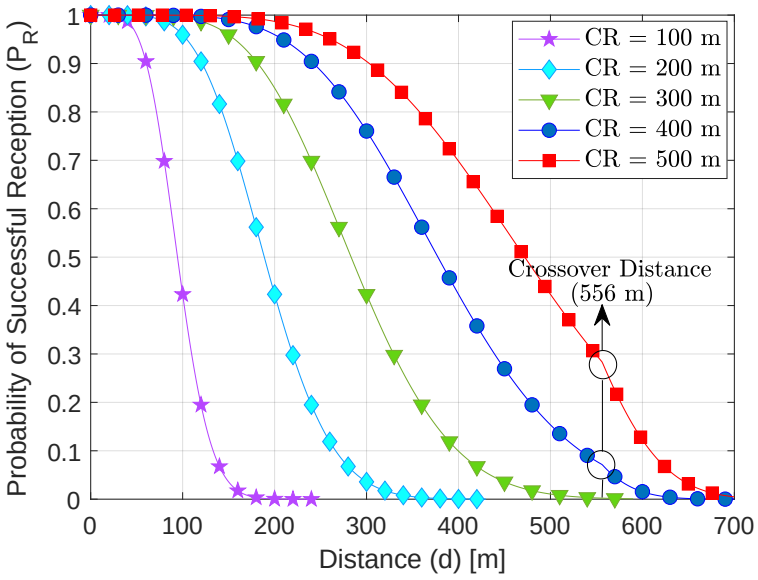

(a)

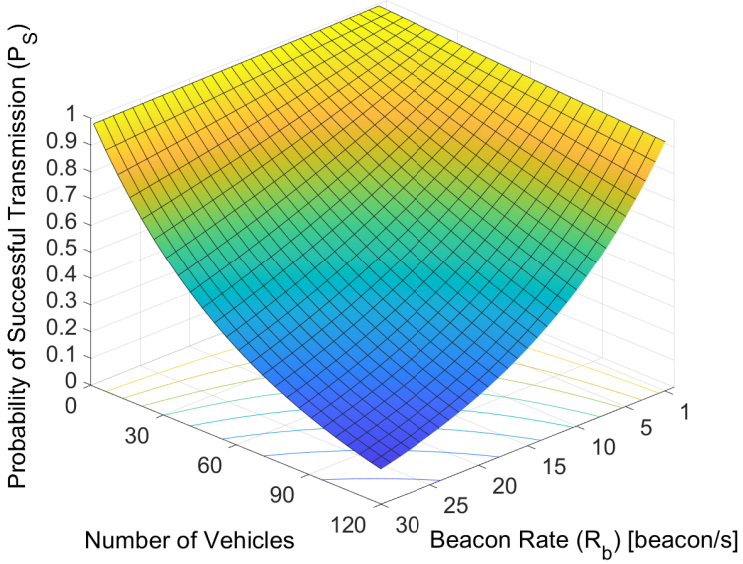

(b)

Figure 2.2: (a) P_{R_k} as a function of d with carrier frequency of 5.89 GHz and antenna heights of 1.5 m, (b) P_{S_k} as a function of the number of vehicles and R_{b_i} with $b_z = 250$ bytes and $R_D = 6$ Mbps.

2.2.3 Joint Power/Rate Dynamic Control

Dynamic Control of Beacon Transmission Rate and Power (DC-BTR&P) combines the control strategies DC-BTR and DC-BTP, in order to meet the position error requirements of cooperative safety applications. DC-BTR&P adopts the position error as a priority metric due to its impact on vehicular systems to detect and mitigate potentially dangerous traffic situations in real-time. DC-BTR&P is executed before each beacon transmission, but the LDM database is updated on each beacon reception. The joint control allows adapting to the vehicular traffic dynamics and to the vehicle movement status, adjusting the transmit power

Algorithm 2: DC-BTP

Data: $\{R_{b_i}, R_{b_k}, b_z, R_D, L_o, P_{T_{\min}}, P_{T_{\max}}\}$
Result: $\{P_{T_i}\}$

Rx: *Section to execute on each beacon reception*:
Begin
1 Get R_{b_k};
2 Compute P_{R_k} according to [65, Eq. 1-2];
3 Compute P_{S_k} according to [25, Sec. IV];
4 $L_{b_k} \leftarrow b_z R_{b_k} P_{R_k} P_{S_k}$;
5 Update LDM Database;
end

Tx: *Section to execute on each beacon transmission*:
Begin
1 $L_{b_i} \leftarrow b_z R_{b_i}$;
2 $L_K \leftarrow 0$;
3 **for** $k \leftarrow 1$ **to** N_i - *Number of Nodes in LDM* **do**
4 $L_K \leftarrow L_K + L_{b_k}$;
end
5 $L_i \leftarrow (L_{b_i} + L_K)/R_D$;
6 **if** $(L_i > L_o)$ **then**
7 $P_{T_i} \leftarrow P_{T_{\min}}$;
end
8 **else if** $(L_i \leq L_o)$ **then**
9 $P_{T_i} \leftarrow P_{T_{\min}} + (P_{T_{\max}} - P_{T_{\min}})(1 - L_i/L_o)R_{b_i}^{-\beta}$;
end
10 **return** P_{T_i};
end

to decrease packet collisions, at the same time that the minimum warning range is guaranteed. As a result, vehicles use a beacon rate and transmit power that change constantly

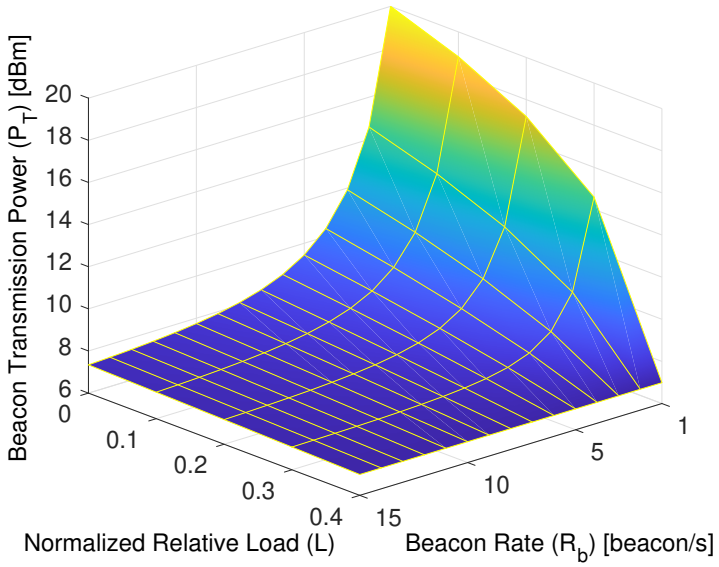

Figure 2.3: P_{T_i} as a function of L_i and R_{b_i} with $P_{T_{\min}} = 7$ dBm, $P_{T_{\max}} = 20$ dBm, $L_o = 0.4$, and $\beta = 2$.

Algorithm 3: DC-BTR&P

Data: $\{v_i, a_i, t_D, I_{b_c}, \overline{E_i}, R_{b_i}, R_{b_k}, b_z, R_D, L_o, P_{T_{min}}, P_{T_{max}}\}$
Result: $\{R_{b_i}, P_{T_i}\}$

Algorithm to execute on each beacon transmission:
Begin
1 Execute **Algorithm 1**;
2 Execute **Algorithm 2**;
3 **return** R_{b_i};
4 **return** P_{T_i};

over time, according to the vehicular context. **Algorithm 3** shows that DC-BTR&P is composed of two phases. First, DC-BTR dynamically controls the beacon transmission rate as a function of the vehicle movement status to limit the position error perceived by neighboring vehicles. Then, DC-BTP computes the transmit power according to the normalized relative channel load and the preset beacon transmission rate in order to mitigate packet collisions.

2.3 Performance Evaluation

The evaluation is carried out in an urban scenario, defined by a real map section of Chicago city, US, with an area of 1 km^2, as shown in Fig. 2.4. The zone has several traffic lights and multi-lane roads with a maximum speed limit of 100 km/h. We use a vehicular traffic model based on flows, where vehicles move between a point of origin and destination. Fig. 2.4 illustrates the seven flows that have been configured with 20, 30, and 40 vehicles in a simulation time of 500 s, resulting in three different vehicle densities: 50, 70, and 100 veh/km^2. The vehicles broadcast beacons to the communication channel by configuring the beacon rate and transmit power, according to the operation of the beaconing approach under evaluation. According to [58], [15], four typical fixed rates between 1 and 10 beacon/s have been investigated: high (10 beacon/s), medium (5 beacon/s), low (2 beacon/s), and

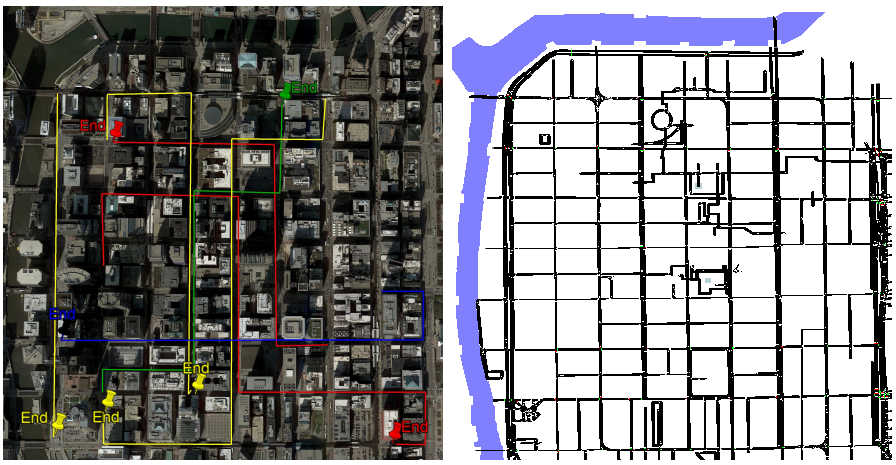

(a) (b)

Figure 2.4: Real map section of Chicago city, US, seen from: (a) Google Earth and (b) SUMO Traffic Simulator.

minimum (1 beacon/s) beacon rate. The maximum transmit power has been set to 20 dBm, and the minimum power level to 7 dBm [7]. We define a position accuracy of 1 m according to cooperative safety-critical applications such as Longitudinal Collision Risk Warning[3] (LCRW) [12]. We perform the simulations by using the Veins framework [66] with the IEEE 802.11p MAC/PHY model introduced by Eckhoff and Sommer in [67]. The radio signal propagation is modeled with the Two-Ray Interference model (with a dielectric constant ϵ_r equal to 1.02), which has been validated based on an extensive set of road measurements [68]. The communications are established on the CCH channel without considering the multi-channel operation. The beacon messages have 250 bytes [36] and are transmitted with a priority corresponding to the voice access category (AC_VO) [67]. Each vehicle is 5 m long, 2 m wide, and has a maximum acceleration of 0.8 m/s^2 and deceleration up to 4.5 m/s^2. The antenna height is 1.5 m [65] and data-rate is 6 Mbps [8]. According to [15], we utilize a normalized critical channel load equal to 0.4. The most important simulation parameters are given in Table 2.1.

Table 2.1: Simulation Parameters

Parameter	**Value**
CCH Frequency	5.89 GHz [7]
CCH Bandwidth	10 MHz [7]
Min. and Max. Transmit Power	7 and 20 dBm [7]
Normalized Critical Load (L_o)	0.4 [15]
Weight Factor (β)*	2
Critical Beacon Interval (I_{b_c})†	0.2 s [15]
Average Position Error ($\overline{E}$)	1 m [12]
Beacon Size (b_z)	250 bytes [36]
Access Category (AC)	AC_VO [67]
Receiver Sensitivity	-82 dBm [8]
Thermal Noise	-110 dBm
Modulation	QPSK [8]
Coding Rate	1/2 [8]
Data-Rate (R_D)	6 Mbps [8]
Antenna Gain	0 dB
Antenna Height	1.5 m [65]
Propagation Model	Two-Ray Interference [68]
Traffic Density (ρ)	50, 70, 100 veh/km^2

$*$ β has been selected from the integer range of 1 to 4 based on extensive simulations, considering its impact on the warning range. † $I_{b_c} = 0.2$ s is equal to 5 beacon/s, setting a good trade-off between position tracking and beaconing load.

2.3.1 DC-BTR: Simulation Result

This experiment focuses on the performance evaluation of DC-BTR. In this case, all vehicles in the scenario are using DC-BTR (with a fixed transmit power of 20 dBm), to dynamically adjust the beacon rate in real-time.

Fig. 2.5 illustrates the movement status of a generic vehicle in the scenario. The acceleration and velocity are represented in color blue and red, respectively. It should be noted that the mobility pattern shows a continuous change in vehicle status between acceleration,

[3]Relevant use cases of the LCRW application are: safety relevant lane change, safety relevant vehicle overtaking warning, and collision risk warning from third party, in ETSI TS 101 539-3 v1.1.1-2013.

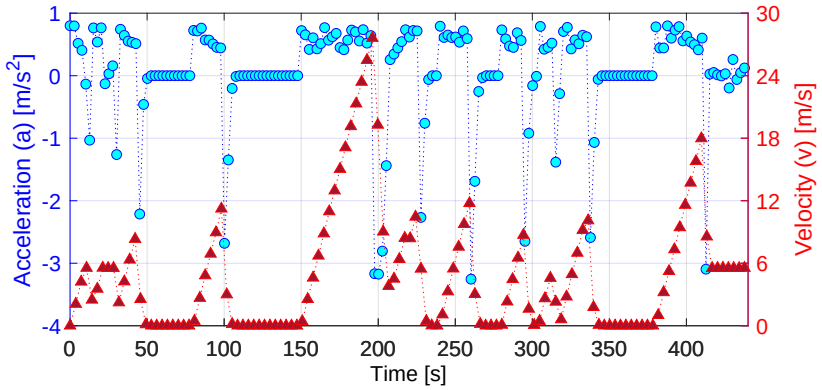

Figure 2.5: Acceleration and velocity developed by the vehicle during 440 s of the simulation time.

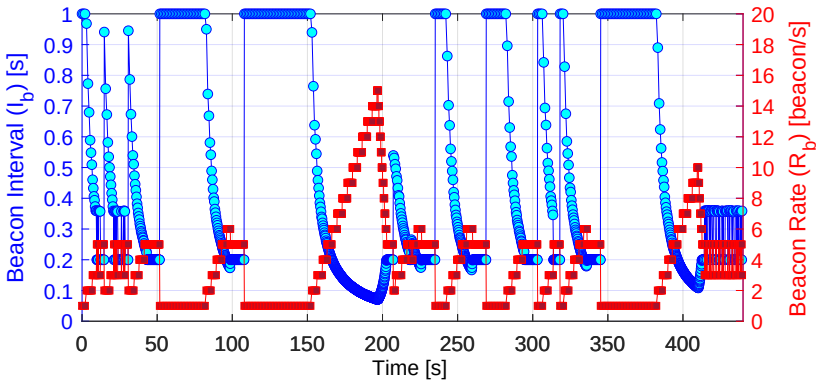

Figure 2.6: Beacon interval and beacon rate computed by the vehicle during 440 s of the simulation time.

deceleration, and repose, which are typical changes of urban environments. Fig. 2.6 shows the adjustments that the DC-BTR imposes, in real-time, on beacon interval (color blue) to meet a target average position error of 1 m (see Fig. 2.7). To gain clarity Fig. 2.6 also shows in color red the beacon transmission rate corresponding to the beacon interval required by DC-BTR. A high correspondence can be observed between Fig. 2.5 and Fig. 2.6. Note that, in the different stages of the accelerated movement, the increase in velocity demands an increase in the beacon transmission rate, ensuring that for high velocity values the beacon interval is shortened to maintain the target position accuracy, as illustrated in the interval from 150 s to 200 s. In this time interval the velocity achieves 28 m/s, demanding 15 beacon/s; whereas in the interval from 380 s to 410 s, the velocity achieves 18 m/s and it is demanding 10 beacon/s. It should be emphasized that the adjustment not only responds to changes in speed, but also to variations of acceleration, as illustrated in the last 30 s. In this time interval, the transmission rate oscillates between 5 and 3 beacon/s. Note also that, when the vehicle is stopped, DC-BTR sets a beacon rate of 1 beacon/s, which is considered the minimum beacon rate. In special cases where the vehicle slows down (see interval from 100 s to 105 s), DC-BTR uses a critical beacon interval equal to 0.2 s, so that neighboring vehicles immediately record any changes in their movement status. Fig. 2.7 demonstrates the effectiveness of DC-BTR for the dynamic control of the beacon transmission rate, restricting the average position error computed by surrounding vehicles to a value that remains most of the time below 1 m. However, packet collisions involve loss of information for the receiv-

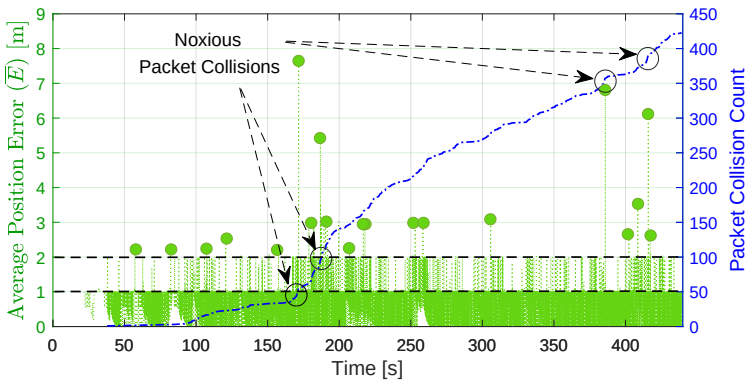

Figure 2.7: Average position error and packet collisions with DC-BTR (20 dBm) and $\rho = 50$ veh/km^2.

ing vehicle, as shown by the blue marks, which increases the difference between the actual position of the transmitter vehicle and the last registered position in the LDM database. It should be noted that the highest occurrence of packet collisions corresponds to the intervals in which the highest beacon transmission rate is required, exceeding 6 m the average position error.

2.3.2 DC-BTP: Simulation Result

This experiment focuses on the performance evaluation of DC-BTP. In this case, all vehicles are using DC-BTP with a fixed beacon rate, to dynamically adjust the transmit power as a function of the relative channel load.

Fig. 2.8 shows the required transmit power as a function of the relative channel load for different beacon transmission rates. Note that the transmit power decreases when the channel load increases. Additionally, low beacon rates lead to high transmit powers, see for instance the blue line corresponding to DC-BTP with 1 beacon/s. On the contrary, high beacon rates lead to low transmit powers, consequently to low warning ranges, as illustrated by the red line corresponding to DC-BTP with 10 beacon/s. Fig. 2.9 compares the probability of successful transmission of DC-BTP (5 beacon/s) with a basic beaconing algorithm set with a fixed transmission rate of 5 beacon/s and a fixed transmit power of 20 dBm, called fixed beaconing algorithm (FB). The power control in DC-BTP (5 beacon/s) achieves a higher successful transmission probability all the time, reducing the impact of hidden nodes. Table 2.2 shows a comparison of the average packet collisions per vehicle as a function of the vehicle density for both DC-BTP and FB algorithms at different beacon rates. Note that high vehicle density leads to more packet collisions as well as the increase of beacon rate. Despite this, the power control in DC-BTP reduces the packet collisions for high channel load (10 beacon/s), being less than 30 % in comparison to the FB algorithm. The best results in terms of packet collisions are related to low beacon rates (1 beacon/s), but these beacon rates lead to high average position error, as shown in Fig. 2.10. However, the small position error achieved by a high beacon transmission rate has a high cost in terms of packet collisions and warning ranges.

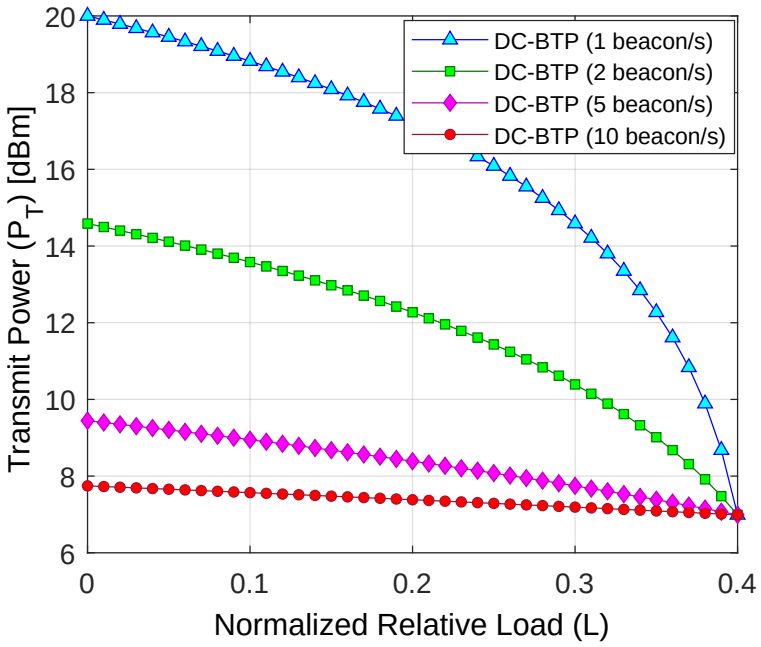

Figure 2.8: Transmit power as a function of the relative load for DC-BTP (1, 2, 5, and 10 beacon/s).

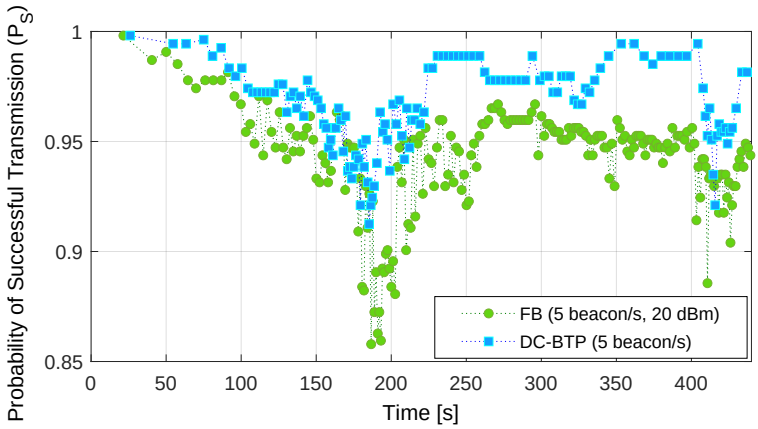

Figure 2.9: Probability of successful transmission for DC-BTP vs FB (20 dBm), with 5 beacon/s and $\rho = 50$ veh/km^2.

2.3.3 DC-BTR&P: Simulation Result

This experiment focuses on the performance evaluation of DC-BTR&P. In this case, all vehicles in the scenario are using DC-BTR&P to dynamically adjust the beacon rate and transmit power in real-time. Previous results have shown that transmitting all the time with low power compromises the warning range, while transmitting with high power leads to high packet collisions rates. Fig. 2.11 shows how DC-BTR&P adjusts the transmit power according to the vehicular traffic dynamics. It should be noted that, when the required beacon transmission rate is low, it is transmitted with high transmit power, which has a low negative impact on the channel load and allows to achieve high warning range (see Fig. 2.6, from 100 s to 150 s). However, when the required beacon transmission rate is high, it is transmitted with low transmit power so as not to increase the channel load (see Fig. 2.6, from

Table 2.2: Average Packet Collisions: FB vs DC-BTP

Beaconing strategy vs ρ [veh/km^2]	Packet collisions 50	70	100
FB (1 beacon/s, 20 dBm)	134	304	407
DC-BTP (1 beacon/s)	184	285	536
FB (2 beacon/s, 20 dBm)	481	752	1558
DC-BTP (2 beacon/s)	228	829	1354
FB (5 beacon/s, 20 dBm)	2027	5928	11094
DC-BTP (5 beacon/s)	**876**	**2531**	**3885**
FB (10 beacon/s, 20 dBm)	8879	21275	38012
DC-BTP (10 beacon/s)	**2162**	**5740**	**10592**

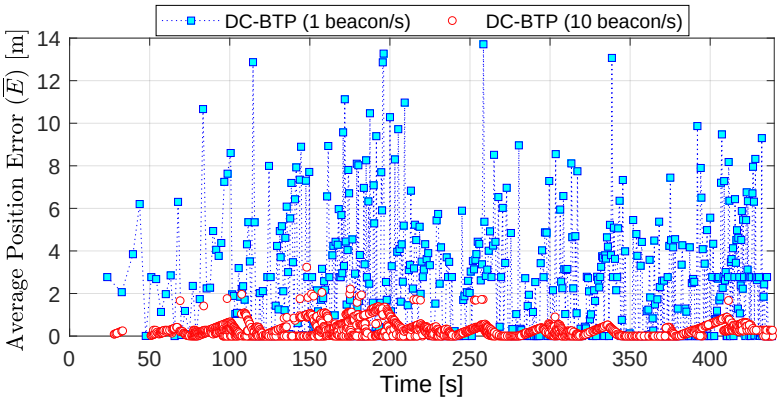

Figure 2.10: Average position error for DC-BTP with 1 beacon/s vs 10 beacon/s, and ρ = 50 veh/km^2.

Table 2.3: Trade-off between Beaconing Algorithms

Beaconing strategy vs ρ [veh/km^2]	$\overline{E} > 1$ m 50	70	100	Packet collisions 50	70	100	Vehicles in LDM 50	70	100
FB (10 beacon/s, 20 dBm)	2081	3065	4442	8879	21275	38012	29	40	56
DC-BTP (10 beacon/s)	431	412	620	2162	5740	10592	7	10	13
DC-BTR (20 dBm)	603	1225	2006	559	1261	2263	34	51	72
DC-BTR&P	**261**	**480**	**868**	**267**	**617**	**1169**	**20**	**31**	**42**

150 s to 200 s). Table 2.3 shows that DC-BTR&P has the best trade-off among the studied beaconing control algorithms in terms of position accuracy, average packet collisions, and warning range. Note that the average number of vehicles registered in the LDM database is directly related to the warning range. DC-BTR&P outperforms FB (10 beacon/s, 20 dBm), DC-BTR and DC-BTP in terms of average packet collisions. Besides, DC-BTR&P outperforms FB (10 beacon/s, 20 dBm) and DC-BTR in terms of position accuracy, being the number of harmful position errors ($\overline{E} > 1$ m) less than 50 %. However, DC-BTR&P has more harmful position errors that DC-BTP for higher vehicle densities, but DC-BTR&P outperforms DC-BTP in terms of average warning range, registering more than three times the average number of vehicles in the LDM database.

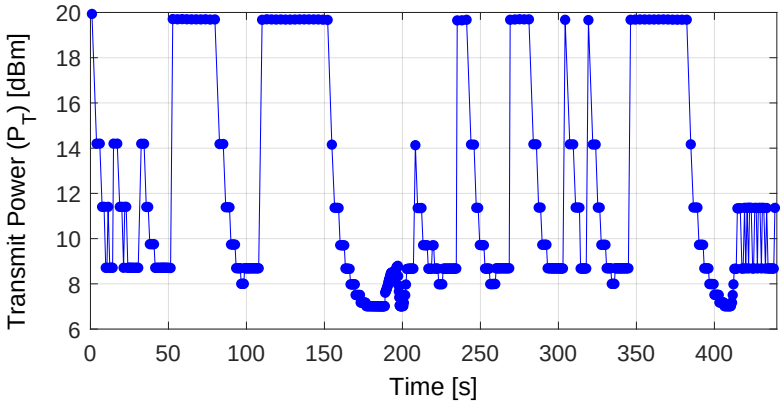

Figure 2.11: Transmit power computed by the vehicle during 440 s of the simulation time.

2.4 Conclusion

In this paper we have proposed the use of a novel joint power/rate control distributed algorithm in cooperative vehicular networks, which dynamically adjusts the beacon rate and transmit power to meet a target position error according to the requirements of cooperative safety applications. The algorithm has the capability to adapt to vehicular traffic dynamics of each scenario and vehicle movement status. The simulation results have shown that the dynamic control of beacon transmission rate limits the average position error, but the use of maximum transmit power leads to an increase of packet collisions. Further, the dynamic control of beacon transmission power decreases the average packet collisions, but the use of a fixed beacon transmission rate is unable to simultaneously achieve a good performance in terms of warning range and position accuracy. However, the joint power/rate control allows to constrain the average position error computed by surrounding vehicles, adjusting opportunistically the communication range to reduce packet collisions. We have shown that DC-BTR&P outperforms other beaconing strategies addressed in this paper, in terms of a trade-off between the main performance metrics.

2.5 Acknowledgements

The authors acknowledge the financial support of CONICYT Doctoral Grant No. 21171722; FONDECYT Postdoctoral Grant No. 3170021; Project ERANET-LAC ELAC2015/T10-0761; as well as Project FONDECYT Iniciación 11140045.

Chapter 3

Dynamic Beaconing using Probability Density Functions in Cooperative Vehicular Networks

Vehicular networks comprise Vehicle-to-Vehicle (V2V) and Vehicle-to-Infrastructure (V2I) communications based on wireless radio access technologies. These networks require the periodic exchange of beacon messages between neighboring vehicles, to support cooperative road safety applications. The regular broadcast of beacon in the common control channel (CCH) using the IEEE 802.11p standard can lead to interference and recurrent packet collisions. This issue impacts negatively on the quality and freshness of the beaconing information, which is essential to detect and mitigate potentially dangerous traffic situations on time. In this paper, we evaluate the performance of a dynamic beaconing strategy where both beacon rate and transmit power are assigned by means of probability density functions (PDFs). The idea is to better understand the benefits and limitations of this approach related to road safety, as well as to know which PDF is more convenient to increase the system's performance according to traffic characteristics of the vehicular scenario. We investigate four types of PDFs, attending to four different performance metrics, in four distinct vehicular scenarios, using the well-established Vehicles in network simulation (Veins) framework. The simulation results show that a beaconing strategy based on uniform PDF is convenient in scenarios with high vehicle density and low relative speed, whereas the normal PDF is suitable in scenarios with high relative speed and low vehicle density.

3.1 Introduction

Vehicular networks include Vehicle-to-Vehicle (V2V) and Vehicle-to-Infrastructure (V2I) communications using the IEEE 802.11-OCB[1] radio access technology in the 5.9 GHz frequency band [7], [8]. Cooperative awareness is the core of several active road safety and traffic efficiency vehicular applications [69]. The main premise is that, knowing the status of neighboring vehicles, the active road safety systems will be able to detect and mitigate

[1]The Outside the Context (OCB) mode allows vehicles that are not members of a Basic Service Set (BSS) to transmit/receive data without preliminary authentication and association.

potentially dangerous traffic situations on time, and successfully coordinate the traffic in certain points or sections of a road. To make neighbors aware of its presence, each vehicle periodically transmits one-hop broadcast messages, called beacons, containing its position, speed, acceleration, and heading [58]. This process, known as beaconing, occurs on the so called control channel (CCH) and allows the receiver vehicles to create a Local Dynamic Map (LDM) based on surrounding environment information, which is essential for the proper performance of cooperative safety applications.

Different beaconing approaches have been proposed in the literature which adapt the beacon transmission parameters to control the channel load or improve cooperative awareness [29]. For instance, the approach proposed by Sepulcre et al. in [36] integrates a congestion and awareness control process. First, the packet transmission rate of each vehicle is configured taking into consideration the minimum required by the application, plus a certain margin. Then, the transmission power is set to the minimum power level needed to ensure the demanded packet reception rate at the application warning distance. On the other hand, the approach proposed by Aygun et al. in [60] adjusts the beacon transmission power in order to reach a desired awareness ratio at the target distance, while controlling the communication channel load by adjusting the beacon transmission rate to keep the current channel busy ratio below a certain threshold. Finally, Kloiber et al. in [34] proposed to mitigate recurring interferences by randomly selecting the transmit power of vehicles while using a fixed beacon transmission rate. Such randomization reduces the chances that a vehicle is found in the common packet collision area from multiple senders.

In this paper, we evaluate the performance of a dynamic beaconing approach where both beacon rate and transmit power are assigned by means of probability density functions (PDFs). The PDFs-based beaconing approach is compared with the algorithm proposed by Kloiber et al. in [34], which also explores the benefits of randomizing the beacon transmission power. The goal is to better understand the benefits and limitations of these approaches related to road safety, as well as to know which PDF is more suitable to increase the system's performance according to traffic characteristics of the vehicular scenario. The main contributions of this paper are the following: ***i)*** to model the beaconing process adjusting both beacon rate and transmit power by means of PDFs; ***ii)*** to evaluate the impact of the PDFs-based beaconing approach on the system's performance, when the same distribution (Constant, Uniform, Normal or Triangular) is used to control the beacon rate and transmit power; ***iii)*** to evaluate the PDFs-based beaconing in four different vehicular scenarios (Spider, Manhattan, Highway, and Urban) using a realistic simulation framework; and ***iv)*** to set a relationship between the use of a certain PDF and the traffic characteristics of the vehicular scenario.

3.2 Dynamic Beaconing using Probability Density Functions

The regular broadcast of beacon messages provides updated information in real-time of the transmitting vehicle status [69]. Through this process, receiving vehicles obtain accurate information of the surrounding environment, being able to avoid accidents on time helping to coordinate the traffic on the road. One of the main issues of the beaconing process is

the high load it can generate on the communication channel. In scenarios with high vehicle density, the beaconing load can lead to channel congestion, increasing significantly packet collisions [59]. As a consequence, the degradation of cooperative awareness due to recurring packet collisions impacts negatively on the system's performance.

The random dynamic beaconing is based on using a certain PDF to set beacon transmission parameters. The vehicles compute the beacon rate and transmit power by means of PDFs over a certain valid range on each beacon transmission. Fig. 3.1 shows the concept of random distribution of beacon transmission rate and power for four different PDFs. In the normal and triangular distributions, the values closer to the mean (5 beacon/s in Fig. 3.1a and 50 mW in Fig. 3.1b) present a higher chance of occurrence. The benefits of randomizing the transmit power are described in [34]. Next, we present the main benefits when both beacon rate and transmit power are assigned randomly.

• **Reduction of recurring packet collisions**: randomize the beacon rate and transmit power by means of symmetric PDFs can significantly decrease recurring interferences. In scenarios with high vehicle density and low relative speed, the periodicity of beacon transmission leads to recurring packet collisions. The random selection of beacon transmission rate decreases the probability that two or more vehicles transmit at the same time, whereas the random selection of beacon transmission power decreases the probability that a vehicle is in the interference area of multiple senders.

• **Local and global fairness**: in vehicular networks, it is commonly desired to achieve local fairness among neighboring vehicles in their contribution to cooperative awareness, and to achieve overall fairness among all the vehicles of the network in their contribution to communication channel load. PDFs harmonize the access to channel resources, and guarantee equity in the selection of beacon rate and transmit power of vehicles. For example, vehicles that broadcast beacons with a higher transmission rate will have greater use of the communication channel resources, and vehicles that transmit with a high power negatively affect

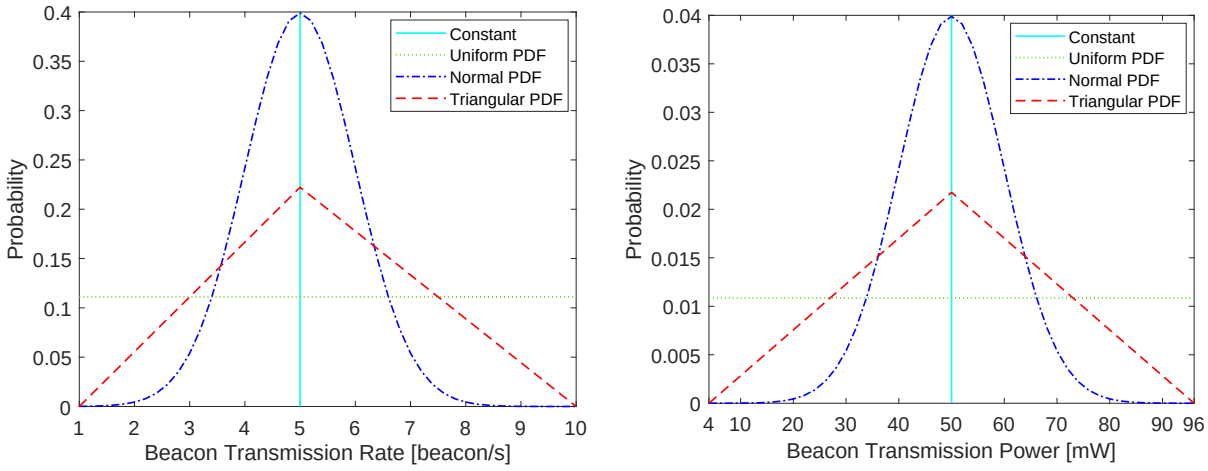

(a) (b)

Figure 3.1: Representation of the probability density functions for the random assignment of: (a) Beacon rate and (b) Transmit power.

vehicles that transmit with a lower energy level. However, the random selection of beacon transmission parameters avoids such unfairness, for an extended period of time, providing local and global fairness.

• **Implicit congestion control**: the random selection of beacon transmission parameters implicitly controls the communication channel congestion, because vehicles use on average the mean value of beacon rate and transmit power of the target PDF. For example, if a vehicle transmits constantly with the maximum beacon transmission rate and power, it will generate the highest possible beaconing load and reach the pre-established maximum communication range. However, with the random selection of beacon transmission parameters considering a uniform PDF over the valid range, the effective beacon transmission rate and power are reduced to the mean value of the PDF. Even so, the minimum beacon inter-reception time and the maximum communication range can still be achieved.

• **Quality of cooperative awareness**: adjusting the parameters of the PDFs (mean and variance), the quality of cooperative awareness can be adapted dynamically according to communication requirements of different applications or vehicular context. For example, the mean can be established to meet a certain target beacon transmission rate and power, and by adapting the variance it is possible to control the way in which selected values are distributed around the mean. Further, it is possible to adapt the limits of the valid range of the PDF according to the vehicle speed or vehicular density in order to improve cooperative awareness.

3.3 Simulation Setup

The experiments have been conducted using the Veins[2] framework [70], which couples the OMNeT++ network simulator and the SUMO road traffic simulator.

3.3.1 Simulation Scenarios

The performance of the dynamic beaconing approach based on PDFs has been evaluated in four different scenarios, as shown in Fig. 3.2.

Spider 8x6x100m: it consists of 8 axes, which have a length of 600 m and converge in the center of the scenario, and by 6 regular octagons all spaced at a distance of 100 m (see Fig. 3.2a). Each road has two lanes in opposite directions and intersections are managed by priority. The speed limit for each street is 70 km/h and the surface has an approximate area of 1 km^2. In this scenario, a traffic flow of 30 vehicles was defined for each principal axis. Therefore, there are eight vehicle flows that move from one end to the other of the axes of the outer octagon at a simulation time of 220 s.

Manhattan 7x7: it has 8 horizontal and vertical roads, with a separation between streets of 100 m. The layout of the roads defines a total of 49 blocks, which have an approximate area of 0.5 km^2 (see Fig. 3.2b). The intersections are managed by priority, while each road has a speed limit of 70 km/h and two lanes in opposite directions. In this scenario were

[2]Vehicles in network simulation - http://veins.car2x.org/

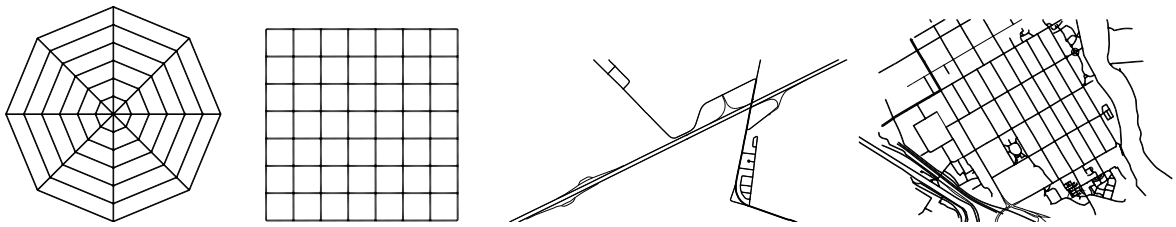

Figure 3.2: Scenarios seen from SUMO road traffic simulator: (a) Spider 8x6x100m, (b) Manhattan 7x7, (c) Highway - Montreal, and (d) Urban - Ottawa.

defined 8 traffic flows of 30 vehicles each. The flows move through the four central roads located vertically; four traffic flows from the top to the bottom and the four remaining from the bottom to the top. Therefore, the target roads have two vehicle flows that are moving in the opposite direction, in a simulation time of 220 s.

Highway: defined by a real map portion of Montreal city with an area close to 5.1 km^2 (see Fig. 3.2c). The zone has two main roads, in the opposite direction with a length of 3.4 km. Each road has two lanes in the same direction and a maximum speed limit of 100 km/h. Two traffic flows of 150 vehicles were defined, one by each main road. Therefore, we have two vehicle flows that are moving on parallel roads, one to meet the other, intersect and move away again, in a simulation time of 500 s.

Urban: defined by a real map portion of Ottawa city with an area close to 1 km^2 (see Fig. 3.2d). The zone has two traffic lights and roads with speed limits of 60 km/h and 100 km/h. Two traffic flows of 30 vehicles were defined, which move along one of the main roads but in opposite directions. The flows intersect in one of the traffic lights so, during the time that takes the change of light, vehicles remain clustered. Then, the groups are dispersed, moving away to reach the final destination of the route, in a simulation time of 220 s.

3.3.2 Simulation Parameters

The vehicles use the IEEE 802.11p model [67] of the Veins framework to represent the physical (PHY) and medium access control (MAC) layers. This is an open-source model, which fully captures the distinctive properties of the IEEE 802.11p radio access technology. The vehicles broadcast beacon messages to the communication channel setting the beacon rate and transmission power by means of PDFs. We define the parameters of the PDFs according to the standards [7], [58], as shown in Table 3.1. The dynamic beaconing process uses the same PDF to adjust both the beacon rate and transmit power on each beacon transmission. We also use the beaconing approach proposed by Kloiber et al. in [34] as a baseline for the evaluation. The parameters of the two implemented variants of Kloiber's approach are shown in Table 3.2. The radio signal propagation is modeled with the Two-Ray Interference model [68], using $\epsilon_r = 1.02$. This model has been validated based on an extensive set of measurements on the road, improving the accuracy of the simulation of radio transmissions, especially at short and medium distances. The communications are established on the CCH without considering the effect caused by the multi-channel operation. The beacon messages have 250 bytes [36] and are transmitted with a priority corresponding to the voice access

Table 3.1: Parameters of the Probability Density Functions

PDF	**Value**
Constant	5 beacon/s, 50 mW [7], [58]
Uniform	a = 1 beacon/s, 4 mW [7], [58] b = 10 beacon/s, 96 mW [7], [58]
Normal	mean = 5 beacon/s, 50 mW [7], [58] variance = 1 beacon/s, 10 mW [7], [58]
Triangular	a = 1 beacon/s, 4 mW [7], [58] b = 5 beacon/s, 50 mW [7], [58] c = 10 beacon/s, 96 mW [7], [58]

Table 3.2: Parameters of the Kloiber's Approach

Approach	**Value**
Kloiber - var1 [34]	10 beacon/s, uniform (4 mW - 96 mW)
Kloiber - var2 [34]	2 beacon/s, uniform (4 mW - 96 mW)

Table 3.3: Simulation Parameters

Parameter	**Value**
CCH Frequency	5.89 GHz [7]
CCH Bandwidth	10 MHz [7]
Beacon Size	250 bytes [36]
Access Category (AC)	AC_VO [67]
Receiver Sensitivity	-82 dBm [8]
Thermal Noise	-110 dBm
Modulation	QPSK [8]
Coding Rate	1/2 [8]
Data-Rate (R_D)	6 Mbps [8]
Antenna Gain	0 dB
Antenna Height	1.5 m
Propagation Model	Two-Ray Interference [68]

category (AC_VO) [67]. Each vehicle is 5 m long, 2 m wide and has a maximum acceleration of 0.8 m/s^2, and deceleration up to 4.5 m/s^2. The antenna height is 1.5 m and data-rate is 6 Mbps [8]. The most important simulation parameters are given in Table 3.3.

3.3.3 Performance Metrics

We use Monte-Carlo simulations and four performance metrics to evaluate the cooperative awareness provided by the PDFs-based beaconing approach.

• **Average packet collisions**: number of packet collisions that, on average, is perceived by each vehicle.

• **Average hidden nodes**: number of nodes that, on average, are hidden from each vehicle.

• **Average vehicles in LDM**: number of surrounding nodes that, on average, each vehicle registers in its LDM database.

• **Average position error**: average position error computed by a receiving vehicle in real-time due to the movement of a surrounding node during the beacon interval.

3.4 Results and Discussion

Fig. 3.3 and Fig. 3.4 show the histogram of the beacon rate and transmit power used by a generic vehicle. In the uniform distribution, the values of the valid interval (1 beacon/s to 10 beacon/s in Fig. 3.3b and 4 mW to 96 mW in Fig. 3.4b) have the same chances of occurrence. The result is a fair dynamic assignment of the possible values of beacon rate and transmission power. Unlike uniform distribution, on the normal PDF, see Fig. 3.3c (mean 5 beacon/s and variance 1 beacon/s) and Fig. 3.4c (average 50 mW and variance 10 mW), the values clustered to one and two variance of the mean have approximately 95 % and 65 % chance of being selected, respectively. This causes that the random values of beacon rate and transmission power with more chance of occurrence to be clustered on both sides of the mean, and the values that remain at the ends of the valid interval occur with very low frequency (only a 5 % of probability). In the triangular distribution, see Fig. 3.3d (mean 5 beacon/s) and Fig. 3.4d (mean 50 mW), the values with higher probability are still around the mean. However, these values occur with less probability than in normal distribution. On the other hand, the values that remain at the ends of the valid interval have more chance of occurrence than in the normal distribution.

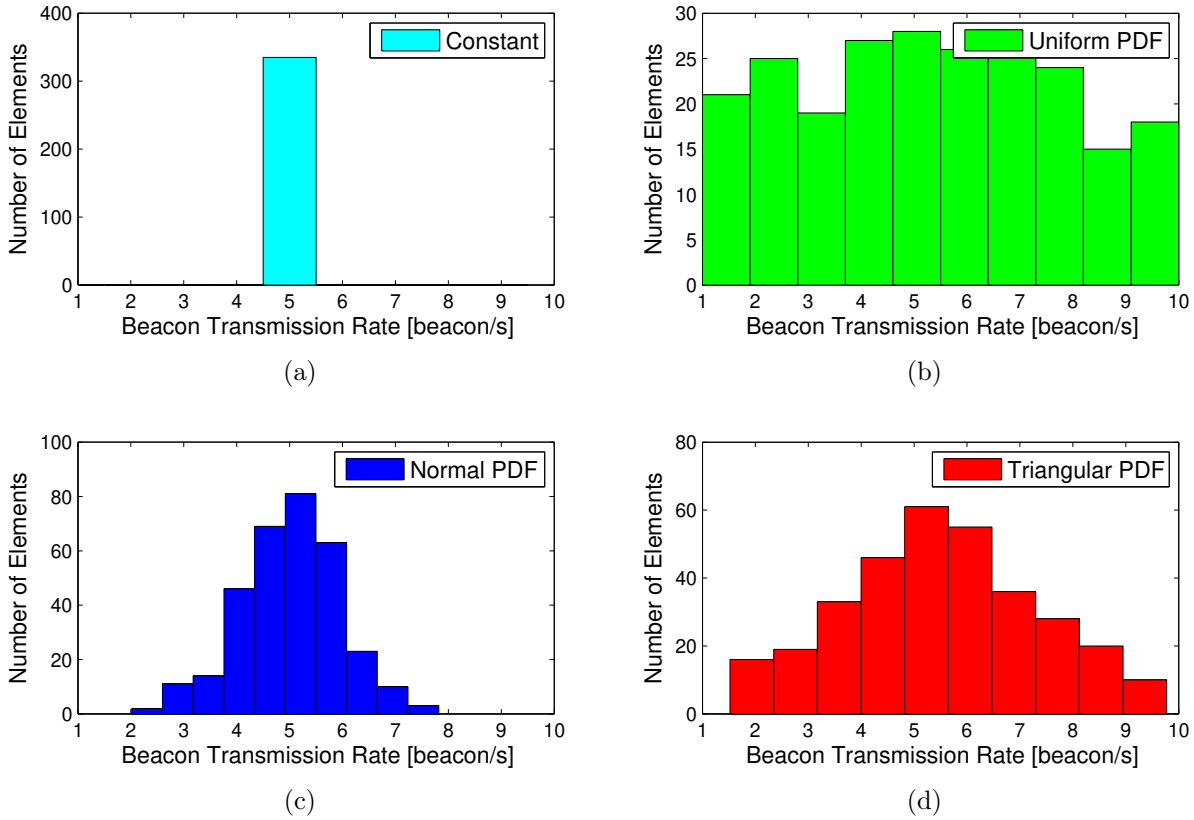

Figure 3.3: Distribution of the beacon rate used by a generic vehicle: (a) Constant, (b) Uniform, (c) Normal, and (d) Triangular.

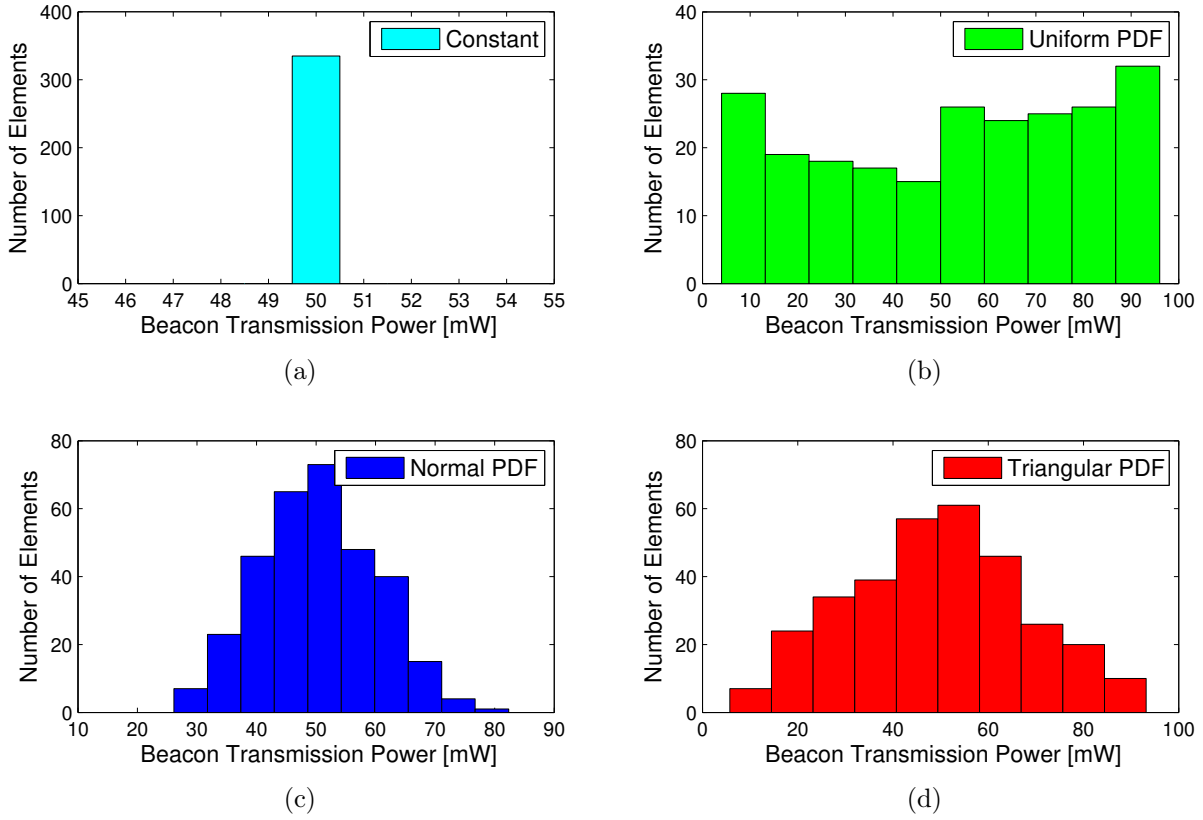

Figure 3.4: Distribution of the transmission power used by a generic vehicle: (a) Constant, (b) Uniform, (c) Normal, and (d) Triangular.

Fig. 3.5 shows the performance of the PDFs-based beaconing approaches on the different scenarios. We also include the two variants of Kloiber's approach (see Table 3.2). Fig. 3.5a illustrates that the Kloiber - var1 beaconing approach leads to the highest number of average packet collisions in all scenarios, followed by the beaconing approach with constant transmission parameters. This is because the Kloiber - var1 beaconing approach uses a high beacon rate (10 beacon/s), which increases the channel load and recurring packet collisions, especially in scenarios with high vehicle densities. The uniform distribution shows the benefits of randomizing the beacon transmission rate compared to the Kloiber - var1 beaconing approach. Note that in all scenarios, the uniform distribution achieves a number of average packet collisions similar to obtained by the Kloiber - var2 approach, despite this Kloiber variant uses a fixed transmission rate of 2 beacon/s. Accordingly, the uniform distribution of transmission parameters in the valid range reduces recurring interferences. Randomizing the beacon transmission rate reduces the probability that two vehicles transmit at the same time while randomizing the transmission power reduces the probability that a vehicle is in the interference area of multiple senders. On the other hand, the normal and triangular distributions achieve similar performances on the different scenarios. However, as expected, the triangular distribution computes a lower number of packet collisions (see Fig. 3.5a) and registers more vehicles in the LDM database (see Fig. 3.5c) than the normal distribution, but computes a greater number of hidden terminals (see Fig. 3.5b). Finally, dynamic beaconing based on PDFs as well as Kloiber's variants computes a similar number of vehicles in LDM

and hidden nodes for the Grid, Highway, and Urban scenario, as shown in Fig. 3.5b and Fig. 3.5c.

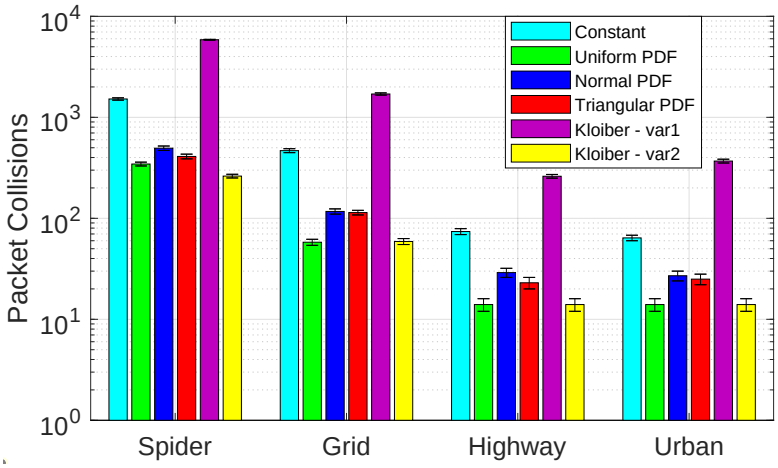

(a)

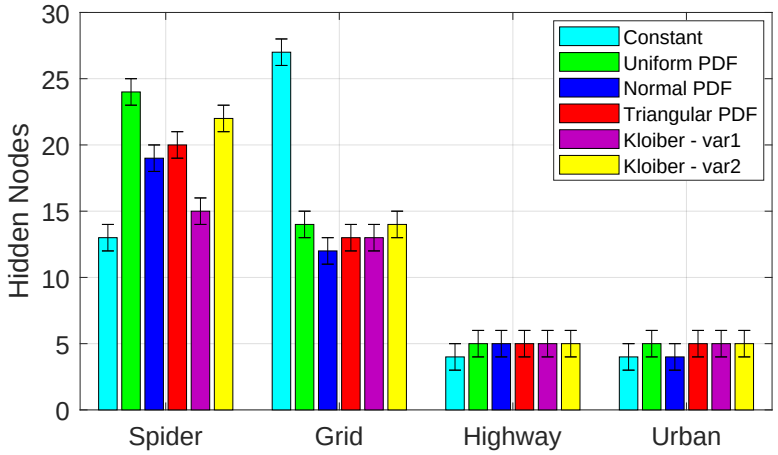

(b)

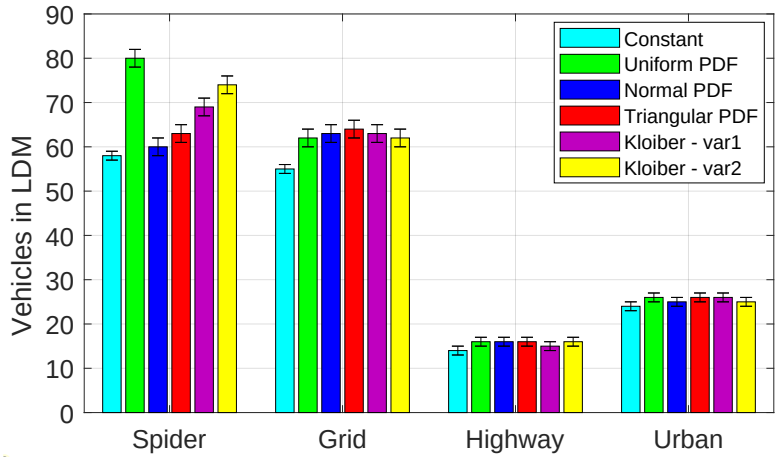

(c)

Figure 3.5: Performance of the PDFs-based beaconing approaches on the different scenarios: (a) Packet collisions, (b) Hidden nodes, and (c) Vehicles in LDM.

Fig. 3.6 and Fig. 3.7 illustrate the cumulative probability of the average position error computed by a generic vehicle when its neighbors use the dynamic beaconing based on PDFs, in the Highway and Urban scenarios, respectively. On the other hand, Fig. 3.8a and Fig. 3.8b show the same situation when the surrounding vehicles use the Kloiber's approach. As can be observed in Fig. 3.6a, the beaconing approach with constant transmission parameters produces an average position error less than 3 m most of the time in the Highway scenario. However, the high number of packet collisions (see Fig. 3.5a) leads to peak values of average position error that can exceed 5 m and 10 m. This means that at high vehicular densities more vehicles will be affected by error peaks due to recurrent packet collisions. This behavior is similar in the Urban scenario (see Fig. 3.7a), where the average position error is close to 1.5 m due to the low speed of vehicles, but exceeding 4 m due to recurrent packet collisions. The good performance of the uniform distribution in the previous metrics is degraded in terms of average position error for both scenarios (see Fig. 3.6b and Fig. 3.7b). Using low beacon rates when vehicles move at high speeds leads to a greater average position error. In contrast, dynamic beaconing with the normal distribution experiences a lower number of harmful position errors than those obtained with the uniform and triangular distributions in both scenarios. Fig. 3.6 shows that the normal distribution outperforms the uniform

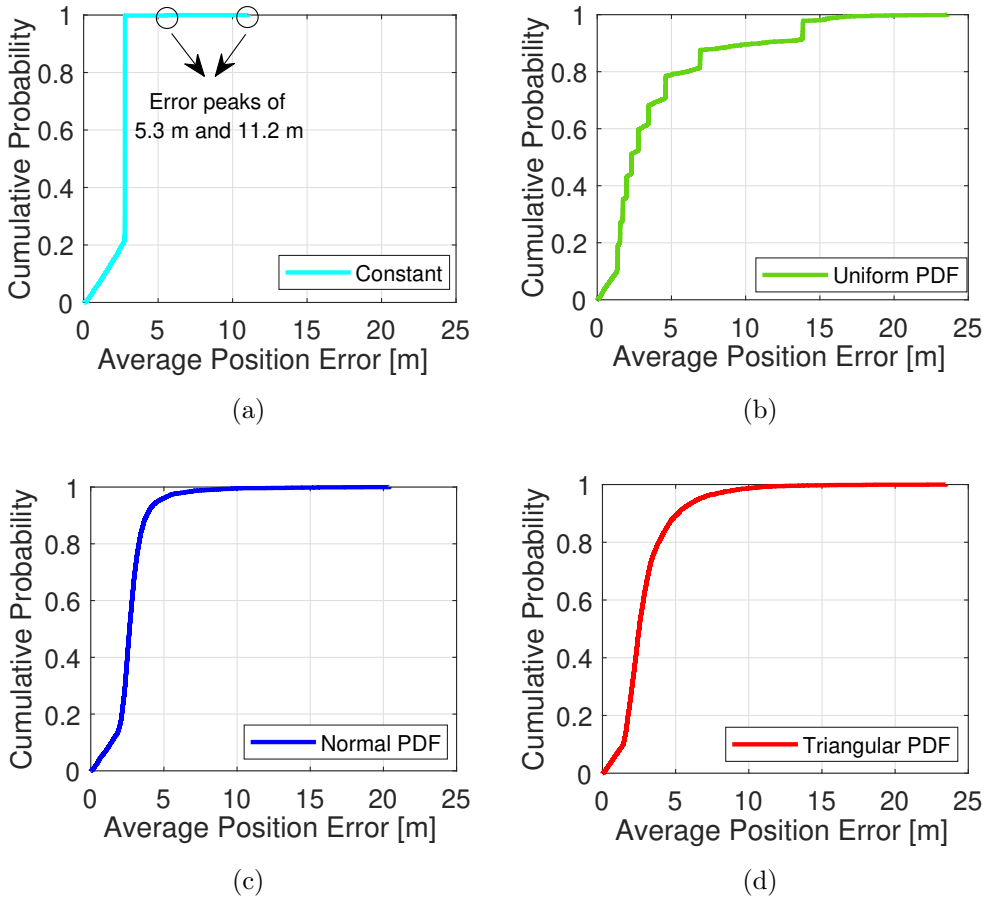

Figure 3.6: Cumulative probability of the average position error computed by a generic vehicle during 70 s in the Highway scenario: (a) Constant, (b) Uniform, (c) Normal, and (d) Triangular.

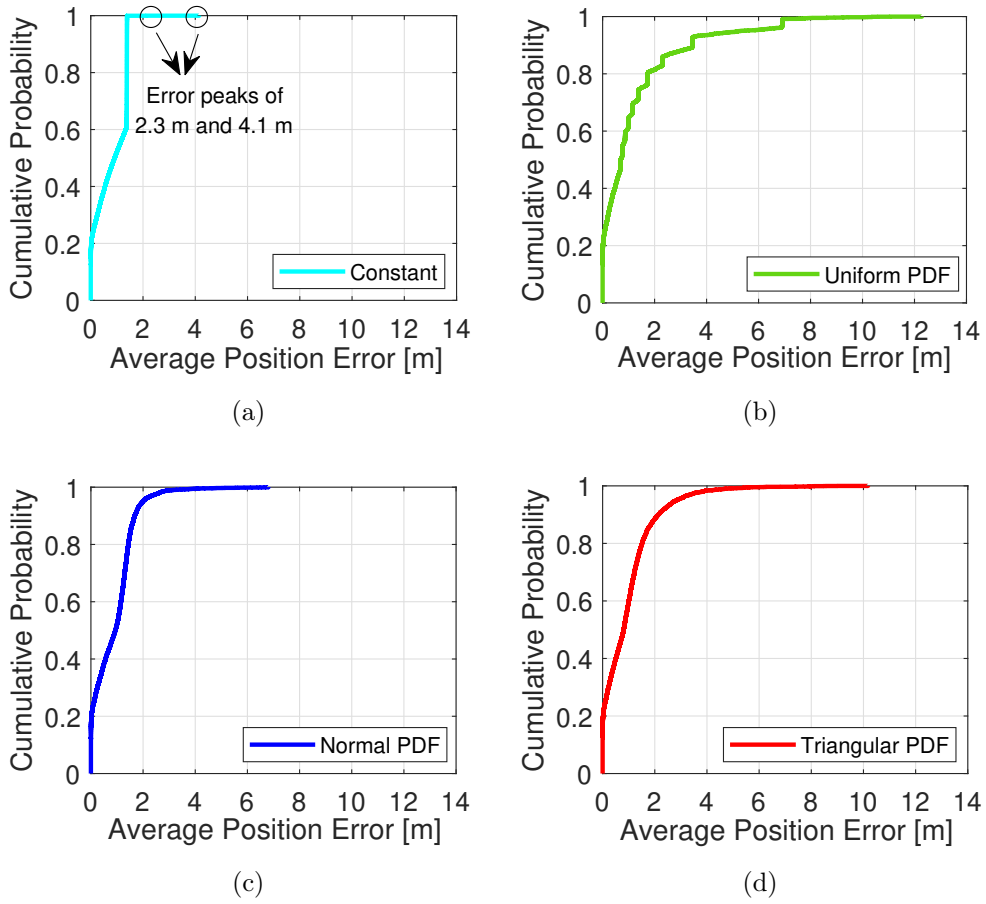

Figure 3.7: Cumulative probability of the average position error computed by a generic vehicle during 60 s in the Urban scenario: (a) Constant, (b) Uniform, (c) Normal, and (d) Triangular.

and triangular distribution in terms of average position error and the number of times that this position error exceeds 5 m. In the urban scenario (see Fig. 3.7), the same behavior is observed, with the normal distribution the maximum average position error does not exceed 7 m and the highest number of average position errors is concentrated below 3 m. It could be thought that the use of a fixed transmission rate of 10 beacon/s in the Kloiber - var1 approach would lead to a small average position error. However, it leads to several harmful peaks of average position error due to the noxious impact of packet collisions, as can be observed in Fig. 3.8. In the Highway and Urban scenario, recurring packet collisions lead to a maximum average position error of 19 m and 9.7 m, respectively. The Kloiber - var2 approach computes a low number of packet collisions (see Fig. 3.5a). However, the use of a low transmission rate (2 beacon/s) leads to a high average position error (see Fig. 3.8), especially in the Highway scenario where error peaks exceed 25 m, as can be observed in Fig. 3.8a.

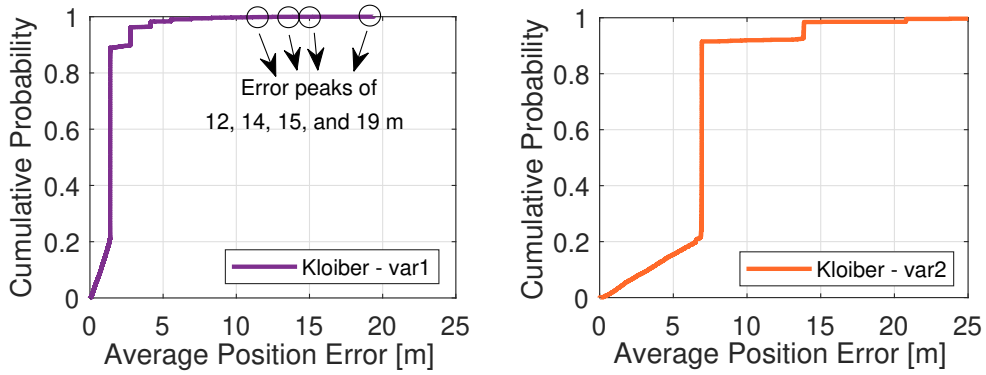

(a)

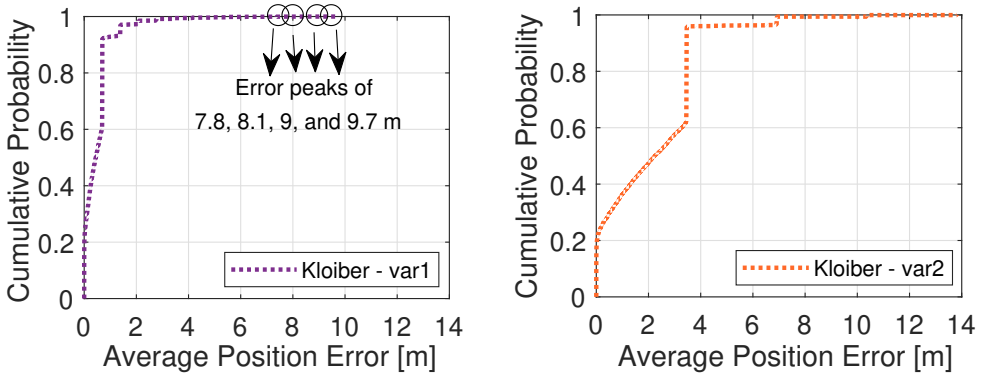

(b)

Figure 3.8: Cumulative probability of the average position error computed by a generic vehicle using the Kloiber's approach in: (a) Highway and (b) Urban.

3.5 Conclusion

In this paper, we evaluated the performance of different dynamic beaconing approaches that use PDFs to randomize beacon transmission parameters. The performance of the beaconing approaches was evaluated through a realistic simulation framework in four different vehicular scenarios. The simulation results showed that some PDFs are more convenient than others for certain scenarios. The uniform PDF is convenient in scenarios with a high vehicle density and low relative speed, whereas the normal PDF is suitable in scenarios with a high relative speed and low vehicle density. The uniform distribution allows reducing interferences while the low speed of the vehicles does not significantly affect the average position error computed by neighboring vehicles. On the other hand, by adjusting the mean of the normal distribution it is possible to reduce the average position error perceived in high-speed scenarios, while the low density of vehicles reduces the noxious impact of packet collisions. In future works, we intend to develop an adaptive beaconing algorithm, where PDFs are selected and adjusted, according to vehicular context to simultaneously provide the communication requirements of cooperative safety applications.

3.6 Acknowledgements

The authors acknowledge the financial support of CONICYT Doctoral Grant No. 21171722; Project ERANET-LAC ELAC2015/T10-0761; FONDECYT Postdoctoral Grant No. 3170021; as well as FONDECYT Iniciación 11140045.

Chapter 4

POSACC: Position-Accuracy based Adaptive Beaconing Algorithm for Cooperative Vehicular Safety Systems

Cooperative vehicular safety systems are expected to revolutionize the driving experience by providing road safety applications based on incident detection. Two vital quality parameters for cooperative safety applications are the position accuracy and communication reliability of the status information. The receiver may take erroneous decisions if the received data does not correspond to the latest situation of the transmitter (e.g., position, velocity, and trajectory of the target vehicle). In this paper, we propose and evaluate a POSition-ACCuracy (POSACC) based adaptive beaconing algorithm for cooperative vehicular safety systems. POSACC integrates three different control mechanisms to guarantee specific performance metrics. It adopts position accuracy and communication reliability as the highest priority metrics, due to their direct impact on the vehicle's systems capability to avoid potential traffic accidents in real-time. In addition, it guarantees the priority metrics, maintaining the vehicle's warning distance, channel load, and end-to-end latency into the operative range of cooperative safety applications. POSACC is compared with three different state-of-the-art adaptive beaconing algorithms; ETSI DMG, LIMERIC, and DC-BTR&P. Extensive evaluation results show that POSACC successfully controls the beacon rate, transmission power, and the size of the minimum contention window. Simulation results also demonstrate that POSACC is more effective than the benchmark algorithms by guaranteeing the operational requirements of cooperative safety applications in a wider range of traffic situations.

4.1 Introduction

Cooperative vehicular safety systems are being designed to provide accident-free and efficient road systems [71]. The new paradigm relies on equipping the vehicle with wireless communication devices to increase its perception about the surrounding environment. Cooperative safety applications aim to detect potential crashes on the road and to notify vehicles in advance. The communication on these systems relies on the IEEE 802.11p [7] radio access technology in the 5.9 GHz frequency band, which specifies the medium-access-control (MAC)

and physical (PHY) layers of Wireless Access in Vehicular Environments (WAVE) [9]. The IEEE 802.11p MAC layer is based on the Carrier Sense Multiple Access with Collision Avoidance (CSMA/CA) protocol and includes the Outside of the Context of a Basic Service Set (OCB) operation mode recently defined in [8]. The IEEE 802.11p PHY layer is based on the IEEE 802.11a standard, but it uses channels of 10 MHz to reduce the negative impact of multipath delay spread and Doppler effect [72].

Cooperative vehicular safety systems rely on the continuous exchange of status information between neighboring vehicles on a common control channel (CCH). To make neighbors aware of its presence, each vehicle regularly transmits one-hop broadcast messages, called beacons. The beacons are formally known as Basic Safety Messages (BSM) [10] in the US or Cooperative Awareness Messages (CAM) [11] in Europe. These messages include information about the status of the transmitting vehicle; such as its position, speed, acceleration, and heading. The beaconing process allows the receiving vehicle to create a Local Dynamic Map (LDM) based on the status information of its neighborhood [11]. The status information is used by cooperative safety applications to detect and mitigate potential crashes in real-time (e.g., the crash risk can be estimated by analyzing the movement status of vehicles) [11].

Finding the appropriate beacon transmission rate for each vehicular scenario is essential for the proper performance of cooperative safety applications. The beacon transmission rate is directly related to the position accuracy perceived by neighboring vehicles [22]. In realistic scenarios, some vehicles could have high dynamics (high speed and acceleration), whereas other vehicles could have low dynamics (low speed and acceleration). This may lead to differences in position accuracy since position error depends on beacon rate and vehicle dynamics. In traffic jams, a beacon transmission rate of 1 beacon/s could be enough to provide the position accuracy needed for most safety-related applications. However, this beacon rate is not enough to achieve the required level of position accuracy on a multi-lane high-speed highway with frequent lane changes. The technical report of the Vehicle Safety Communications Consortium (VSCC) [14] specifies that 10 beacon/s is the minimum beacon rate required to meet the position accuracy of several safety-related applications, while some safety-critical applications can demand a beacon rate up to 50 beacon/s.

The operational requirements of cooperative safety applications can be defined mainly in terms of position accuracy, communication reliability, and end-to-end latency [12], [13]. The European Telecommunication Standards Institute (ETSI) has specified in the technical specification ETSI TS 101 539-3 [12] that cooperative safety-critical applications, such as Longitudinal Collision Risk Warning (LCRW) (e.g., safety-relevant lane change and safety-relevant vehicle overtaking), demand a position accuracy equal or less than 1 m with a confidence level of 95 %, a communication range of 300 m in a line of sight situation and when the channel load is at a relaxed state, and an end-to-end latency equal or less than 300 ms. Similarly, cooperative safety-critical applications, such as Intersection Collision Risk Warning (ICRW) (e.g., turning collision risk warning and merging collision risk warning) defined by ETSI in ETSI TS 101 539-2 [13], require a position accuracy equal or better than 2 m with a confidence level of 95 %, a communication range of 300 m in a line of sight situation and when the channel load is at a relaxed state, and an end-to-end latency equal or less than 300 ms. ETSI also specifies in [12], [13] that the required communication range may be reduced in certain situations (e.g., in congested channel situations).

Congestion and awareness control approaches have been proposed in the literature [28], [29] to provide reliable and efficient vehicular communications. However, both approaches have drawbacks in terms of road safety. Congestion control approaches [30]-[33] aim at keeping the channel load below a certain target threshold and to achieve local/global fairness. However, these approaches usually do not consider the operational requirements of safety-related applications or vehicle dynamics. In contrast, awareness control approaches [11], [35]-[38] can consider road safety or vehicle dynamics, but they usually are not designed to simultaneously satisfy the operational requirements of cooperative safety applications. Furthermore, channel busy ratio (CBR) is generally used as a priority metric; however other critical metrics directly related to road safety, such as position error, packet collision rate, packet delivery ratio (PDR), and end-to-end latency are not considered.

4.1.1 Challenges of Beaconing Approaches

A high beacon rate is desirable from the viewpoint of providing fresh information and ensuring that vehicles have high levels of awareness [37]. However, a high beacon rate also could lead to a congested channel, especially, in scenarios with a high vehicular density. Channel congestion leads to a degradation of communication reliability caused by packet collisions [73]. Even if the channel is not congested, a high beacon transmission rate can still cause severe interference due to the hidden terminal problem and the CSMA/CA Distributed Coordination Function (DCF) procedure of IEEE 802.11p [41]. Simultaneously, packet collisions have a negative impact on position accuracy. This underlying trade-off also applies to the beacon transmission power [42]. A high beacon transmission power increases the probability of successful reception of a single transmission, but at the same time increases the probability of packet collisions for all transmissions.

A contradictory behavior is also observed regarding the size of the minimum contention window used by the backoff algorithm in IEEE 802.11p. Beacons are usually transmitted with the highest priority access category [29]. Due to the short temporal validity of beacons, the size of the minimum contention window used by the backoff algorithm in IEEE 802.11p is often kept small. However, reducing the size of the minimum contention window increases the probability of packet collisions in broadcast communications where no exponential backoff is considered [26]. The probability of packet collisions can be reduced by increasing the size of the minimum contention window; but, it has a negative effect on end-to-end latency.

Meeting the operational requirements of cooperative safety applications is a very challenging task. The responsibility for meeting the requirements of a specific performance metric in the worst-case scenario (more demanding applications) can lead to not meeting the requirements of these and other applications in other metrics. In this context, we propose a novel POSition-ACCuracy (POSACC) based adaptive beaconing algorithm for cooperative vehicular safety systems. It aims to satisfy the operational requirements of cooperative safety applications. POSACC is compared with relevant state-of-the-art beaconing algorithms via a realistic simulation framework and considering performance metrics directly related to road safety.

The contribution of this paper is threefold:

1. We adopt the position accuracy and communication reliability as the highest priority metrics due to their direct impact on the decision-making process, in real-time, of cooperative safety applications. We establish a design strategy that reduces the conflict between the required goals. The strategy focuses on providing the position accuracy and communication reliability required by cooperative safety applications, maintaining the vehicle's warning distance, channel load, and end-to-end latency into the operative range of cooperative safety applications.
2. We design three different control mechanisms to guarantee specific performance metrics. We design a beacon rate control mechanism that adapts the beacon rate depending on vehicle movement status to achieve the desired position accuracy. In addition, we design a transmission power control mechanism that computes the vehicle's transmission power depending on its movement status to maximize the probability of successful reception of beacon messages at the target warning distance. Finally, we design a control mechanism that computes the size of the minimum contention window depending on the maximum reported size of the LDM database in order to minimize the probability of packet collisions.
3. We propose an adaptive beaconing algorithm, called POSACC, to simultaneously guarantee the operational requirements of cooperative safety applications. Extensive evaluation results show that POSACC successfully controls the beacon rate, transmission power, and the size of the minimum contention window. Simulation results also demonstrate that POSACC is more effective than three state-of-the art algorithms: ETSI DMG [11], LIMERIC [31], and DC-BTR&P [43], by adapting to the vehicle dynamics as well as guaranteeing the operational requirements of cooperative safety applications in a wider range of traffic situations.

4.2 Related Work

In the ETSI EN 302 663 standard [74], ETSI has defined a 10 MHz common control channel for vehicular communications at 5.9 GHz, known as the ITS-G5 radio channel. To enable cooperative awareness within ITS-G5, ETSI also has delivered the standard ETSI EN 302 637-2 [11] specifying the rules for the exchange of CAMs. The cooperative awareness basic service is mandatory for all nodes operating in ITS-G5. In this service, vehicles regularly broadcast their status data by using the CSMA/CA protocol with no acknowledgments or retransmissions. One key problem of the beaconing activity is the channel congestion that can arise due to the aggregated load. In this context, ETSI has defined the Cross-Layer Decentralized Congestion Control (DCC) Management Entity to avoid overloading the ITS-G5 radio channel [75]. Channel congestion can limit the transmission of event-driven messages, such as the Decentralized Environmental Notification Messages (DENMs) defined by ETSI in ETSI EN 302 637-3 [76]. Channel congestion can also negatively affect the proper performance of cooperative safety applications. In the following, we overview some congestion and awareness control approaches.

Some examples of congestion control approaches available in the literature are PULSAR [30], LIMERIC [31], FABRIC [32], and DCC [33]. Two of the most important current

congestion control approaches are PULSAR [30] and LIMERIC [31]. Both approaches adapt the beacon rate based on the channel load and set the transmission power to a fixed value. PULSAR relies on a binary rate control using the Additive Increase Multiplicative Decrease (AIMD) technique. To fulfill the global fairness design principle, vehicles share two-hop CBR information. In LIMERIC, the underlying function linearly controls the beacon rate of each vehicle according to local CBR measurements. LIMERIC converges to a fair and efficient channel utilization in deterministic environments. To ensure the convergence in very dense scenarios, it uses an effective gain saturation technique. PULSAR and LIMERIC are able to maintain the channel load below a certain target threshold independently of the vehicular traffic density. In LIMERIC, noisy CBR measurements produce unfairness in rate allocations, see [77].

FABRIC [32] is based on a network utility maximization problem. In FABRIC, the beacon rate of each vehicle in the one-hop neighborhood is recursively optimized. To enable this, it is proposed that all vehicles share their beacon rates. The main drawback of FABRIC is controlling the speed of convergence in practical scenarios [37]. ETSI has also specified a set of DCC mechanisms [33] that adapt the beacon transmission parameters to keep the channel load below a target threshold. All the mechanisms rely on a state machine that distinguishes three states: *relaxed*, *active*, and *restrictive*, in increasing order of channel congestion. State transitions are driven by the channel load conditions locally measured by each node during a sampling interval. DCC is naturally oscillatory, which implies unstable state transitions [20].

Several awareness control approaches exist in the literature. For example, the awareness control approach proposed by ETSI is the dynamic message generation mechanism [11], which we call here ETSI DMG. It adapts the beacon rate depending on the changes in position, velocity, and heading of the transmitting vehicle. This approach aims to limit the position error perceived by neighboring vehicles while implicitly controls the channel load. ETSI DMG has a synchronization problem for cooperative maneuvers that degrades its performance [78]. It also suffers from a divergence effect that leads to oscillations in the beacon rate [40]. IVTRC [35] is an awareness control approach that also considers the position accuracy as a design goal. It controls the beacon rate depending on differences from position predictions. However, beaconing based on position prediction has serious drawbacks for road safety, as specified in [15]. Further, in situations where the channel load increases, IVTRC reduces the beacon transmission rate of vehicles at the cost of decreasing the position accuracy.

Other awareness control approaches available in the literature are INTERN [36], NORAC [37], TTCC [38], and DC-BTR&P [43]. INTERN [36] assigns the beacon transmission rates required by the applications, and then equitably shares the excess capacity. It also controls the transmission power to generate certain level of awareness. NORAC [37] is a rate and awareness distributed control approach based on non-cooperative game theory. The underlying congestion control mechanism limits the bandwidth usage of each vehicle and reduces the beaconing rate in congested situations. NORAC assigns a beacon transmission rate to each vehicle proportional to its requirements while ensuring fairness between vehicles with the same requirement. Similarly, TTCC [38] aims to satisfy the constraints on channel availability, whereas the safety of the surrounding traffic situation is captured with a time-to-collision metric. TTCC increases the beacon transmission rate of the vehicles involved in more dangerous situations, so it yields higher rates and better usage of channel capacity.

DC-BTR&P [43] is an awareness control approach designed to satisfy the position accuracy requirements of cooperative safety applications. This approach is based on the dynamic control of the beacon rate and transmission power. The underlying control mechanisms limit the position error perceived by neighboring vehicles and reduce packet collisions. However, such benefits are achieved at the cost of decreasing the communication range of vehicles with higher dynamics. This issue is critical for road safety because drivers need to be notified at a sufficient distance from the expected impact to initiate a maneuver, as defined by ETSI technical specifications [12], [13].

4.2.1 Limitations related to Road Safety

The primary motive for using vehicular communications is to improve road safety. Therefore, congestion and awareness control approaches not only should prevent channel congestion or improve cooperative awareness, but also ensure the quality of service required for the proper performance of cooperative safety applications. ETSI specifies that safety applications such as LCRW [12] and ICRW [13] have strict operational requirements in terms of position accuracy, communication reliability, and end-to-end latency, as shown in Table 4.1. However, most of the current congestion and awareness control approaches have not been designed to satisfy the requirements simultaneously.

Table 4.1: Operational Requirements of LCRW and ICRW Applications

Application	**Position Accuracy**	**Communication Range**†	**End-to-end Latency**
LCRW [12]	$\leq$ 1 m, 95 %	300 m	$\leq$ 300 ms
ICRW [13]	$\leq$ 2 m, 95 %	300 m	$\leq$ 300 ms

† As specified by ETSI, the communication range may be reduced (e.g., in congested channel situations) but without affecting the safety time required by cooperative safety applications [12], [13].

The main drawback of congestion control approaches such as PULSAR [30], LIMERIC [31], FABRIC [32], and DCC [33] is that they do not explicitly consider the operational requirements of cooperative safety applications or vehicle dynamics. Congestion control approaches generally adapt beacon rate based only on the channel load, without considering the traffic situation of neighboring vehicles. This could be critical for road safety in vehicular scenarios such as a highway with a traffic jam in one direction, resulting in a congested channel, and a free-flow condition in the opposite direction with high-speed vehicles. The vehicles in free-flow are forced to reduce their beacon rates due to channel congestion even if they require a high beacon rate to maintain a certain level of position accuracy. In addition, the interference generated by the vehicles in the traffic jam can significantly affect the communication reliability of vehicles in free-flow, reducing the effectiveness of cooperative safety applications.

Regarding current awareness control approaches, most of them have not been designed to simultaneously satisfy the operational requirements of cooperative safety applications. Some awareness control approaches aim to maintain a certain level of position accuracy. For instance, ETSI DMG [11] and IVTRC [35] adapt the beacon transmission rate according to the vehicle dynamics to limit the position error perceived by neighboring vehicles. ETSI DMG does not consider an additional control mechanism to guarantee communication reliability in dense traffic situations. IVTRC mitigates packet collisions, but at the cost of reducing the

beacon rate, which directly affects the position accuracy. In contrast, INTERN [36] does not consider the position accuracy or vehicle dynamics. Furthermore, it also has difficulties to guarantee the beacon rates and warning distances required by the safety applications. This issue is represented by feasible regions [36] where the requirements of all vehicles could be satisfied without overloading the channel. Another drawback is that the feasible regions change with the vehicular density, so it is a challenge to avoid the regions where the requirements are not satisfied.

NORAC [37] and TTCC [38] aim to improve cooperative awareness by increasing the beacon rate of certain vehicles. However, these approaches have not been designed to satisfy a pre-defined position accuracy, nor do they have a mechanism to mitigate packet collisions. Improving cooperative awareness is not sufficient to guarantee the quality of service required by safety-critical applications. The main reason is that increasing the beacon rate also leads to more packet collisions, especially for high vehicular densities and low minimum contention windows [26], [25]. Further, CBR is generally used as a priority metric, and other critical performance metrics directly related to road safety, such as position error, packet collision rate, PDR, and end-to-end latency are not considered.

Finally, DC-BTR&P [43] defines a minimum fixed transmission power independently of the vehicle dynamics. Further, it reduces packet collisions by decreasing the communication range of vehicles with higher dynamics. This issue is critical for road safety because vehicles with high speed should use a higher transmission power in order to increase their notification capacity. Another limitation is that vehicles adapt the beacon transmission parameters based on their own dynamics, without considering information from the surrounding environment. Therefore, in this paper, we design the POSACC approach to overcome these issues and guarantee the operational requirements of cooperative safety applications.

4.2.2 Approaches used as Benchmark

As a benchmark for comparison, we utilize three different beaconing approaches; ETSI DMG [11], LIMERIC [31], and DC-BTR&P [43]. ETSI DMG is the awareness control approach specified by European standards, whereas LIMERIC is one of the most important congestion control approaches available in the literature. ETSI DMG adapts the beacon rate depending on vehicle dynamics to provide a target position accuracy. In contrast, LIMERIC adapts the beacon rate based on the locally measured CBR to maintain the channel load below a certain target threshold and to achieve fairness. We also include our previous approach DC-BTR&P, which is an awareness control algorithm that adapts the beacon rate and transmission power to provide a target position accuracy and reduce interference. The evaluation of these beaconing approaches will help understand their benefits and limitations when referring to road safety.

4.3 Proposed Algorithm

This section presents the design of the POSition-ACCuracy (POSACC) based adaptive beaconing algorithm for cooperative vehicular safety systems. POSACC aims to satisfy the operational requirements of cooperative safety applications. The POSACC system architecture is illustrated in Fig. 4.1. We assume that each vehicle obtains its own location from

the Global Positioning System (GPS) device, as well as its own movement parameters (e.g., velocity, acceleration, and heading) from on-board sensors. Each vehicle also has an LDM database, where the beaconing information from its neighbors is stored. One entry is created for each neighboring vehicle. The LDM database provides information from the surrounding traffic situation (e.g., the number of neighboring vehicles as well as their movement parameters). Entries are updated at beacon receptions. If a neighbor does not announce its presence once the entry expiration time has been reached, the entry is erased from the LDM database. Cooperative safety applications require fresh status information to successfully detect possible threats. If a hazardous situation is detected, the safety-critical application provides warnings to the driver or it may trigger collision avoidance actions (e.g., in autonomous driving).

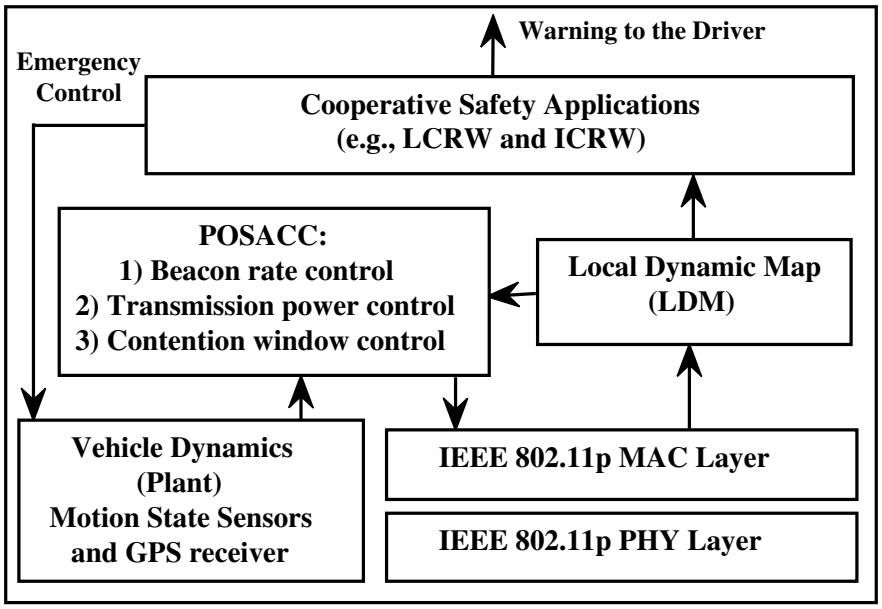

Figure 4.1: POSACC system architecture.

To fulfill the design goals, POSACC utilizes three different control mechanisms:

- **Beacon rate control**: it adapts the beacon rate depending on vehicle dynamics to provide the required position accuracy.
- **Transmission power control**: it adapts the transmission power depending on vehicle dynamics to guarantee the required warning distance.
- **Contention window control**: it takes advantage of the LDM database information to adapt the size of the minimum contention window by minimizing the probability of packet collisions.

In the following subsections, the control mechanisms and POSACC algorithm are presented in detail.

4.3.1 Beacon Rate Control Mechanism

The beacon rate control mechanism adapts the beacon rate in real-time to limit the position error perceived by neighboring vehicles. In this mechanism, the beacon rate is controlled

according to the transmitter vehicle dynamics. Therefore, the beacon rate is reduced when the vehicle has low dynamics, alleviating the channel load and decreasing the interference on its neighbors. Furthermore, the resulting beaconing load is implicitly controlled by the relationship between average velocity and traffic density [15]. As a consequence, the channel load remains stable when more vehicles drive at lower velocities.

Fig. 4.2 illustrates relevant time parameters that influence position accuracy. If the event of looking up the vehicle's position in the LDM database is uniformly distributed between the minimum and maximum time difference of the beacon transmission event, the average position error ($\overline{E}$) perceived by neighboring vehicles is [15],

$$\overline{E} = \frac{E_{\min} + E_{\max}}{2}, \tag{4.1}$$

where $E_{\min}$ is the minimum error resulting from the transmission delay (t_D), and $E_{\max}$ is the maximum error resulting from the beacon interval and transmission delay.

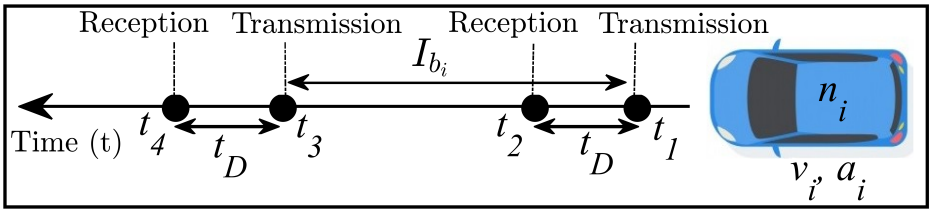

Figure 4.2: Relevant time parameters that determine the position accuracy.

We assume constant acceleration during the beacon interval. So, from kinematic equations, $\overline{E}$ is expressed as a function of velocity[1] (v_i) and acceleration (a_i) of the transmitting vehicle (n_i),

$$2\overline{E_\mathrm{i}} = v_\mathrm{i} t_D + I_{b_\mathrm{i}} \left(v_\mathrm{i} + \frac{a_\mathrm{i} I_{b_\mathrm{i}}}{2} \right) + t_D (a_\mathrm{i} I_{b_\mathrm{i}} + v_\mathrm{i}), \tag{4.2}$$

where I_{b_i} is the beacon interval of n_i (equal to the inverse of beacon transmission rate, R_{b_i}). We assume beacon messages of the same size (b_z) and equal data-rate (R_D), so t_D is the same for all vehicles, $t_D = b_z / R_D$.

A quadratic function, $f(I_{b_\mathrm{i}}) = A I_{b_\mathrm{i}}^2 + B I_{b_\mathrm{i}} + C$, can be obtained from (4.2) as follows,

$$f(I_{b_\mathrm{i}}) = a_\mathrm{i} I_{b_\mathrm{i}}^2 + 2(v_\mathrm{i} + a_\mathrm{i} t_D) I_{b_\mathrm{i}} + 4(v_\mathrm{i} t_D - \overline{E_\mathrm{i}}). \tag{4.3}$$

In the general case of $a_\mathrm{i} \neq 0$, the discriminant (D) and solutions ($I_{b_{\mathrm{i}\{1,2\}}}$) of the quadratic function are computed as follows,

$$D = 4 \left[(v_\mathrm{i} + a_\mathrm{i} t_D)^2 - 4 a_\mathrm{i} \left(v_\mathrm{i} t_D - \overline{E_\mathrm{i}} \right) \right], \tag{4.4}$$

[1]The velocity vector is not used since position error considers the movement in a straight line between the last received position and the current position of the vehicle. Therefore, in order to reduce the complexity, it is assumed that the vehicle moves in a single dimension (direction of longitudinal displacement).

$$I_{b_{\mathrm{i}\{1,2\}}} = \frac{-v_{\mathrm{i}} - a_{\mathrm{i}} t_D \pm \left[v_{\mathrm{i}}^2 + (a_{\mathrm{i}} t_D)^2 - 2a_{\mathrm{i}}\left(v_{\mathrm{i}} t_D - 2\overline{E_{\mathrm{i}}}\right)\right]^{\frac{1}{2}}}{a_{\mathrm{i}}}. \tag{4.5}$$

Otherwise, if $a_{\mathrm{i}} = 0$, the solution $(I_{b_{\mathrm{i}}})$ is computed by using the following linear equation,

$$I_{b_{\mathrm{i}}} = \frac{2(\overline{E_{\mathrm{i}}} - v_{\mathrm{i}} t_D)}{v_{\mathrm{i}}}. \tag{4.6}$$

Fig. 4.3 shows the numerical solutions of the beacon interval by using (4.3) for different setups: acceleration (deceleration), velocity, and average position error. To better relate the analysis with real traffic scenarios, velocity is shown in kilometers per hour. In the analysis only positive solutions $(0 < I_{b_{\mathrm{i}}})$ are considered. A real root in the interval $(0, 1]$ exists in most traffic situations. However, the root may be outside the range $(0, 1]$ in acceleration (see Fig. 4.3a, $v_{\mathrm{i}} = 30$ km/h and $\overline{E_{\mathrm{i}}} = 5$ m), or even the root may not exist in deceleration (see Fig. 4.3b, $v_{\mathrm{i}} = 30$ km/h and $\overline{E_{\mathrm{i}}} = 5$ m).

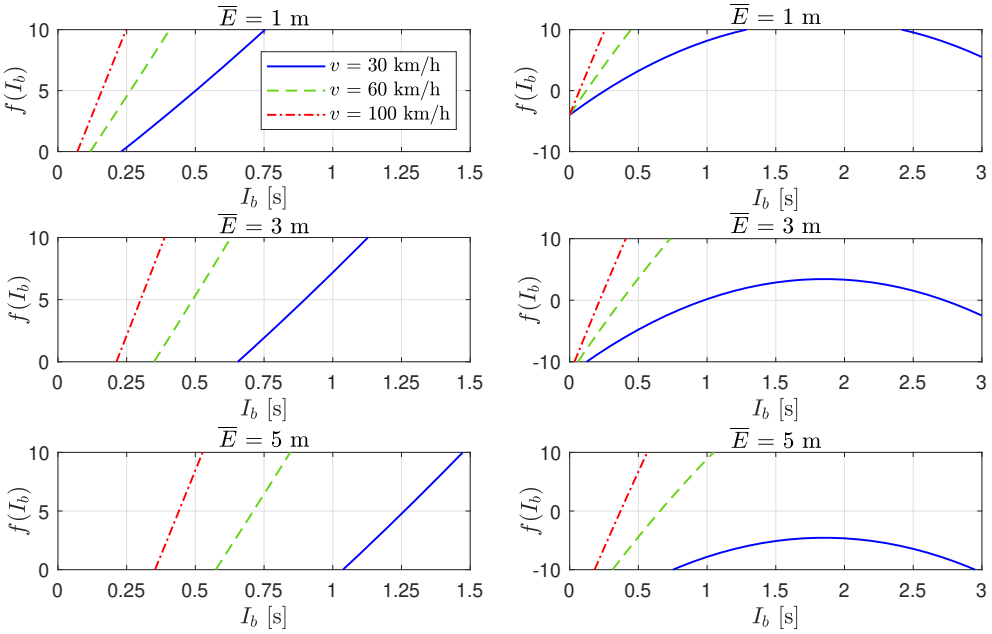

(a) $a = 2.5\ m/s^2$ (b) $a = -4.5\ m/s^2$

Figure 4.3: Numerical solutions of the beacon interval computed using (4.3) for $b_z = 378$ bytes and $R_D = 6$ Mbps, equivalent to a transmission delay of 500 μs.

Fig. 4.4 shows the beacon interval computed by using (4.5) and (4.6) in the accelerated and uniform movement for different average position errors. As expected, an increase in velocity demands a shorter beacon interval to guarantee the desired position accuracy. The beacon interval not only responds to changes in velocity, but also to variations of acceleration. Note that the impact of acceleration is especially significant at low velocities since for a short beacon interval the velocity variation is low.

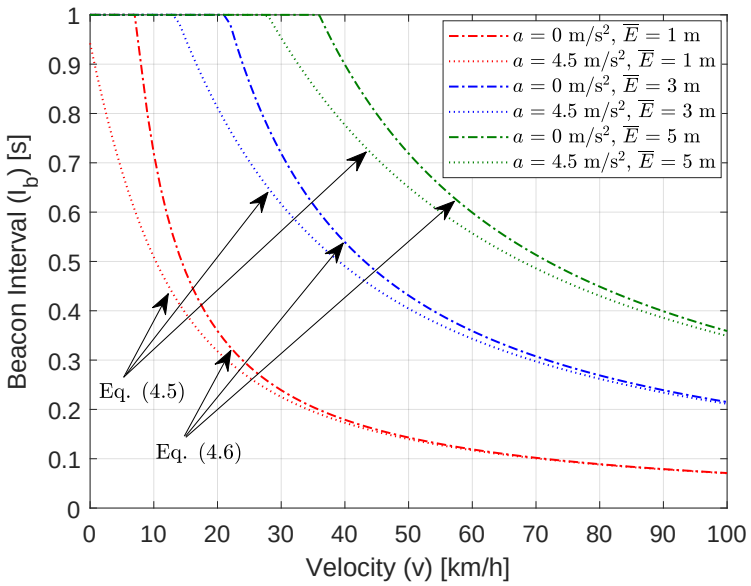

Figure 4.4: Beacon interval computed by using (4.5) and (4.6) for $b_z = 378$ bytes and $R_D = 6$ Mbps, equivalent to a transmission delay of 500 μs.

Algorithm 4 shows the steps followed by the beacon rate control mechanism to compute the beacon transmission rate in real-time depending on the vehicle movement status. On each beacon transmission, the vehicle n_i gets its velocity v_i and acceleration a_i, and sets the desired position accuracy $\overline{E_\text{i}}$. Lines 1-20 involve the decisions associated depending on the movement status of n_i: repose (Line 1-2), the beacon transmission rate is set to 1 beacon/s equivalent to the minimum value required for the proper performance of the less demanding vehicular applications [11]; accelerated movement (Line 3-7), the beacon transmission rate is computed using (4.5); uniform movement (Line 8-11), the beacon transmission rate is

Algorithm 4: Beacon Rate Control Mechanism

Data: $\{v_\text{i}, a_\text{i}, t_D, I_{b_c}, \overline{E_\text{i}}\}$
Result: $\{R_{b_\text{i}}\}$
Begin
1 **if** *(v_i == 0 && a_i == 0)* **then**
2 $I_{b_\text{i}} \leftarrow 1$;
end
3 **else if** *(v_i >= 0 && a_i > 0)* **then**
4 *Compute* $I_{b_{\text{i}\{1,2\}}}$ using (4.5);
5 $I_{b_\text{i}} \leftarrow maximum\{I_{b_{\text{i}\{1\}}}, I_{b_{\text{i}\{2\}}}\}$;
6 **if** *(I_{b_i} > 1)* **then**
7 $I_{b_\text{i}} \leftarrow 1$;
end
end
8 **else if** *(v_i > 0 && a_i == 0)* **then**
9 *Compute* I_{b_i} using (4.6);
10 **if** *(I_{b_i} > 1)* **then**
11 $I_{b_\text{i}} \leftarrow 1$;
end
end
12 **else if** *(v_i > 0 && a_i < 0)* **then**
13 *Compute D* using (4.4);
14 **if** *(D > 0)* **then**
15 *Compute* $I_{b_{\text{i}\{1,2\}}}$ using (4.5);
16 $I_{b_\text{i}} \leftarrow maximum\{I_{b_{\text{i}\{1\}}}, I_{b_{\text{i}\{2\}}}\}$;
17 **if** *(I_{b_i} > I_{b_c})* **then**
18 $I_{b_\text{i}} \leftarrow I_{b_c}$;
end
end
19 **else if** *(D <= 0)* **then**
20 $I_{b_\text{i}} \leftarrow I_{b_c}$;
end
end
21 $R_{b_\text{i}} \leftarrow ceil(1/I_{b_\text{i}})$;
22 **return** R_{b_i};
end

computed according to (4.6); deceleration (Line 12-20), in order to notify with immediacy to surrounding vehicles a possible braking [15], it is set a critical beacon interval (I_{b_c}). We demonstrate the applicability of the beacon rate control mechanism in [43].

4.3.2 Transmission Power Control Mechanism

We design the transmission power control mechanism based on the *"Dynamic Safety Shield"* concept presented by ETSI in [12], [13]. The dynamic safety shield is a virtual dynamic area surrounding the transmitting vehicle, as shown in Fig. 4.5. The size of the safety area is estimated by the transmitting vehicle in real-time. In order to react to a potential crash, a driver needs to be informed at a sufficient distance from the expected impact to initiate a maneuver [12], [13]. From the transmitting vehicle's point of view, this means that it has to guarantee that its beacon messages are received within a certain distance, which we denote as target warning distance. The target warning distance ($\mathrm{d}_{w_\mathrm{i}}$) depends on the velocity v_i of the transmitting vehicle n_i, and the required safety time (t_s). Acceleration (deceleration) is not taken into account to avoid undesired oscillations on the warning distance. The safety time must consider the maximum latency time (e.g., 300 ms [12], [13]), the average driver's reaction time (e.g., 1.5 s [79]), the required action time (e.g., 0.75 s [80]), and a certain time margin.

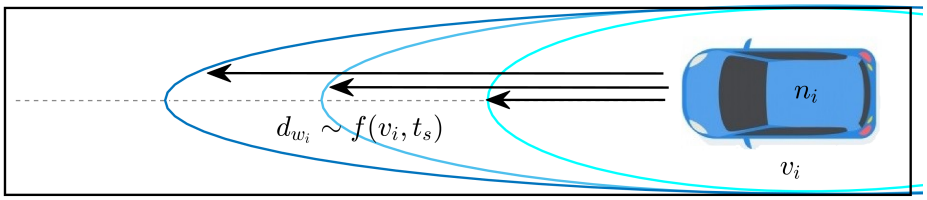

Figure 4.5: Dynamic safety shield for the transmitting vehicle n_i depending on its velocity v_i and the safety time t_s.

We adopt the model based on Nakagami-m proposed by Killat et al. in [65] and used in [41], [43], [81] to compute the probability of successful reception of beacon messages in the presence of a single transmitter-receiver pair. This analytical model has been validated based on extensive evaluations via a discrete-event network simulator, achieving a perfect match [65]. The model combines the Nakagami-m distribution fast fading model and the Friis/Two-Ray-Ground path loss model. The probability of successful reception (P_{SR}) is computed depending on the distance (d) between the transmitter and receiver as follows [65],

$$P_{SR} = \begin{cases} \mathrm{e}^{-3\left(\frac{\mathrm{d}}{CR}\right)^2}\left(1+3\left(\frac{\mathrm{d}}{CR}\right)^2+\frac{9}{2}\left(\frac{\mathrm{d}}{CR}\right)^4\right), & \mathrm{d} \le \mathrm{d}_{c_o}, \quad (4.7) \\ \mathrm{e}^{-3\gamma\left(\frac{\mathrm{d}^2}{CR}\right)^2}\left(1+3\gamma\left(\frac{\mathrm{d}^2}{CR}\right)^2+\frac{9}{2}\gamma^2\left(\frac{\mathrm{d}^2}{CR}\right)^4\right), & \mathrm{d} > \mathrm{d}_{c_o}, \quad (4.8) \end{cases}$$

where the crossover distance, $\mathrm{d}_{c_o} = 4\pi\left(\frac{h_t h_r}{\lambda}\right)$, depends on the wavelength of the signal (λ) and the height of the antennas (h_t), (h_r), and $\gamma = (\mathrm{d}_{c_o})^{-2}$.

The Friis path loss model is considered for distances equal to or less than d_{c_o}. The Two-Ray-Ground path loss model is used for distances greater than d_{c_o}. The intended communication range (CR) depends on the configured transmission power. CR is the maximum achievable communication distance when only assuming path loss according to Friis/Two-Ray-Ground and neglecting fast fading effects. Fig. 4.6 shows P_{SR} for different intended communication ranges and distances between the transmitter and receiver over a crossover distance of 556 m, equivalent to a carrier frequency of 5.89 GHz and antenna heights of 1.5 m.

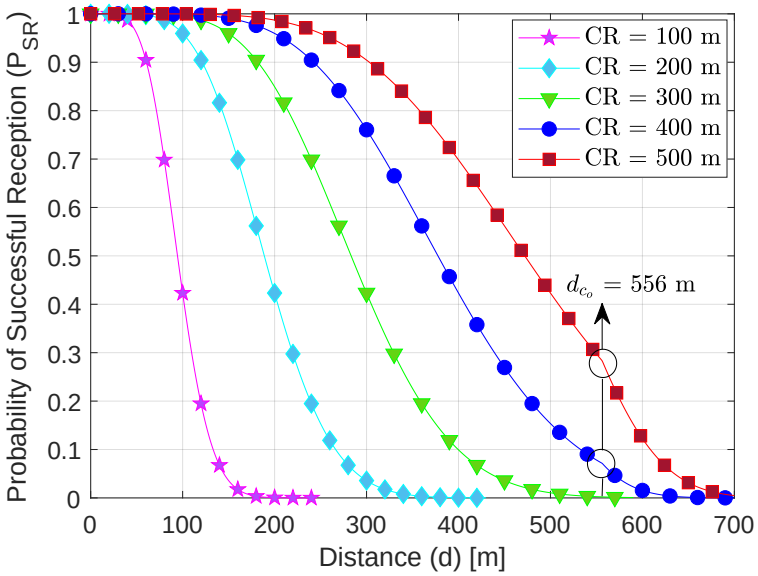

Figure 4.6: Probability of successful reception as a function of distance, using a carrier frequency of 5.89 GHz and antenna heights of 1.5 m.

The transmission power control mechanism computes the optimal vehicle's transmission power (P_{T_i}) to maximize the probability of successful reception P_{SR} at the target warning distance. This control mechanism aims to ensure that the beacons are received at the target warning distance with certain reliability (r_t). If the values of the intended communication range CR that satisfy the condition $P_{SR} \geq r_t$ are grouped into a discrete set $S = \{CR_1, CR_2, ..., CR_s\}$, the valid value of CR in (4.7) or (4.8) that maximizes P_{SR} at the target warning distance can be computed by solving the following optimization problem,

$$\begin{aligned} \max_{CR} \quad & P_{SR} \\ \text{s.t.} \quad & \mathrm{d} = \mathrm{d}_{w_i}, \\ & CR = CR_1 \in S \;\forall\; P_{SR} \geq r_t. \end{aligned} \tag{4.9}$$

Algorithm 5 describes the steps followed by the transmission power control mechanism to compute the optimal beacon transmission power in real-time depending on the vehicle movement status and the desired safety time. On each beacon transmission, the vehicle n_i gets its velocity v_i and sets the desired safety time t_s. The target warning distance d_{w_i} is computed according to basic kinematic equations (see Line 1). A minimum warning distance (d_{w_o}) is guaranteed in Lines 2-3. This is especially useful in low dynamic situations. The P_{SR}

Algorithm 5: Transmission Power Control Mechanism

```
Data: {v_i, t_s, r_t, d_{w_o}, d_{c_o}}
Result: {P_{T_i}}
Begin
1   d_{w_i} ← v_i t_s;
2   if (d_{w_i} < d_{w_o}) then
3   |   d_{w_i} ← d_{w_o};
    end
4   if (d_{w_i} <= d_{c_o}) then
5   |   P_SR ← (4.7) with d ← d_{w_i};
6   |   P_T ← Friis model [26];
    end
7   else if (d_{w_i} > d_{c_o}) then
8   |   P_SR ← (4.8) with d ← d_{w_i};
9   |   P_T ← Two-Ray-Ground model [26];
    end
10  CR_k ← d_{w_i};
11  while P_SR < r_t do
12  |   CR_{k+1} ← CR_k − P'_SR(CR_k)/P''_SR(CR_k);
13  |   P_SR ← P_SR(CR_{k+1});
14  |   CR_k ← CR_{k+1};
    end
15  P_{T_i} ← P_T(CR_{k+1});
16  return P_{T_i};
End
```

optimization function and the propagation model (used to compute the transmission power) are defined in Lines 4-9. We use the Newton-Raphson method to compute the intended communication range CR that maximizes P_{SR} at the target warning distance under the restriction $P_{SR} \geq r_t$ (see Line 10-14). Note that the first value of CR that satisfies the restriction is selected. Finally, the transmission power P_{T_i} is computed by evaluating the valid value CR_1 in the chosen model (see Line 15).

4.3.3 Contention Window Control Mechanism

IEEE 802.11p [7] considers the DCF procedure for medium contention. It includes the Hybrid Coordination Function (HCF), which provides prioritization techniques according to IEEE 802.11e. HCF defines different Arbitration Inter-Frame Space (AIFS) and contention window range depending on the access category (priority) of the packet. Highest priority packets have the shortest AIFS and the shortest contention window to ensure a high probability of medium access. The initial contention window size is limited by the minimum contention window. For broadcast communication, there is no error-handling (e.g., no acknowledgments) and hence no exponential backoff growth [26]. As the contention window size is not increased, the size of the minimum contention window always defines the upper limit for the backoff counter. This limits the prioritization and increases the probability of packet collisions.

To compute the probability of packet collisions, we utilize the analytical model proposed by Bianchi in [27]. Bianchi's work is regarded as a standard in this research field. His model allows analyzing the performance of broadcast communications in vehicular networks based on IEEE 802.11p [26], [82], [83]. Applying Bianchi's model to vehicular communications where no exponential backoff is considered, the probability of packet collisions (p) can be computed as follows,

$$p = 1 - (1 - \tau)^{N-1}, \tag{4.10}$$

where N is the number of contending vehicles, and τ is the probability of a vehicle transmitting in a randomly chosen slot within the contention window size (CW) with no exponential backoff,

$$\tau = \frac{2}{CW + 1}. \tag{4.11}$$

Fig. 4.7 shows the probability of packet collisions for integer values[2] of CW in the range from 3 to 1023 [8]. Note that the probability of packet collisions p is significantly high for small values of minimum contention windows, even if there is a low number of contending vehicles. Since interference cannot be completely eliminated in the IEEE 802.11p DCF procedure, the proposed control mechanism focuses on achieving the lowest possible value of the probability of packet collisions.

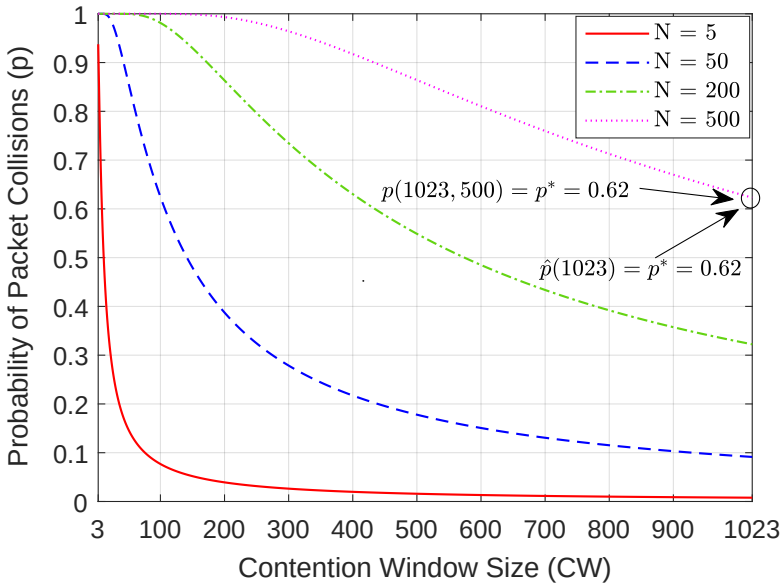

Figure 4.7: Probability of packet collisions according to the contention window size for different numbers of contending vehicles.

We design the contention window control mechanism to perform a linear distribution of the size of CW according to N. Let $CW_{\max}$ be the maximum value of CW and $N_{\max}$ be the maximum value of N. We denote as p^* the probability of packet collisions resulting from the evaluation of $N_{\max}$ and $CW_{\max}$ in (4.10) and (4.11), respectively. We utilize the linear function of the probability of packet collisions $\hat{p} = mCW$ that satisfies the condition $\hat{p}(CW_{\max}) = p^*$, so the slope is $m = \frac{p^*}{CW_{\max}}$. The solution $CW > 0$ for each $N > 1$ that satisfies the condition $p(CW, N) = \hat{p}(CW)$ (intersection point) can be computed by finding the zero of the following function,

$$P(CW) = 1 - \left(1 - \frac{2}{CW + 1}\right)^{N-1} - mCW. \tag{4.12}$$

[2]As specified in [8], CW is divided into equidistant time slots. The valid range of integers for CW is between 3 to 1023. The length of each time slot is 13 μs.

The value of CW that minimizes P can be computed by solving the optimization problem,

$$\begin{aligned} \min_{CW} \quad & P \\ \text{s.t.} \quad & p^* = 1 - \left(1 - \frac{2}{CW_{\max} + 1}\right)^{N_{\max}-1}, \\ & m = \frac{p^*}{CW_{\max}}, \\ & N > 1. \end{aligned} \tag{4.13}$$

We design the control mechanism to provide the lowest value of p by using Bianchi's model when $CW = CW_{\max}$ and $N = N_{\max}$. For example, if $CW_{\max} = 1023$ and $N_{\max} = 500$, the lowest value of p according to Bianchi's model is $p(1023, 500) = p^* = 0.62$ (see Fig. 4.7). However, $\hat{p}(1023) = p^* = 0.62$ is the maximum value of probability of packet collisions according to $\hat{p}$. As we are interested in the intersection point between both functions, the optimal value of the minimum contention window CW provides the lower probability of packet collisions in the interval $(0, p^*]$, for each N in the interval $1 < N \leq N_{\max}$ following a linear distribution. Fig. 4.8 shows the numerical solutions of CW computed by using (4.12) for different numbers of contending vehicles.

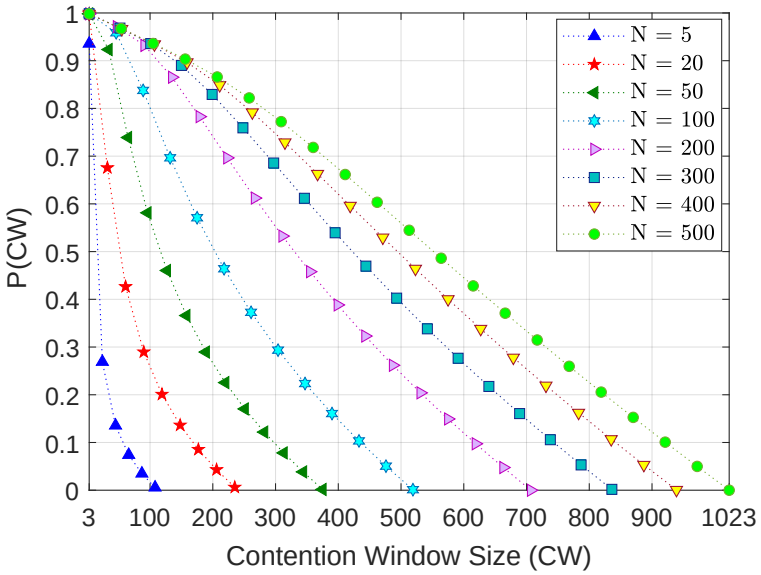

Figure 4.8: Numerical solutions of the minimum contention window computed by using (4.12) for $CW_{\max} = 1023$ and $N_{\max} = 500$.

The proposed mechanism focuses on the collision domain of the transmitting vehicle in saturation condition, as specified by Bianchi's model assumptions [27]. The saturation condition assumption means that the control mechanism is able to operate in the worst-case scenario. This is a key design assumption since communication reliability is critical in safety communications. We reduce the number of contending vehicles N to the number of neighbors of the transmitting vehicle. This is a valid assumption since Bianchi's model [27] only focuses on the collision domain of the transmitter, neglecting the impact of the hidden terminals.

Further, computing the number of contending vehicles in ad-hoc scenarios is a challenge because it involves the vehicles within the carrier-sensing-range.

To fulfill the steady-state principle of Bianchi's model [27], vehicles compute the optimal size of CW based on the maximum LDM database size ($\hat{N}$) reported on their neighborhood. Vehicles attach to the beacon the maximum value between its LDM database size and the maximum size announced by their neighbors, as shown in Fig. 4.9. Initially, vehicles n_1 and n_2 announce that their LDM databases are empty. At step 3, the vehicle n_3 announces a maximum LDM database size equal to 2. At step 5, the maximum size reported by the vehicles converges to the same value. The dissemination process allows vehicles to see the system in a steady-state.

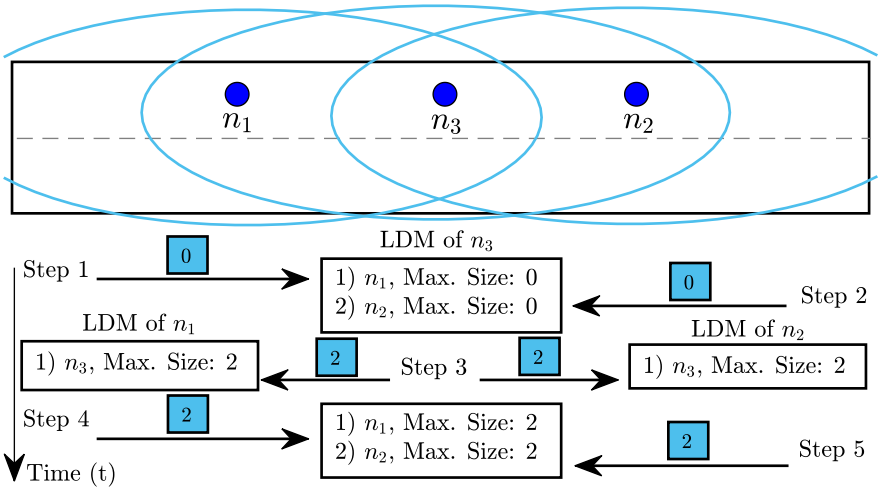

Figure 4.9: Representation of the LDM database size dissemination process.

Algorithm 6 describes the steps followed by the contention window control mechanism to compute the optimal size of the minimum contention window in real-time. On each beacon transmission, the vehicle n_i gets the maximum LDM database size $\hat{N}_\text{i}$ reported on its neighborhood. Lines 1-13 involve the decisions associated with the calculation of CW_i depending on $\hat{N}_\text{i}$. The smallest size of the minimum contention window CW_min is set in Lines 1-2. The Newton-Raphson method is used to compute the optimal size of the minimum contention window when $1 < \hat{N}_\text{i} \leq N_\text{max}$ (see Line 3-11). Note that the optimal size of CW_i is computed with an accuracy (σ) of one slot (see Lines 7 and 9). Finally, the largest value of the minimum contention window CW_max is set in Lines 12-13.

4.3.4 POSACC Algorithm

POSACC controls the beacon transmission parameters based on the vehicle dynamics and surrounding situation. POSACC integrates the control mechanisms described above to provide the position accuracy and communication reliability required by cooperative safety applications. It also focuses on maintaining the vehicle's warning distance, channel load, and end-to-end latency into the operative range of cooperative safety applications. POSACC takes advantage from the relationship between average velocity and traffic density [15] to reduce the conflict between the design goals. The interference is decreased without affecting the position accuracy and warning distance. In addition, a balance between the end-to-end

Algorithm 6: Contention Window Control Mechanism

Data: $\{\hat{N}_{\mathrm{i}}, CW_{\min}, CW_{\max}, N_{\max}\}$
Result: $\{CW_{\mathrm{i}}\}$
Begin
1 **if** *(*$\hat{N}_{\mathrm{i}} <= 1$*)* **then**
2 $CW_{\mathrm{i}} \leftarrow CW_{\min}$;
end
3 **else if** *(*$\hat{N}_{\mathrm{i}} > 1$ *&&* $\hat{N}_{\mathrm{i}} <= N_{\max}$*)* **then**
4 $CW_k \leftarrow CW_{\min}$;
5 *Compute* p^* using (4.10) and (4.11);
6 $m \leftarrow p^*/CW_{\max}$;
7 **while** $\sigma > 1$ **do**
8 $CW_{k+1} \leftarrow CW_k - P(CW_k)/P'(CW_k)$;
9 $\sigma \leftarrow fabs(CW_{k+1} - CW_k)$;
10 $CW_k \leftarrow CW_{k+1}$;
end
11 $CW_{\mathrm{i}} \leftarrow round(CW_{k+1})$;
end
12 **else if** *(*$\hat{N}_{\mathrm{i}} > N_{\max}$*)* **then**
13 $CW_{\mathrm{i}} \leftarrow CW_{\max}$;
end
14 **return** CW_{i};
end

latency and beacon interval is maintained in order to avoid packet losses due to expiration time reached.

Algorithm 7 describes the steps followed by POSACC on each beacon transmission. First, the beacon rate is computed depending on vehicle movement status to guarantee the desired position accuracy (see Line 1). Then, the optimal vehicle's transmission power is computed to maximize the probability of successful reception at the target warning distance (see Line 2). Finally, the optimal size of the minimum contention window is computed depending on the maximum LDM database size reported in the neighborhood of the transmitting vehicle to minimize the probability of packet collisions (see Line 3).

Algorithm 7: POSACC

Data: {data-set: Algorithm 4, Algorithm 5, Algorithm 6}
Result: $\{R_{b_{\mathrm{i}}}, P_{T_{\mathrm{i}}}, CW_{\mathrm{i}}\}$
Begin
1 Execute **Algorithm 4**;
2 Execute **Algorithm 5**;
3 Execute **Algorithm 6**;
4 **return** $R_{b_{\mathrm{i}}}$;
5 **return** $P_{T_{\mathrm{i}}}$;
6 **return** CW_{i};
end

4.4 Simulation Setup

In this section, we present the simulation setup in detail. The basic settings of the evaluation scenario, as well as communication parameters, are introduced in Section 4.4.1. The configurations of ETSI DMG, LIMERIC, DC-BTR&P and POSACC are given in Section 4.4.2.

4.4.1 Scenarios and Basic Configuration

We conduct our simulations using the Veins framework [84] with the IEEE 802.11p MAC/PHY model introduced by Eckhoff and Sommer in [67]. We assume a dedicated CCH that is solely used by safety applications. Consequently, the beaconing process occurs on the CCH without considering multi-channel operation. The evaluation scenario is a one-way two-lane highway with a total length of 3 km. Vehicles are randomly located on the first kilometer of the highway. To address a wide range of vehicular situations (e.g., from low vehicular density - high average speed to high vehicular density - low average speed), we define eight different traffic setups, as shown in Table 4.2.

Table 4.2: Traffic Settings

Traffic Setup	**1**	**2**	**3**	**4**	**5**	**6**	**7**	**8**
Traffic Density (ρ) [veh/km/lane]	10	20	30	40	50	60	70	80
Maximum Velocity [km/h]	100	90	80	70	60	50	40	30

The transmission power is set to 20 dBm [7]. We utilize the Two-Ray Interference model [68] with a dielectric constant $\epsilon_r = 1.02$ to simulate the radio signal propagation. This model has been validated based on an extensive set of road measurements, capturing complex signal effects, especially at short and medium distances [68]. The beacons have 378 bytes [31] and are transmitted with a priority corresponding to the voice access category (AC_VO) [8], [29]. Each vehicle is 5 m long, 2 m wide, with a maximum acceleration of 2.5 m/s^2, and deceleration up to 4.5 m/s^2. We utilize omnidirectional antennas with a height of 1.5 m [65] and a data-rate equal to 6 Mbps [8]. In order to validate statistically the results, we conducted a total of 800 simulations with random seeds: 8 traffic setups, 5 beaconing algorithms configurations, and 20 repetitions. The most important simulation parameters are given in Table 4.3.

Table 4.3: Simulation Parameters

Parameter	**Value**
CCH Frequency	5.89 GHz [7]
CCH Bandwidth	10 MHz [7]
Transmission Power	20 dBm [7]
Receiver Sensitivity	-82 dBm [36]
Carrier Sense Threshold	-90 dBm [36]
Thermal Noise	-104 dBm [26]
Data-Rate (R_D)	6 Mbps [8]
Beacon Size (b_z)	378 bytes [31]
Access Category (AC)	AC_VO [8], [29]
Backoff Slot Time	13 μs [8], [67]
Propagation Model	Two-Ray Interference [68]

4.4.2 Configuration of the Algorithms

POSACC is compared with two relevant state-of-the-art beaconing algorithms, such as ETSI DMG [11] and LIMERIC [31]. POSACC is also compared with our previous adaptive beaconing algorithm, DC-BTR&P [43]. We developed a new simulation model using the Veins framework, which captures the full operation mode of the four adaptive beaconing algorithms.

As specified in [11], ETSI DMG transmits a new CAM if one of the following conditions has been detected:

- The difference between current and previous position exceeds 4 m (e.g., $\Delta pos \geq 4$ m);
- The difference between current and previous velocity exceeds 0.5 m/s (e.g., $\Delta vel \geq 0.5$ m/s);
- The difference between current and previous heading exceeds 4° (e.g., $\Delta head \geq 4°$);

CAM trigger rules are checked at a time interval denoted as Status Monitoring and Decision Interval (SMDI).

In LIMERIC [31], each vehicle adapts its beacon transmission rate such that the channel load converges to a specified threshold. The beacon rate of vehicle j at time instant t is computed according to,

$$\hat{r}_j(t) = (1-\alpha)\hat{r}_j(t-1) + \beta(\hat{r}_g - \hat{r}_C(t-1)), \tag{4.14}$$

where $\hat{r}_C$ is the aggregate rate of all vehicles participating in congestion control, $\hat{r}_g$ is the goal for the total rate, and α and β are adaptation parameters that control stability, fairness, and steady-state convergence.

To ensure convergence in very dense scenarios, LIMERIC introduces a novel gain saturation approach. The modified linear rate-control equation based on (4.14) with gain saturation is,

$$\hat{r}_j(t) = (1-\alpha)\hat{r}_j(t-1) + \text{sign}(\hat{r}_g - \hat{r}_C(t-1))\min[X, \beta\,|(\hat{r}_g - \hat{r}_C(t-1)|], \tag{4.15}$$

where X is a threshold that limits the update offset. We utilize LIMERIC with the gain saturation approach [31] for comparison purposes. The CBR is measured at a fixed time interval of 200 ms, as specified in [30]. This time interval is denoted as Channel Monitoring and Decision Interval (CMDI).

DC-BTR&P [43] adapts the beacon rate and transmission power of the vehicle j to provide the desired position accuracy. The beacon rate is adjusted according to the beacon rate control mechanism presented in Section 4.3.1. The transmission power is computed as [43],

$$\hat{P}_{t_j} = \hat{P}_{t_{\min}} + (\hat{P}_{t_{\max}} - \hat{P}_{t_{\min}})\left(1 - \frac{L_j}{L_o}\right)\hat{R}_{b_j}^{-\phi}, \tag{4.16}$$

where $\hat{P}_{t_{\min}}$ is a minimum fixed transmission power, $\hat{P}_{t_{\max}}$ is the maximum allowed transmission power, L_o is the channel load threshold, ϕ is a weight factor which controls the impact of the beacon rate $\hat{R}_{b_j}$ on the transmission power, and L_j is the channel load on j.

In POSACC, we specify an average position error of 1 m according to cooperative safety-critical applications, such as LCRW [12] and ICRW [13]. The critical beacon interval is set to 0.2 s [15], achieving a good trade-off between position tracking and the generated interference. We set a minimum warning distance of 50 m, which is within the minimum safety range used in [36]. We define a safety time of 5 s, that is long enough to include a maximum latency of 300 ms [12], [13], an average driver's reaction time of 1.5 s [79], a required action time of 0.75 s [80], and a margin of 2.45 s. To achieve a high probability of successful reception of beacon messages, the target reliability is set to 0.99. According to [8], an interval from 3 to 1023 is used for the contention window. As specified in [85], an optimal contention window must keep a balance between the expired beacons and the collided ones. Since the trade-off between communication reliability and end-to-end latency depends on $N_{\max}$, two different setups are investigated. We set the maximum value of $\hat{N}$ to 200 and 500 vehicles, which are values into the range of the vehicular density studied in [31]. The algorithms settings are shown in Table 4.4.

Table 4.4: Algorithms Settings

Algorithm	**Parameter**	**Value**
ETSI DMG	Δpos	$\geq$ 4 m [11]
ETSI DMG	Δvel	$\geq$ 0.5 m/s [11]
ETSI DMG	$\Delta head$	$\geq 4^{\circ}$ [11]
ETSI DMG	SMDI	20 ms [11]
LIMERIC	alpha (α)	0.1 [31]
LIMERIC	beta (β)	1/150 [31]
LIMERIC	Goal for Total Rate ($\hat{r}_g$)	0.6 [31]
LIMERIC	Threshold (X)	0.0005 [31]
LIMERIC	CMDI	200 ms [30]
DC-BTR&P	Min. Transmission Power	7 dBm [43]
DC-BTR&P	Max. Transmission Power	20 dBm [43]
DC-BTR&P	Channel Load Threshold (L_o)	0.6 [31]
DC-BTR&P	Weight Factor (ϕ)	2 [43]
DC-BTR&P	Average Position Error ($\overline{E}$)	1 m [12], [13]
DC-BTR&P	Critical Beacon Interval (I_{b_c})	0.2 s [15]
POSACC	Average Position Error ($\overline{E}$)	1 m [12], [13]
POSACC	Critical Beacon Interval (I_{b_c})	0.2 s [15]
POSACC	Min. Warning Distance (d_{w_o})	50 m [36]
POSACC	Desired Safety Time (t_s)	5 s [80]
POSACC	Target Reliability (r_t)	0.99
POSACC	Maximum value of $\hat{N}$ ($N_{\max}$)	200, 500 [31]
POSACC	Minimum value of CW ($CW_{\min}$)	3 [8]
POSACC	Maximum value of CW ($CW_{\max}$)	1023 [8]

4.5 Evaluation

POSACC relies on the adaptation of beacon rate, transmission power, and the size of the minimum contention window. Therefore, we first verify the aforementioned three points in Section 4.5.1. Then, we present the performance of POSACC and compare it with ETSI DMG, LIMERIC, and DC-BTR&P in Section 4.5.2.

4.5.1 Performance of the Control Mechanisms

POSACC controls in real-time the beacon rate, transmission power, and the size of the minimum contention. Therefore, the first step is to evaluate the performance of the iteration

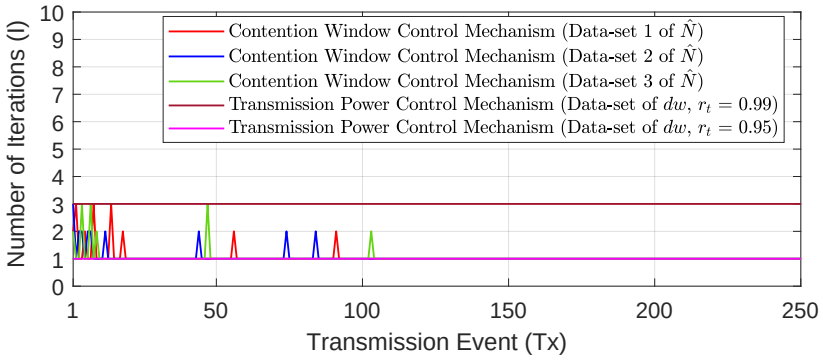

Figure 4.10: Complexity of the Newton-Raphson based control mechanisms.

processes. We use small scale Matlab simulations based on data-sets to evaluate the complexity of the iteration processes. Fig. 4.10 shows that the Newton-Raphson based control mechanisms solve the optimization problems with a really low number of iterations.

To better understand how POSACC reacts to vehicular traffic dynamics, we illustrate in Fig. 4.11 the acceleration and velocity of a generic vehicle in the scenario during 100 s of the simulation time. Since the impact of the acceleration on the beacon interval computed

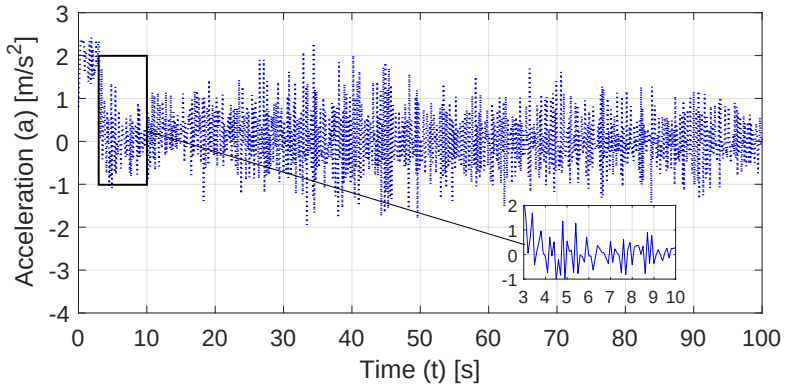

(a)

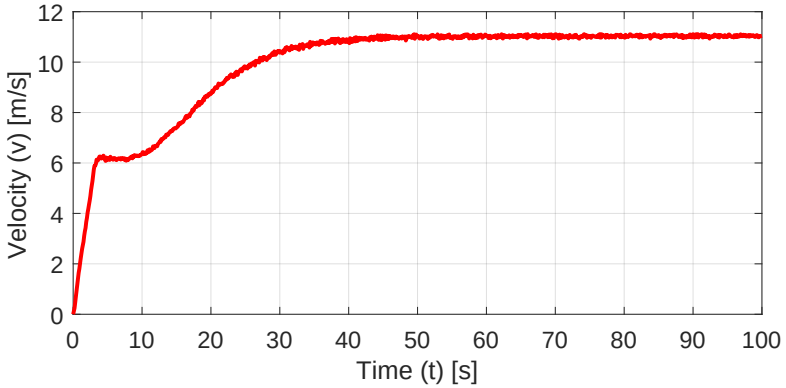

(b)

Figure 4.11: (a) Acceleration and (b) velocity developed by the vehicle during 100 s of simulation time with $\rho = 70$ veh/km/lane.

by the beacon rate control mechanism is more significant at lower velocities, we show the mobility pattern of the vehicle in the traffic scenario of 70 veh/km/lane (40 km/h).

Fig. 4.12a illustrates the adjustment that POSACC imposes in real-time on the beacon interval to achieve an average position error of 1 m. The beacon rate corresponding to the beacon interval required by POSACC is shown in Fig. 4.12b. In accelerated movement, an increase in velocity demands an increase in the beacon rate computed by POSACC, ensuring that for high-velocity situations the beacon interval is shortened to guarantee the target position accuracy, as shown in the interval from 10 s to 30 s. POSACC not only responds to variations in speed but also to changes of acceleration, as shown in the interval from 3 s to 10 s. In this time interval, the vehicle moves with a velocity of 6.2 m/s (22 km/h) and the beacon interval (beacon rate) oscillates between 0.32 s (4 beacon/s) and 0.2 s (5 beacon/s). Positive or zero acceleration leads to a beacon interval close to 0.32 s, as predicted by (4.5) and (4.6) (see Fig. 4.4). Nevertheless, when the vehicle slows down, POSACC sets a critical beacon interval equal to 0.2 s. Consequently, surrounding vehicles are more likely to detect sudden braking.

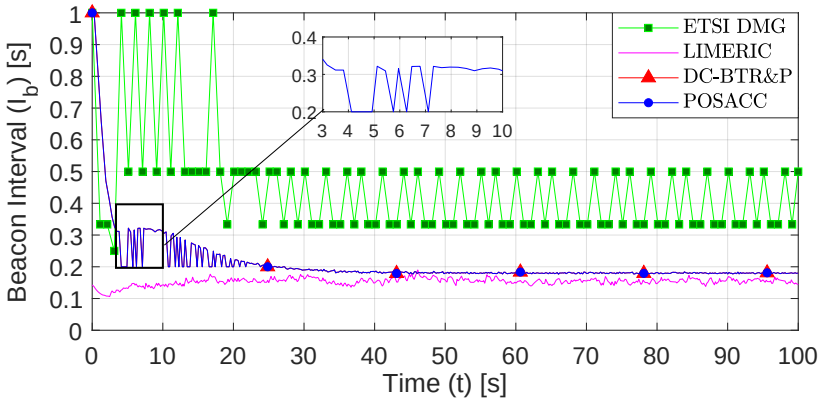

(a)

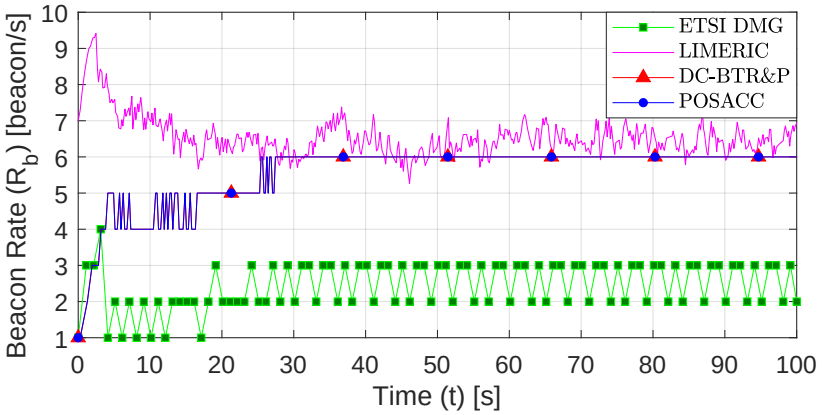

(b)

Figure 4.12: (a) Beacon interval and (b) beacon rate computed by the vehicle during 100 s of simulation time with $\rho = 70$ veh/km/lane.

For comparison purposes, we also include in Fig. 4.12 the beacon interval (beacon rate) computed by ETSI DMG and LIMERIC in the same traffic scenario. Note that POSACC

and DC-BTR&P utilize the same beacon rate control mechanism. The vehicle dynamics is also taken into account by ETSI DMG. However, the asynchrony between the CAM trigger limit and the SMDI leads to oscillations in the beacon rate. For instance, if the vehicle has a constant speed of 12 m/s going straight ahead, it is expected that ETSI DMG generates exactly 3 beacon/s considering $\Delta pos \geq 4$ m (see [11]). Accordingly, the requirements of the vehicle dynamics are not fully fulfilled implying a potential risk for road safety. This divergence effect has been reported in [40]. On the contrary, POSACC achieves a stable beacon transmission rate once the velocity has increased and the impact of the acceleration is negligible, as shown in the interval from 30 s to 100 s. LIMERIC adjusts the beacon transmission rate based on the measured CBR without taking into account the specific vehicle dynamics. As specified in [77], noisy CBR measurements produce unfairness in rate allocation even with gain saturation.

Both POSACC and DC-BTR&P adapt the communication range and transmission power in real-time depending on vehicle dynamics, as shown in Fig. 4.13. Initially, the vehicle moves

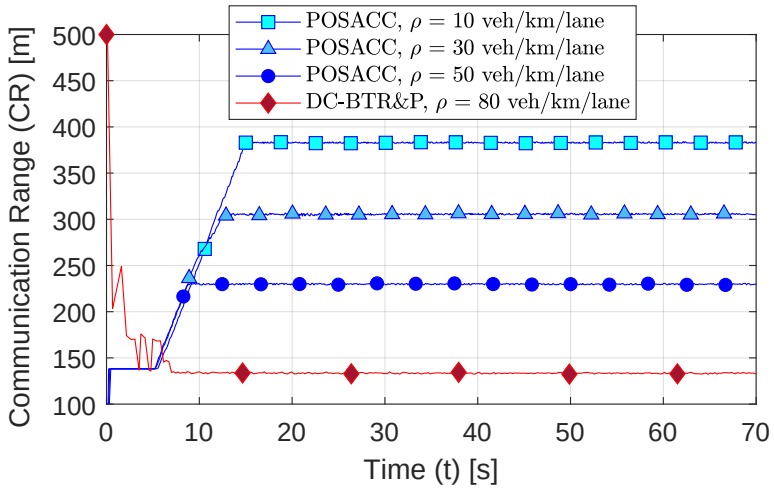

(a)

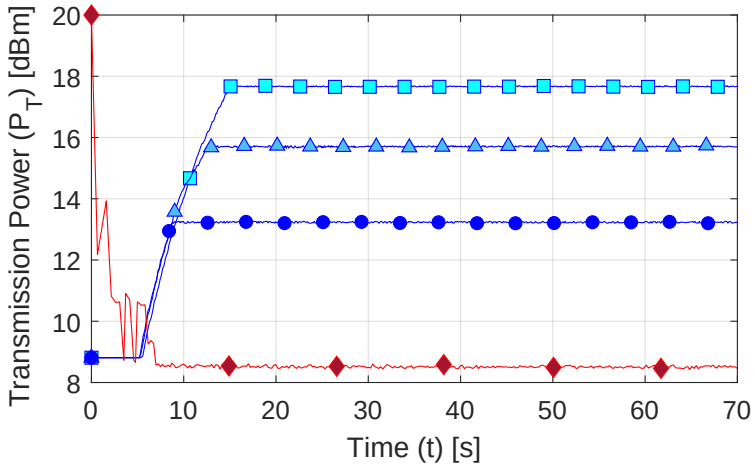

(b)

Figure 4.13: (a) Communication range and (b) transmission power computed by the vehicle for different traffic situations.

with low dynamics, so POSACC computes an intended communication range of 140 m to guarantee the default minimum warning distance of 50 m with reliability equal to 0.99. As velocity increases, POSACC increases the size of the safety shield by adjusting the warning distance to ensure a safety time of 5 s. For instance, in the traffic scenario of 30 veh/km/lane, the vehicle moves with a maximum velocity of 22.2 m/s (80 km/h) in the interval from 13 s to 70 s, resulting in a warning distance and intended communication range of 111 m and 310 m, respectively. Accordingly, POSACC increases the transmission power up to 15.7 dBm to maximize the probability of successful reception of beacon messages at the computed warning distance. In contrast, DC-BTR&P reduces the communication range and transmission power as the vehicle's velocity increases, as shown in Fig. 4.13. DC-BTR&P aims to mitigate packet collisions at the cost of decreasing the vehicle's warning distance. This strategy is suitable for urban environments where the vehicles' mobility pattern usually shows a continuous change between acceleration, deceleration, and repose (see [43]). However, on a highway, this issue is critical for road safety because drivers need to be notified at a sufficient distance from the expected impact, as specified in [12], [13]. Note that even in the traffic setup of the lowest velocity (80 veh/km/lane), the design of DC-BTR&P leads to a stable transmission power less than 9 dBm.

Fig. 4.14 demonstrates the effectiveness of POSACC to control the size of the minimum contention window in real-time on different traffic situations. Note that the dissemination of the maximum LDM database size ensures global fairness in the calculation of the optimal size of the minimum contention window, as well as the steady-state principle (see [27]). In POSACC, the size of the minimum contention window increases as more vehicles are registered in the LDM database, as defined by (4.12). Vehicles converge to the same optimal size of the minimum contention window. This not only minimizes the probability of packet collisions in the neighborhood of the transmitting vehicle but also decreases the negative impact of the hidden terminals.

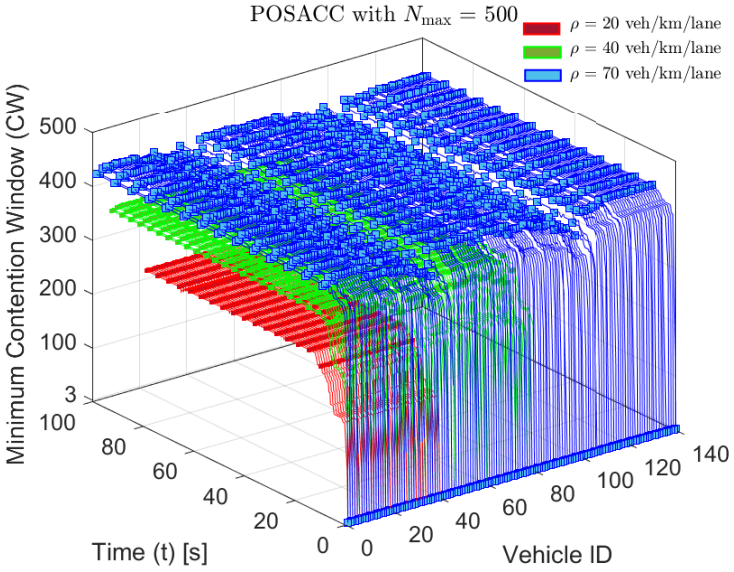

Figure 4.14: Size of the minimum contention window computed in real-time by the vehicles on different traffic situations with POSACC.

Fig. 4.15 shows the average transmission parameters computed by the beaconing algorithms on each traffic scenario. POSACC adapts to vehicular traffic dynamics by using the proposed control mechanisms. Note that the design strategy reduces the conflict between the required goals. The beacon rate and transmission power decrease for higher traffic densities, since the velocity of the vehicles is reduced and more vehicles are involved in interferences. Further, the size of the minimum contention window decreases as the beacon rate increases because the traffic density is reduced and the end-to-end latency becomes more critical. For instance, in the traffic scenario of 10 veh/km/lane (100 km/h), POSACC increases the transmission rate up to 14 beacon/s to limit the average position error to 1 m, but at the same time, it sets the smallest size of the minimum contention window (e.g., 200 and 300) to reduce the latency and minimize the probability of packet collisions.

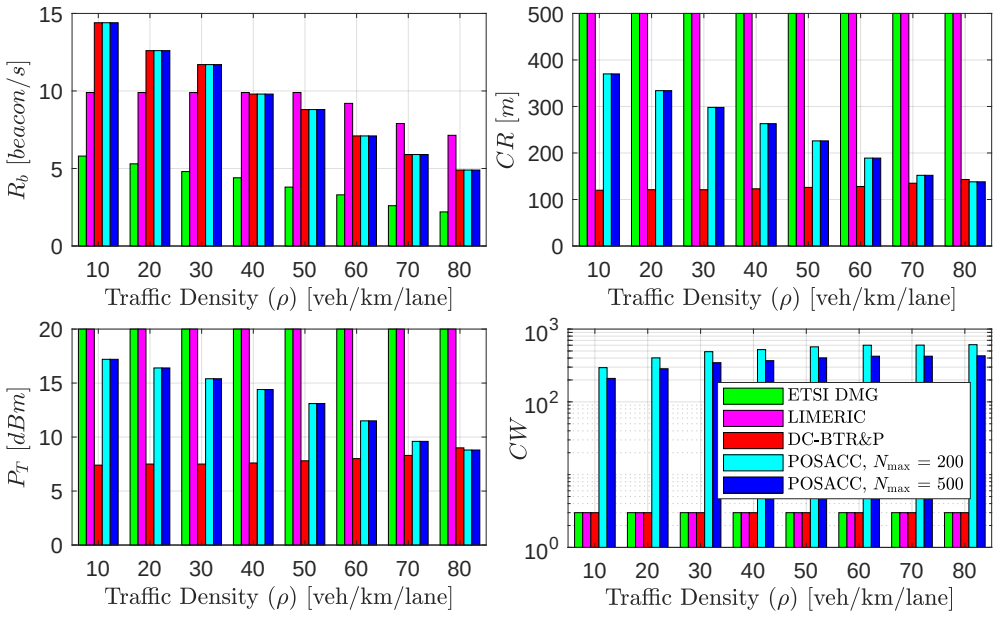

Figure 4.15: Transmission parameters computed by the beaconing algorithms.

4.5.2 Performance of the POSACC Algorithm

This subsection presents the evaluation results of POSACC compared with ETSI DMG, LIMERIC, and DC-BTR&P in terms of position accuracy, communication reliability, channel load, and end-to-end latency.

Fig. 4.16 shows the histograms with the relative probability of the average and maximum position error achieved by the beaconing algorithms in the traffic setups of 50 veh/km/lane (60 km/h) and 10 veh/km/lane (100 km/h). As defined by (4.1), the maximum position error is twice the average position error. We can observe the effectiveness of POSACC to achieve an average position error of 1 m. However, ETSI DMG only achieves half of the position accuracy provided by POSACC. Unlike ETSI DMG and POSACC, LIMERIC cannot guarantee a pre-defined position error. Note that the position error increases as the velocity of the vehicle increases. The reason is that LIMERIC controls the beacon transmission rate according to the channel load, without taking into account the vehicular traffic dynamics. The gain saturation technique limits the transmission rate to 10 beacon/s in low density - high speed scenarios (see Fig. 4.15). Despite that a beacon rate of 10 beacon/s provides a

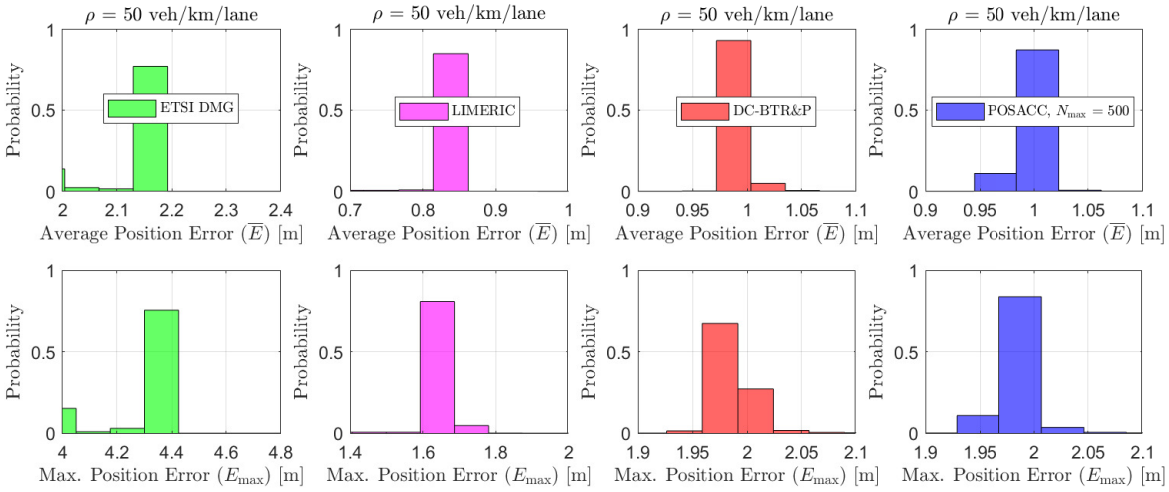

(a)

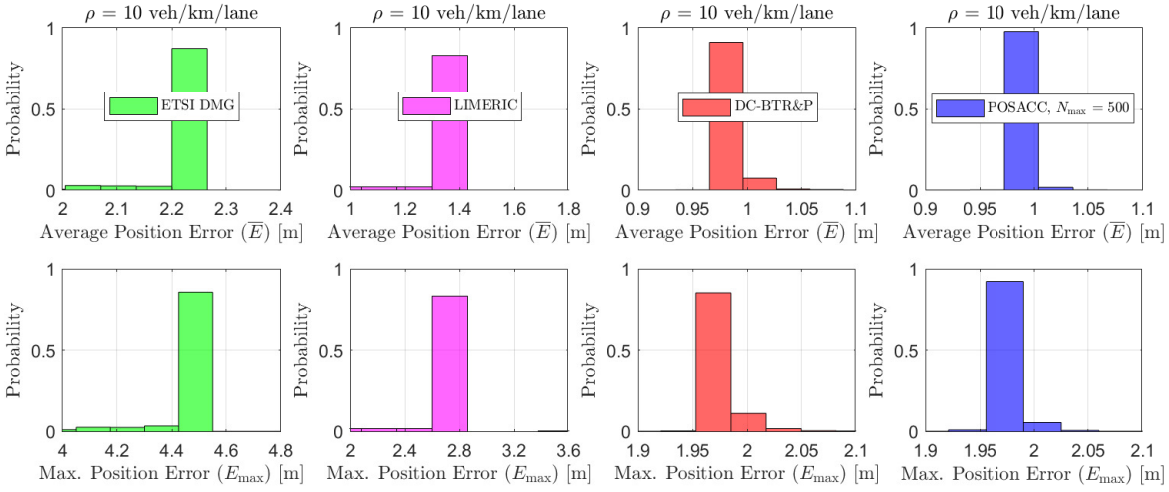

(b)

Figure 4.16: Probability-based histograms of the average and maximum position error achieved by the adaptive beaconing algorithms for (a) $\rho = 50$ veh/km/lane and (b) $\rho = 10$ veh/km/lane.

good position accuracy on a wide range of traffic conditions, this transmission rate is not enough to achieve an average position error of 1 m in vehicular scenarios where the velocity exceeds 80 km/h, as shown in Fig. 4.16b.

Fig. 4.17a illustrates that the position accuracy achieved by POSACC is better than the ETSI DMG and LIMERIC in each traffic setup. Note that 95 % of the maximum position error population falls below 2 m, which means that most of the vehicles compute an average position error of 1 m. Further, POSACC also achieves lower peaks of the maximum position error on all conditions, as shown in Fig. 4.17b. Both algorithms ETSI DMG and LIMERIC have limitations when applied to cooperative safety-critical applications. Trigger conditions in ETSI DMG lead to low beacon rates in order to alleviate the channel load and maintain

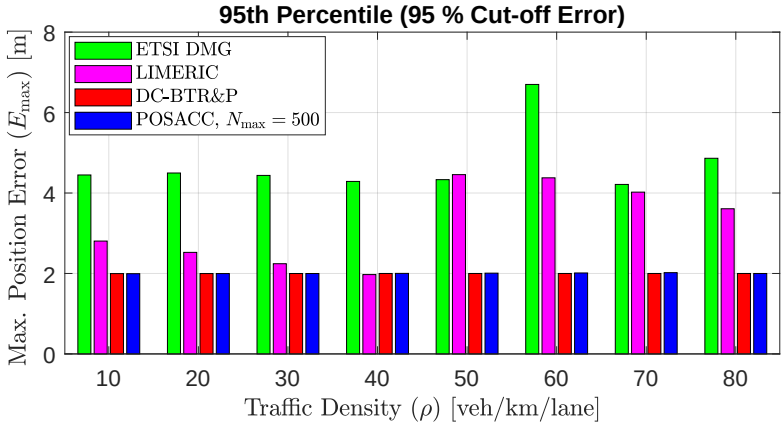

(a)

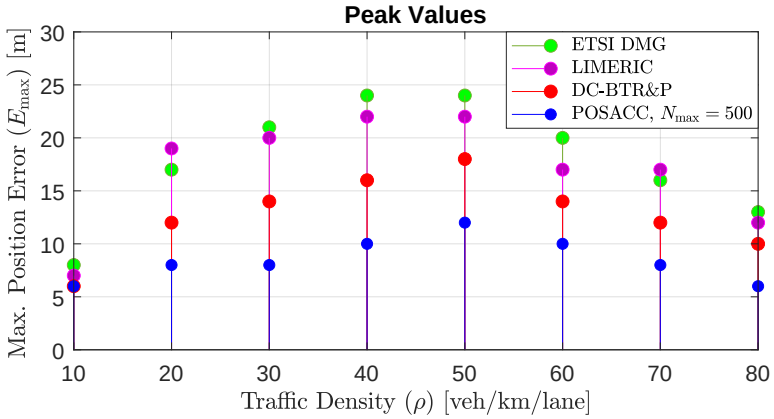

(b)

Figure 4.17: (a) 95 % cut-off and (b) peak values of the maximum position error achieved by the beaconing algorithms.

a certain level of awareness. However, packet losses have more impact on position error at lower beacon rates. This means that for each beacon lost in ETSI DMG, the position error increases by 4 m. Accordingly, the peak values of the maximum position error in ETSI DMG increase up to 24 m, as shown in Fig. 4.17b. In addition, ETSI DMG has the worst performance in the traffic setup of 60 veh/km/lane, achieving a 95 % cut-off error higher than 6 m. This analysis is supported by the packet delivery ratio (PDR) shown in Fig. 4.18. The vertical lines in Fig. 4.18 represent the 25th and 75th percentiles. We can observe that the mean PDR achieved by ETSI DMG in the traffic setup of 60 veh/km/lane is below 0.92.

In LIMERIC, the gain saturation technique leads to a high beacon rate in low densities. Therefore, it only sets a beacon rate lower than 10 beacon/s if the traffic density is high, for example, when exceeds 50 veh/km/lane (see Fig. 4.15). If the beacon transmission rate is high, the impact of packet losses on the position error is lower. However, recurring packet losses eventually will lead to a higher position error, as shown in Fig. 4.17b. Note that the peaks of the maximum position error in LIMERIC are close to the peaks computed by ETSI DMG. This effect also can be observed in the traffic densities from 50 to 80 veh/km/lane, where the 95 % cut-off error achieved by LIMERIC increases up to 4 m (see Fig. 4.17a) and the mean PDR does not exceed 0.91 (see Fig. 4.18). For instance, it is expected that

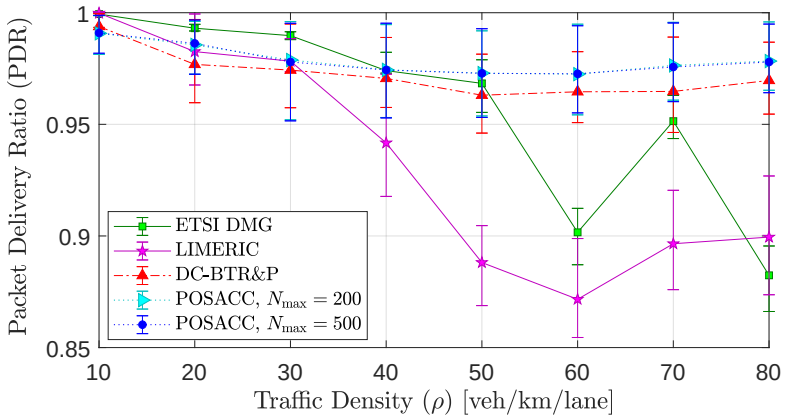

Figure 4.18: Packet delivery ratio computed by the beaconing algorithms on each traffic setup.

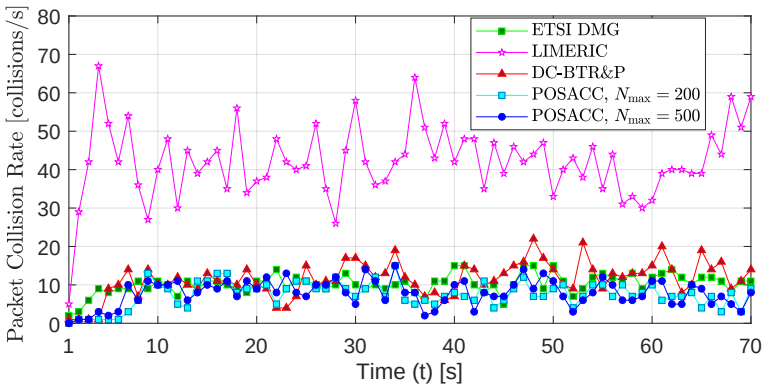

Figure 4.19: Packet collisions per second measured in the traffic setup of 60 veh/km/lane.

the maximum position error computed by LIMERIC be 1.4 m in the traffic density of 70 veh/km/lane (40 km/h). However, the 95 % cut-off maximum position error is almost three times higher than the expected value due to packet losses.

Fig. 4.18 shows that POSACC has also the best performance in terms of communication reliability, achieving a mean PDR higher than 0.95 for each traffic setup. The PDR achieved by LIMERIC decreases as traffic density increases. Since vehicles adjust the beacon rate to achieve fairness, it requires a great number of vehicles sharing the channel resources to set a low transmission rate. Fig. 4.15 shows that even in the more dense setups, the average beacon rate of LIMERIC is higher than 6 beacon/s. Consequently, more vehicles suffer from interference, leading to a higher packet collision rate, as shown in Fig. 4.19. This is critical in non-homogeneous scenarios where vehicles are moving at different speeds (e.g., a two-way highway in free flow and congested state). The interference generated by the congested section leads to a low position accuracy in the vehicles that move at high speed. ETSI DMG is also affected by vehicular density. We notice that controlling the beacon rate according to vehicle dynamics is not sufficient to guarantee a PDR higher than 0.95 on each traffic setup.

Fig. 4.20 shows that POSACC is able to regulate the channel load by adapting the beacon rate according to vehicle traffic dynamics. In this figure, the vertical lines also represent the 25th and 75th percentiles. As expected, ETSI DMG and LIMERIC measure the lower and

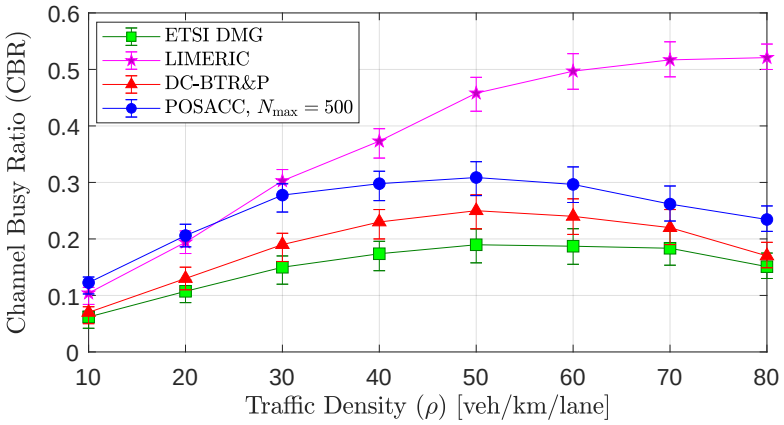

Figure 4.20: Channel busy ratio computed by the beaconing algorithms on each traffic setup.

higher CBR, respectively. ETSI DMG achieves a low CBR at the cost of reducing the position accuracy. Instead, LIMERIC maximizes channel utilization at the cost of reducing communication reliability. Whereas for POSACC, the measured CBR does not exceed 35 % of the channel capacity, and it is controlled by the relationship between the average velocity and traffic density (see [15]). Note that the CBR increases, then it remains stable and finally decreases. However, in the more dense traffic setups, the CBR measured by LIMERIC exceeds 50 % of channel capacity.

In POSACC, the adaptive control of the minimum contention window provides a high position accuracy without significantly affecting communication reliability, as shown in Fig. 4.19. Note that POSACC and ETSI DMG compute a similar packet collision rate, but POSACC achieves a position accuracy two times higher. POSACC guarantees the priority metrics at the cost of increasing the end-to-end latency, as shown in Fig. 4.21. However, the 95 % cut-off end-to-end latency computed in all conditions are far away from the upper limit of 300 ms specified by ETSI for cooperative safety applications (see [12], [13]). In fact, the 95 % cut-off latency does not exceed 11 ms, and it is lower than 8 ms for $N_{max} = 500$. We notice that both setups of N_{max} achieve similar performance in terms of communication reliability (see Fig. 4.18); however, the setup of $N_{max} = 200$ leads to an increase in the

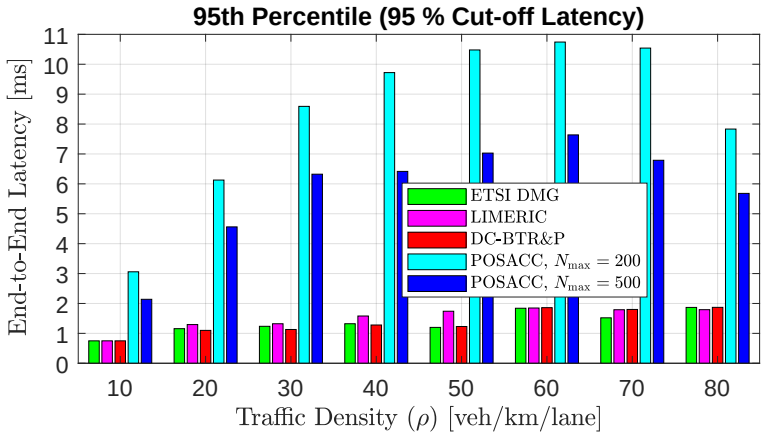

Figure 4.21: End-to-end latency performance (95 % cut-off latency) achieved by the beaconing algorithms.

latency up to 3 ms. POSACC keeps a balance between the end-to-end latency and beacon interval in order to avoid packet losses due to expiration time reached. Note that an increase in the end-to-end latency also corresponds to an increase in beacon interval (see Fig. 4.15). Accordingly, POSACC provides the position accuracy and communication reliability required by cooperative safety applications with a 95 % cut-off latency that does not exceed 8 % of the beacon interval.

4.6 Conclusion

In this paper, we proposed an adaptive beaconing algorithm, called POSACC, for cooperative vehicular safety systems. We designed three different control mechanisms to guarantee specific performance metrics. The performance of POSACC algorithm was evaluated in different traffic setups and compared against three different state-of-the-art beaconing algorithms; ETSI DMG, LIMERIC, and DC-BTR&P. Extensive evaluation results demonstrated that the design strategy was able to reduce the conflict between the required goals. The proposed control mechanisms proved their effectiveness to control the beacon transmission parameters in real-time. POSACC was able to limit the position error and improve communication reliability, while maintaining the warning distance, channel load, and end-to-end latency within the desired limits. POSACC outperformed the benchmark beaconing algorithms by guaranteeing the operational requirements of cooperative safety applications in a wider range of traffic situations. POSACC achieved in each traffic setup a 95 % cut-off average position error of 1 m and PDR higher than 0.95, with a 95 % cut-off end-to-end latency that did not exceed 8 % of the beacon interval. Regarding future works, we intend to study the benefits and limitations of controlling the values of $CW_{\max}$ and $N_{\max}$ in real-time according to the surrounding traffic situation, as well as using nonlinear functions in the contention window control mechanism.

4.7 Acknowledgements

This work has been partially supported by CONICYT Doctoral Grant No. 21171722; Project ERANET-LAC ELAC2015/T10-0761; FONDECYT Post-Doctoral under Grant 3170021; and in Brazil by the National Council for Scientific and Technological Development (CNPq).

Chapter 5

Impact of Awareness Control on V2V-based Overtaking Application in Autonomous Driving

In autonomous driving, IEEE 802.11p-based vehicle-to-vehicle (V2V) communication is considered for overcoming the intrinsic limitations of sensors and supporting safety applications. In this letter, we evaluate the effectiveness of relevant awareness control approaches, such as ETSI DMG, IVTRC, and POSACC, to support the V2V-based overtaking application in autonomous driving. For this, we assess the incident detection capability of the overtaking application when it is running with messages gathered from these approaches, considering packet losses due to channel fading. Simulations show that POSACC is more effective than the remaining approaches for detecting unsafe overtaking maneuvers in different operating conditions.

5.1 Introduction

Autonomous driving is expected to reduce the number of traffic accidents caused by human errors [86]. Currently, autonomous vehicles (AVs) can perform safety operations such as forward collision avoidance, traffic sign detection, and lane departure warning [87]. However, performing other safety operations such as overtaking, which requires to determine whether a gap is safe for the maneuver considering the trajectory of the AVs in the vicinity, is still challenging. This is because sensors (e.g., radars, lasers, and cameras) are incapable of determining the location of oncoming traffic successfully. Further, sensors are unable of detecting potential threats a few blocks away due to their limited view [88]. Despite sensors' limitations, they still are the cornerstone of different proposals to support overtaking applications (e.g., in [89], automotive radars are used for video rate control to improve the visual quality of drivers). A viable solution for overcoming the limitations of sensors is to enable wireless links between the AVs.

By using vehicle-to-vehicle (V2V) communication based on IEEE 802.11p [8], the motion parameters of the AV (e.g., its position, speed, and acceleration) can be regularly transmitted

in the form of cooperative awareness messages (CAMs) [11]. CAMs are essential for tracking highly dynamic neighboring vehicles and supporting high-level safety applications. Standard CAMs are broadcasted at a fixed message transmission frequency ranging from 1 to 10 Hz [11]. However, the varying conditions of the wireless channel and vehicular traffic impose the necessity of considering congestion and awareness control approaches [11], [33], [35], [47], [45]. For instance, the European Telecommunication Standards Institute (ETSI) defined the dynamic message generation (DMG) approach in [11], which is a kinematic-based mechanism that controls CAMs triggering. ETSI also defined a set of decentralized congestion control (DCC) mechanisms [33] that adapt the message transmission parameters to keep the channel load below a target threshold. Unlike ETSI proposals, the Inter-Vehicle Transmit Rate Control (IVTRC) approach set by Huang et al. in [35] and its variant based on tracking error threshold (IVTRC-Th) [47], adapt the message transmission rate in a probabilistic manner based on positioning tracking error. Bolufé et al. [45] introduced a POSition-ACCuracy (POSACC) based awareness control approach where message transmission parameters are controlled depending on vehicle dynamics and surrounding road traffic to limit the position error and improve communication reliability.

Although numerous adaptive approaches with diverse goals have been proposed in the literature, to date little attention has been paid on whether the proposed approaches are adequate or not to support safety applications. In particular, safety-critical applications aimed at detecting new neighboring vehicles with sufficient time to react and avoid a traffic accident, such as the V2V-based overtaking application. To our best knowledge, no literature has put to work together the overtaking application and awareness control approaches so far.

In this letter, we evaluate the effectiveness of relevant awareness control approaches, such as ETSI DMG [11], IVTRC [35], IVTRC-Th [47], and POSACC [45], to support the V2V-based overtaking application in autonomous driving. In particular, we assess the incident detection capability of the overtaking application when it is running with CAMs gathered from these approaches. The main contribution of this work is to evaluate the impact of the addressed awareness control approaches on predicting unsafe overtaking maneuvers, taking into account motion state sensors' errors and packet losses due to channel fading.

5.2 System Model

We consider three AVs, A (AV that intends to overtake), C (AV that will eventually be overtaken by A), and B (AV that oncoming to A and C from the opposite lane), as illustrated in Fig. 5.1. Then, the overtaking application running on A should monitor the movement status of C, and at the same time, use the received CAMs for tracking the position of B in order to evaluate the suitability of the overtaking maneuver and avoid unsafe executions.

5.2.1 Overtaking Time Estimation

Assume that AVs A and C move at the same speed[1] ($v_A = v_C$) at the beginning of the overtaking maneuver, and A starts accelerating with a_A^{ov} to change the lane and overtake

[1]In order to reduce the complexity, the model considers the movement in a single dimension (longitudinal displacement of the vehicle), obviating any transverse movement.

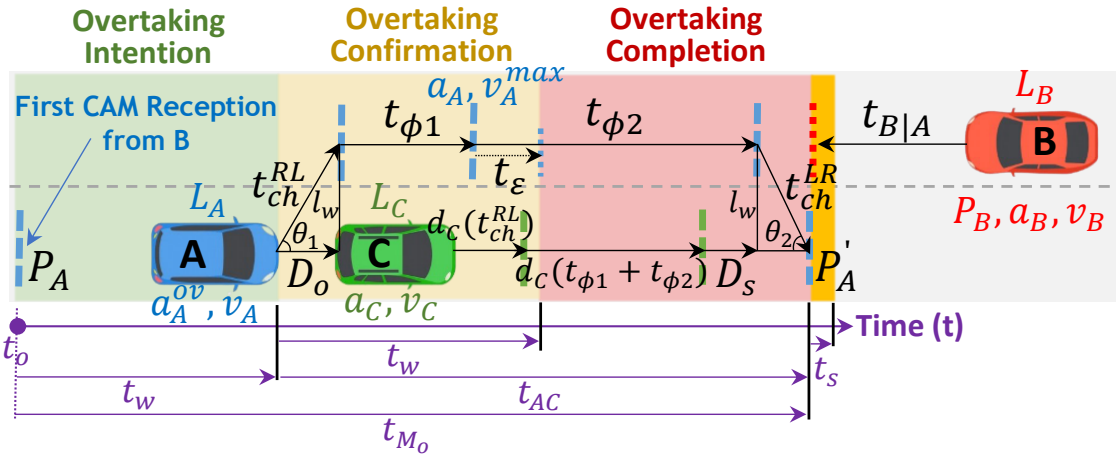

Figure 5.1: Overtaking scenario. AV A changes the lane from its right to left to overtake C. To ensure the reliability of the maneuver, we assume a time window (t_w) for the overtaking intention equal to the overtaking confirmation.

C, as shown in Fig. 5.1. The initial overtaking heading (θ_1) of A can be computed as, $\theta_1 = \tan^{-1}\left(\frac{l_w}{D_o}\right)$ [90], where l_w is the lane width and D_o is the initial distance between A and C (regarding the front side of A and rear side of C). The distance travelled by A during the lane change maneuver (from its right to left) is, $\mathrm{d}_A(t_{ch}^{RL}) = v_A \cdot t_{ch}^{RL} + \frac{a_A^{ov}\cdot(t_{ch}^{RL})^2}{2}$, where t_{ch}^{RL} represents the time needed by A to change the lane (from its right to left), which can be computed as,

$$t_{ch}^{RL} = \frac{-v_A + \left(v_A^2 + \frac{2a_A^{ov} l_w}{\sin\theta_1}\right)^{\frac{1}{2}}}{a_A^{ov}}, \; a_A^{ov} > 0. \tag{5.1}$$

We assume that A accelerates with a_A^{ov} until it reaches the maximum allowed overtaking velocity, $v_A^{\max}$. The time ($t_{\phi 1}$) needed by A to reach $v_A^{\max}$ once the first lane change has been done is,

$$t_{\phi 1} = \frac{v_A^{\max} - \left(v_A + a_A^{ov}\cdot t_{ch}^{RL}\right)}{a_A^{ov}}. \tag{5.2}$$

Then, A completes the overtaking maneuver at uniform motion. In order to carry out the overtaking in a reasonable time and represent a more realistic overtaking situation, we also assume that: i) C moves with uniform motion during the entire overtaking maneuver and ii) sensor's noisy measurements over the real acceleration of A and C are considered, as specified in [91]. Hence, the estimated acceleration of A and C could be non zero even in uniform motion. Accordingly, a_A and a_C are the measured acceleration of A and C, respectively, in uniform motion, as shown in Fig. 5.1. Once $v_A^{\max}$ is reached, the time ($t_{\phi 2}$) needed by A to overtake C in a safety distance, D_s, can be derived from,

$$\mathrm{d}_A(t_{\phi 1}) + \mathrm{d}_A(t_{\phi 2}) = \mathrm{d}_C(t_{ch}^{RL}) + \mathrm{d}_C(t_{\phi 1}+t_{\phi 2}) + D_s + L_A + L_C, \tag{5.3}$$

where L_A and L_C are the length of A and C, respectively. So, $t_{\phi 2}$ can be estimated as follows,

$$t_{\phi 2} = \begin{cases} \dfrac{\mathrm{d}_C(t_{\phi 1}) - \mathrm{d}_A(t_{\phi 1}) + \mathrm{d}_C(t_{ch}^{RL}) + D_s + L_A + L_C}{v_A^{\max} - v_C - a_C t_{\phi 1}}, \\ \qquad\qquad\qquad\qquad\qquad\qquad\qquad\qquad \text{if } a_A = a_C, \forall v_A^{\max} \,/\, \exists\, t_{\phi 2} > 0, \\ \dfrac{-(v_A^{\max} - v_C - a_C t_{\phi 1}) + \Big[(v_A^{\max} - v_C - a_C t_{\phi 1})^2 + 2(a_A - a_C)\big(\mathrm{d}_C(t_{\phi 1}) - \mathrm{d}_A(t_{\phi 1}) + \mathrm{d}_C(t_{ch}^{RL}) + D_s + L_A + L_C\big)\Big]^{\frac{1}{2}}}{a_A - a_C}, \\ \qquad\qquad\qquad\qquad\qquad\qquad\qquad\qquad \text{if } a_A \neq a_C, \forall v_A^{\max} \,/\, \exists\, t_{\phi 2} > 0. \end{cases} \tag{5.4}$$

The time required by A to change the lane (from its left to right) depending on the final overtaking heading (θ_2) can be computed as,

$$t_{ch}^{LR} = \begin{cases} \dfrac{l_w}{v_A^{\max} \sin\theta_2}, & a_A = 0, \\ \dfrac{-v_A^{\max} + \left((v_A^{\max})^2 + \frac{2 a_A l_w}{\sin\theta_2}\right)^{\frac{1}{2}}}{a_A}, & a_A \neq 0. \end{cases} \tag{5.5}$$

Finally, the total time required by A to overtake C can be computed as follows,

$$t_{AC} = t_{ch}^{RL} + t_{\phi 1} + t_{\phi 2} + t_{ch}^{LR}. \tag{5.6}$$

5.2.2 Time Window

As shown in Fig. 5.1, we set the complexity of the overtaking maneuver into three different stages. 1) Overtaking Intention: it starts when AV A receives the first CAM from oncoming AV B, indicating that there is a sufficient gap to perform a safe overtaking maneuver. Here, A follows C with uniform motion maintaining controlled the distance D_o. If one or more CAMs are received into a time window confirming that the overtaking maneuver can be successfully performed, A goes forward to the second stage. 2) Overtaking Confirmation: A (into a time window) determines whether to continue or not the overtaking maneuver depending on previously received information and new CAMs arriving from B; and 3) Overtaking Completion: A completes the overtaking.

We set the same time window for stages 1 and 2. We define this time window as the time required by A to reach C during the overtaking (see Fig. 5.1). This is a suitable assumption since this time interval allows A to abort the maneuver without causing a dangerous situation regarding C. The time window can be computed as,

$$t_w = t_{ch}^{RL} + t_{\phi 1} + t_{\varepsilon}, \tag{5.7}$$

where t_ε is the time required by A to reach C once $v_A^{\max}$ is accomplished, as shown in Fig. 5.1. The time (t_ε) can be derived from,

$$\mathrm{d}_A(t_{\phi 1}) + \mathrm{d}_A(t_\varepsilon) = \mathrm{d}_C(t_{ch}^{RL}) + \mathrm{d}_C(t_{\phi 1} + t_\varepsilon). \tag{5.8}$$

By using kinematic equations in (5.8), t_ε (which is a small time interval) can be estimated as,

$$t_\varepsilon = \frac{v_C(t_{ch}^{RL} + t_{\phi 1}) - \mathrm{d}_A(t_{\phi 1})}{v_A^{\max} - v_C}. \tag{5.9}$$

Note that: $\exists\, t_\varepsilon \;\forall\, v_A^{\max} \,/\, v_C(t_{ch}^{RL} + t_{\phi 1}) > \mathrm{d}_A(t_{\phi 1})$.

5.2.3 Encounter Time Estimation

The AV A utilizes a kinematics-based trajectory prediction model and the received CAMs for tracking the new positions of B. Consider that P_A is the position of A when the first CAM from B is received, and $P_A^{'}$ is the position of A at the end of the overtaking maneuver, as shown in Fig. 5.1. On each received CAM, the position (P_B), speed (v_B), and acceleration (a_B) of B are used by A as input for the following prediction model equation,

$$\begin{bmatrix} P_B^k \\ v_B^k \end{bmatrix} = \begin{bmatrix} 1 & \Delta t \\ 0 & 1 \end{bmatrix} \cdot \begin{bmatrix} P_B^{k-1} \\ v_B^{k-1} \end{bmatrix} + \begin{bmatrix} \frac{\Delta t^2}{2} \\ \Delta t \end{bmatrix} a_B. \tag{5.10}$$

If past a Δt time step no CAM is received, A uses (5.10) and the previous information to predict the new position (P_B^k) and velocity (v_B^k) of B. In (5.10), k and $k-1$ are the current state and previous state, respectively.

Once the position of B has been updated, A can estimate the encounter distance as follows,

$$\mathrm{d}_{B|A} = |P_A - P_B^k| - \mathrm{d}_T, \tag{5.11}$$

where d_T is the euclidean distance between P_A and $P_A^{'}$. This distance is computed as follows,

$$\mathrm{d}_T = \mathrm{d}_A(t_w) + D_o + \mathrm{d}_A(t_{\phi 1}) + \mathrm{d}_A(t_{\phi 2}) + \frac{l_w}{\tan\theta_2}. \tag{5.12}$$

Finally, the time required by B to encounter A is computed as,

$$t_{B|A} = \begin{cases} \dfrac{\mathrm{d}_{B|A}}{v_B^k}, & a_B = 0, \\ \dfrac{-v_B^k + \left({v_B^k}^2 + 2a_B \mathrm{d}_{B|A}\right)^{\frac{1}{2}}}{a_B}, & a_B \neq 0. \end{cases} \tag{5.13}$$

5.2.4 Overtaking Maneuver Decision

As can be observed in Fig. 5.1, the time ($t_{M_\circ}$) needed by A to complete the full maneuver (stage 1 and overtaking) regarding the instant t_o at which the first CAM from B is received, can be computed as,

$$t_{M_\circ} = t_w + t_{AC}. \tag{5.14}$$

As A moves forward, the remaining maneuver time at the k^{th} time step (τ) can be computed as, $t_{M_k} = t_{M_\circ} - k\tau$. To increase safety during the maneuver, we consider an additional margin of time, called safety time (t_s), as illustrated in Fig. 5.1. If ($t_{M_k} + t_s$) is less than ($t_{B|A}$), A deems the maneuver as safe and goes forward. However, if ($t_{M_k} + t_s$) is greater or equal than ($t_{B|A}$), A deems the maneuver as unsafe and it is aborted.

5.3 V2V-based Overtaking Application

The steps followed by the V2V-based overtaking application can be observed in **Algorithm 8**. We assume that the responsibility of setting, controlling, and maintaining the overtaking maneuver parameters rely on the autonomous driven system (ADS) of AV A. Furthermore, AVs A and B can get their position, speed, and acceleration from on-board sensors. A also utilizes short-range sensors to regularly measure the speed and acceleration of C. In addition, A and B utilize Kalman Filters (KFs) to estimate the values of measured status parameters. In consequence, the parameters' values utilized by the overtaking application, as well as the included in CAMs, are the estimated values[2] resulting from applying KFs. Then, on each received CAM or state prediction, A determines whether to continue or abort the overtaking maneuver based on the computed values of t_{M_k} and $t_{B|A}$. To increase the robustness of the overtaking application, the computed values of t_w and $t_{M_\circ}$ are averaged (av) over time. The parameter (γ^*) is a function that returns the current time in milliseconds. Note that state predictions occur at regular time intervals (Δt) after each CAM received from B.

Algorithm 8: V2V-based Overtaking Application on AV A

Initial Conditions: $\{P_A, v_A, a_A, P_B, v_B, a_B, v_C, a_C, t_o\}$
Overtaking Parameters: $\{\theta_{1,2}, a_A^{ov}, v_A^{\max}, t_s, D_o, D_s\}$
Result: {ABORT}
Rx: *On each CAM from AV B, cancel the scheduled task and*, **do**:
begin
1 **call** *D*ecide;
2 **Every** Δt **up to** $t_o + 2t_w^{av}$ **do**
3 Update $\begin{bmatrix} P_B^k \\ v_B^k \end{bmatrix}$ (5.10);
4 **call** *D*ecide;

Function *D*ecide(P_B, v_B, a_B)
1 Compute t_w (5.7), $t_{B|A}$ (5.13), and $t_{M_\circ}$ (5.14);
2 $t_{M_k} \leftarrow t_{M_\circ}^{av} - (\gamma^* - t_o)$;
3 **if** $(t_{M_k} + t_s \geq t_{B|A})$ **then**
4 set ABORT;

[2]Since we assume that B is moving along a straight road, the KF not only allows B to accurately estimate its lateral position, but also allows A to locate B in the correct lane.

5.4 Awareness Control Approaches

To evaluate the impact of awareness control on the V2V-based overtaking application, four different approaches proposed in the literature are used on the AV B: ETSI DMG [11], IVTRC [35], IVTRC-Th [47], and POSACC [45]. The awareness control approach introduced by European standards is ETSI DMG [11]. It transmits a new CAM if one of the following conditions has been detected: i) The difference between current and previous position exceeds 4 m (e.g., $\Delta pos \geq 4$ m); ii) The difference between current and previous velocity exceeds 0.5 m/s (e.g., $\Delta vel \geq 0.5$ m/s); and iii) The difference between current and previous heading exceeds 4° (e.g., $\Delta head \geq 4°$). The objective of ETSI DMG is to provide a certain level of cooperative awareness while implicitly controlling the channel load.

Unlike ETSI DMG, IVTRC [35] computes the CAM transmission probability of B, $p_B(t)$, based on positioning tracking error, $\tilde{e}_B(t)$, as follows: $p_B(t) = 1 - \exp(-\alpha\, \tilde{e}_B^2(t))$, where α is a positive real number, representing the sensitivity to $\tilde{e}_B(t)$. After each CAM transmission, IVTRC uses the packet erasure rate (Ω_B) to stochastically determine the positioning tracking error $\tilde{e}_B(t)$: $\tilde{e}_B(t^+) = (1 - \zeta_B(t))\tilde{e}_B(t)$, where $\zeta_B(t)$ is a Bernoulli trial with probability $Pr(\zeta_B(t) = 0) = \Omega_B$. Then, if successful, i.e., $\zeta_B(t) = 1$, $\tilde{e}_B(t^+)$ is reset to zero; otherwise, $\tilde{e}_B(t^+)$ accumulates from $\tilde{e}_B(t)$ based on first-order kinematic model, as specified in [35]. In this work, Ω_B is estimated every second depending on CAMs received by the AV A. This is a suitable assumption since a symmetric network is considered in [35]. IVTRC-Th [47] is a variant of IVTRC based on tracking error threshold (e_{th}). Here, if the $\tilde{e}_B(t)$ is larger than e_{th}, the CAM transmission probability of B is computed as follows: $p_B(t) = 1 - \exp(-\alpha|\ \tilde{e}_B(t) - e_{th}\ |^2)$. Otherwise, if $\tilde{e}_B(t)$ is smaller than e_{th}, there is no transmission at all from B (i.e., $p_B(t) = 0$). CAM trigger conditions on ETSI DMG, IVTRC, and IVTRC-Th are checked at a fixed time interval, denoted in this work as Status Monitoring and Decision Interval (SMDI).

POSACC [45, Alg. 1] adjusts the message transmission rate in real-time depending on the movement dynamics of B. On each CAM transmission, POSACC gets the velocity (v_B) and acceleration (a_B) of B as well as the transmission delay (t_D). Then, it defines the movement status (e.g., repose, accelerated motion, uniform motion, or deceleration) and uses a kinematic-based model to set the required CAM transmission interval for guaranteeing the pre-define average position error ($\overline{E}_B$). The settings of the awareness control approaches are summarized in Table 5.1.

Table 5.1: Settings of the Awareness Control Approaches

Approach	Parameter	Value
ETSI DMG†	Δpos	≥ 4 m [11]
	Δvel	≥ 0.5 m/s [11]
	SMDI	50 ms [11]
IVTRC	Sensitivity (α)	30 [35]
	SMDI	50 ms [35]
IVTRC-Th	Sensitivity (α)	30 [35]
	Tracking Error Threshold (e_{th})	0.2 m [47]
	SMDI	50 ms [35]
POSACC	Average Position Error ($\overline{E}_B$)	1 m [45]
	Transmission Delay (t_D)	500 μs [45]

† Changes on heading of AV B are not considered since we assume that it moves along a straight road.

5.5 Simulation Results and Discussion

The experiments were conducted with Matlab in a two-lane straight road, as illustrated in Fig. 5.1. To model a wide range of overtaking situations, three different initial velocities (v_A, v_C) for the AVs A and C were considered, as can be observed in Table 5.2. We set initial (D_o) and safety (D_s) distances of 18, 25, and 32 m according to the braking distance[3] required for a velocity (v_A, v_C) of 60, 70, and 80 km/h, respectively. These distances also are within the range analyzed in [92]. We use a normally distributed noise with zero mean and standard deviation of 0.3 m/s^2, 0.27 m/s, and 1.5 m to model sensing errors [91]. These values are also utilized as initial conditions for KFs. Further, we consider communication channel impairments associated with low traffic density environments where overtaking maneuvers are common, such as packet losses due to channel fading. To model packet losses, we utilize an IEEE 802.11p V2V fading channel[4] with additive white Gaussian noise and Doppler spread. According to [8], at the physical (PHY) layer, we set a 10 MHz channel, a PHY service data unit (PSDU) of 350 bytes, a quadrature-phase-shift keying (QPSK) modulation, a code rate of 1/2, resulting in a data-rate of 6 Mbps. The remaining simulation parameters are given in Table 5.2.

Table 5.2: Simulation Parameters

Parameter	**Value**
Road Length	1 km
Lane Width (l_w)	3.5 m [90]
Vehicle Length (L_A, L_B, L_C)	4 m [92]
Vehicle Width	1.8 m
Initial Distance (D_o)	18, 25, 32 m [92]
Safety Distance (D_s)	18, 25, 32 m [92]
Overtaking heading (θ_1, θ_2)	$\approx 11°, 8°, 6°$
Initial Velocity‡ (v_A, v_C)	60, 70, 80 km/h
Maximum Overtaking Velocity ($v_A^{\max}$)	90, 100, 110 km/h
Acceleration in Uniform Motion (a_A, a_C)	0 m/s^2
Overtaking Acceleration (a_A^{ov})	2.5 m/s^2
Safety Time (t_s)	0.5 s
Prediction Interval (Δt)	50 ms
Number of Simulated Incidents	$18 \cdot 10^5$

‡ We utilize typical movement parameters of two-way roads where overtaking maneuvers are common.

Fig. 5.2a illustrates the measurements that AV A gets from its own acceleration and from the acceleration of C, as well as the acceleration estimated by its KFs. By using the estimated acceleration, A computes the t_w which for an initial velocity (v_A, v_C) of 70 km/h is 4.6 s (with t_{ch}^{RL}, $t_{\phi 1}$, and t_ε equal to 1.2 s, 2.1 s, and 1.3 s, respectively). Accordingly, the $t_{M_\circ}$ is 14.1 s, where t_{AC} is 9.5 s with $t_{\phi 2}$ equal to 5.3 s and t_{ch}^{LR} of 0.9 s. In Fig. 5.2a, the AV B moves at 70 km/h and accelerates at 2.5 m/s^2 until reaching a maximum velocity of 90 km/h. To model an incident[5], we configure B to accelerate within the t_w of stage 2, as shown in Fig. 5.2a. An incident occurs when the encounter time $(t_{B|A})$ is less than the remaining maneuver time plus the safety time $(t_{M_k} + t_s)$, as illustrated in Fig. 5.2b for an ideal channel. Note that the probability of detecting an incident strongly depends on the transmissions accomplished

[3]Precise method for calculating the braking distance.

[4]Matlab, "802.11p Packet Error Rate Simulation for a Vehicular Channel," 2020.

[5]We assume our system to work in the worst case, *i.e.*, without channel tracking and that the maneuver is only aborted by A based on CAMs received from B.

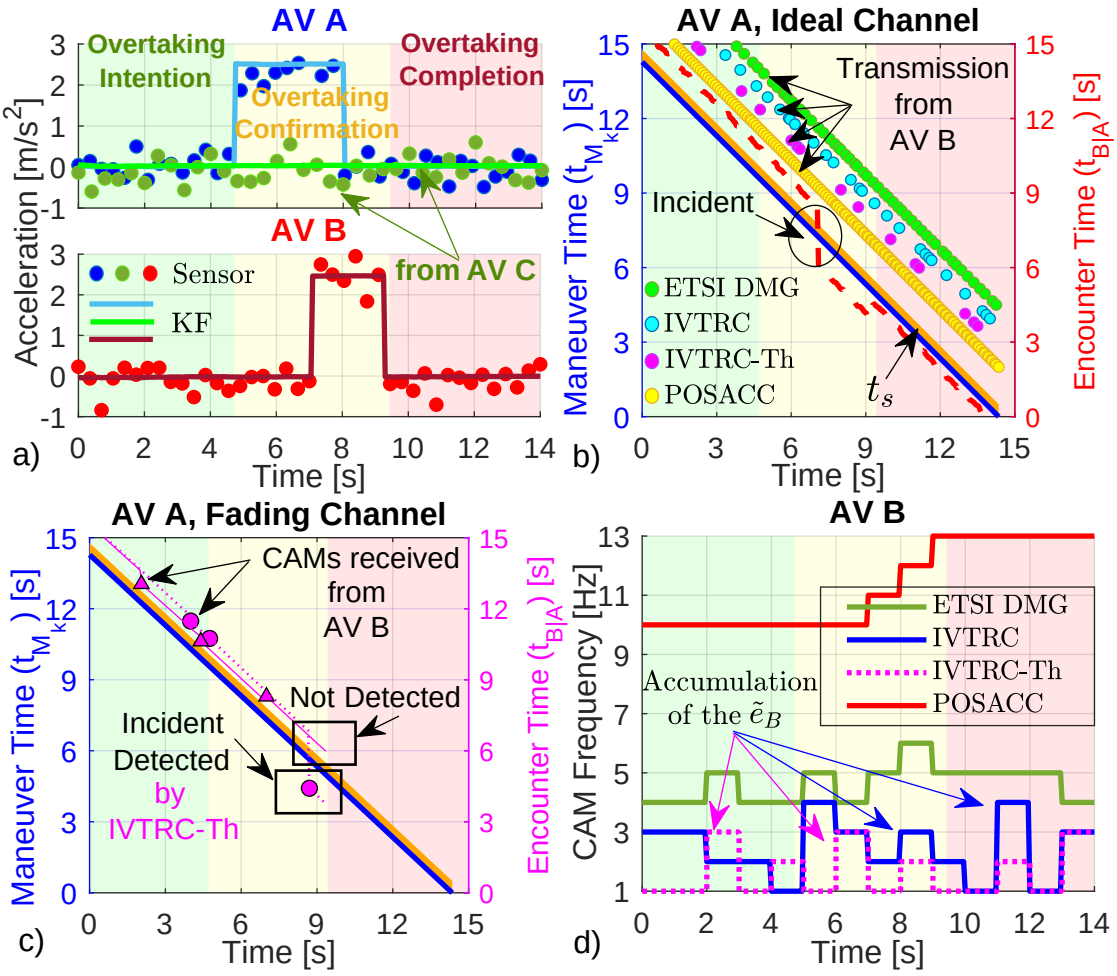

Figure 5.2: Parameters involved in detecting unsafe overtaking maneuvers.

by the awareness control approach running on B. Fig. 5.2c shows that in real operating conditions, packet losses due to channel fading significantly impair the incident detection capability of the V2V-based overtaking application. Here, the overtaking application utilizes the CAMs gathered from the IVTRC-Th approach for tracking the position of B and deciding whether to continue or abort the unsafe overtaking maneuver shown in Fig. 5.2b.

Fig. 5.2d illustrates that POSACC is more effective than ETSI DMG, IVTRC, and IVTRC-Th on reacting to the movement dynamics of the AV B. Note that when B accelerates (see Fig. 5.2a), POSACC increases the message transmission frequency up to 13 Hz (equivalent to 13 CAMs per second) to maintain an average position error of 1 m (see Table 5.1). In consequence, POSACC is also more effective than the other approaches to support the V2V-based overtaking application, achieving the best performance in terms of incident detection rate (IDR), as shown in Fig. 5.3. The IDR is the ratio between the number of detected incidents and the total of simulated incidents. In Fig. 5.3, the error bars represent the standard deviation of the IDR computed for an initial velocity (v_A, v_C) of 60 and 80 km/h. Fig. 5.3 shows the IDR for different operating conditions, where in each simulated incident the instant at which B accelerates is uniformly distributed within the time interval $(t_w, 2t_w)$ of the stage 2. Here, the acceleration (2, 2.5, or 3 m/s^2) and maximum velocity (85, 90, or

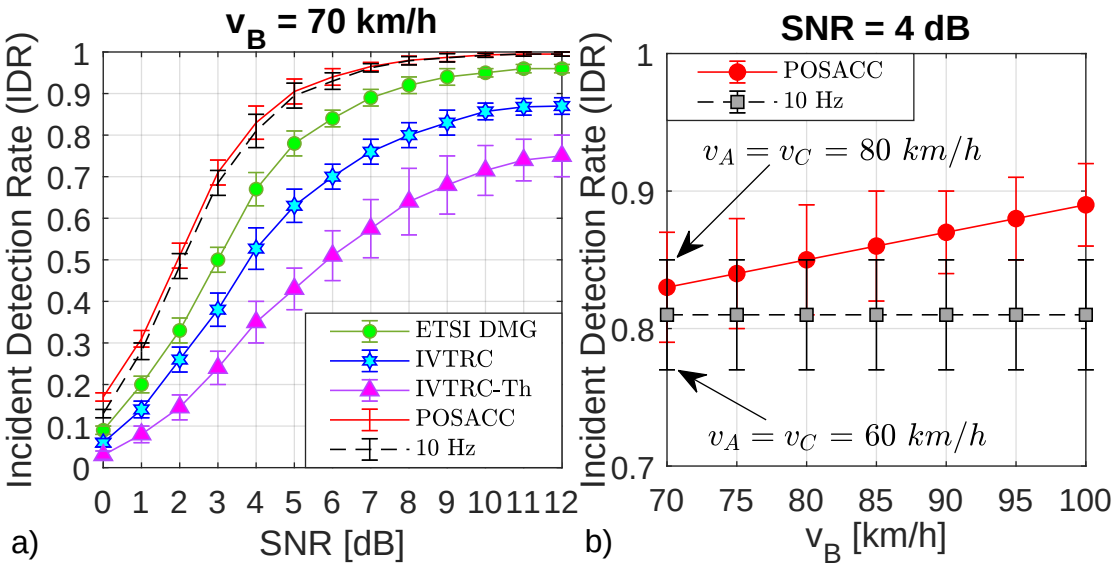

Figure 5.3: Incident detection rate (IDR) for different operating conditions.

100 km/h for Fig. 5.3a) of B were randomly selected on each simulation. Like POSACC, ETSI DMG also considers vehicle dynamics. However, it has serious drawbacks to achieve a stable message transmission frequency as can be observed in Fig. 5.2d. This is because of its divergence effect (see [45]) and the uncertainties associated with the on-board position sensor. Fig. 5.3a demonstrates that CAM trigger conditions specified by ETSI [11] are not sufficient to support the V2V-based overtaking application for values of signal-to-noise ratio (SNR) lower than 10 dB, achieving a mean IDR lower than 0.95. Further, unlike POSACC, ETSI DMG is incapable of achieving a mean IDR greater than 0.99 for an SNR of 12 dB. Fig. 5.3a also shows that IVTRC and IVTRC-Th are not suitable to support the V2V-based overtaking application. The reason is that their CAM transmission probabilities mostly depend on the accumulation of $\tilde{e}_B$, as shown in Fig. 5.2d. Even, once $\tilde{e}_B$ is accumulated, its reset is still stochastic. Therefore, they can not guarantee a high message transmission frequency in critical situations (e.g., when B changes its movement state). Accordingly, for an SNR ranging from 2 dB to 6 dB, POSACC increases the probability of detecting unsafe maneuvers by 10 % and 20 % in comparison to the approaches ETSI DMG and IVTRC, respectively. In Fig. 5.3, we also include a fixed CAM transmission frequency of 10 Hz, which is the higher message frequency specified by ETSI in [11]. Fig. 5.3a illustrates that for velocities of B lower than 70 km/h, the effectiveness of a fixed CAM frequency of 10 Hz to detect incidents is similar to the one achieved by POSACC, especially for SNRs higher than 6 dB. However, the drawbacks of using a fixed message frequency of 10 Hz regarding the vehicle dynamics are shown in Fig. 5.3b. Here, to establish the maximum velocity, we utilize an excess velocity with respect to v_B calculated as v_B + random{15, 20, 30 km/h}. Fig. 5.3b shows that POSACC outperforms the fixed CAM transmission frequency of 10 Hz in terms of IDR for velocities higher than 70 km/h. Note that the effectiveness of POSACC increases as a function of the velocity of B, exceeding by 8 % the IDR achieved by the fixed CAM frequency of 10 Hz for a velocity of 100 km/h and SNR of 4 dB.

5.6 Conclusion

In this letter, we evaluated the suitability of awareness control approaches, such as ETSI DMG, IVTRC, and POSACC, to support the V2V-based overtaking application in autonomous driving. Simulation results showed the feasibility of POSACC for rapidly adapting to changes in vehicle dynamics, achieving a stable CAM transmission rate, which increases its probability of detecting unsafe overtaking maneuvers. POSACC proved its effectiveness regarding the remaining addressed approaches for supporting the V2V-based overtaking application, achieving the best performance in terms of IDR in different operating conditions.

Finally, we conclude that the design and configuration of the addressed awareness control approaches should be further investigated to increase the incident detection rate, especially at low SNRs. In future works, we intend to consider overtaking maneuvers in which the AVs collaborate to avoid an accident for increasing the performance of the V2V-based overtaking application.

5.7 Acknowledgements

This work has been partially supported in Chile by CONICYT Doctoral Grant No. 21171722; Vicerrectoría de Investigación y Desarrollo (VID) de la Universidad de Chile Project ENL 01/20; ANID - Basal Project FB0008; FONDECYT Iniciación No. 11200659; and FONDEQUIP EQM180180.

Chapter 6

Conclusions

6.1 General Conclusions

I designed a joint power/rate control distributed algorithm oriented to provide the position accuracy requirements of cooperative safety applications [43]. First, I adopted position accuracy and communication reliability as the highest priority metrics due to their direct impact on the decision-making process, in real-time, of road safety applications. Second, I proposed a control mechanism that was able of adapting the beacon rate in real-time depending on vehicle movement state and of limiting the position error perceived by neighboring vehicles. I also proposed a control mechanism that was able of adapting the beacon transmission power in real-time according to channel load and beacon rate and of reducing packet collisions. Then, I integrated both control mechanisms in a joint power/rate control distributed algorithm that was effective in setting a good trade-off between position accuracy, packet collisions, and warning range, by outperforming other combinations of fixed and adaptive beaconing algorithms. I demonstrated that, on the one hand, the dynamic control of the beacon rate limited the average position error, but the use of maximum transmission power led to an increase in packet collisions. On the other hand, the dynamic control of beacon transmission power decreased the average packet collisions, but the use of a fixed beacon transmission rate was unable to simultaneously achieve a good performance in terms of warning range and position accuracy. On the contrary, the proposed joint power/rate control algorithm allowed to constrain the average position error computed by surrounding vehicles and opportunistically adjusted the communication range of vehicles to mitigate packet collisions.

I modeled the beaconing process adjusting both beacon rate and transmit power through probability density functions [44]. I also evaluated the impact of the distributions-based beaconing approach on the system's performance in four different vehicular scenarios using a realistic simulation framework and metrics directly related to road safety. The beaconing algorithm introduced by Kloiber et al. in [34] was used as a baseline. I set a relationship between the use of a certain distribution and the traffic characteristics of the vehicular scenario. I highlighted the benefits and limitations of this approach. I demonstrated that the uniform distribution is effective for mitigating packet collisions. I also observed that one of the drawbacks of the uniform distribution for road safety is that vehicles can set a low beacon

transmission rate and power when a high position accuracy or warning range is required to mitigate a critical situation. On the contrary, vehicles with low dynamics can set a high beacon transmission rate and power when a high position accuracy or warning range is not required.

I designed a POSition-ACCuracy (POSACC) based adaptive beaconing algorithm oriented to provide the operational requirements of cooperative safety applications in a wide range of traffic situations [45]. I proposed a control mechanism that was able of computing the vehicle's transmission power according to its movement status and of maximizing the probability of successful reception of beacon messages at the target warning distance. I also proposed a control mechanism that was able of adapting the size of the minimum contention window according to the number of neighboring vehicles and of reducing the probability of packet collisions. I evaluated POSACC with a realistic simulation framework in different traffic setups and compared it with other relevant congestion and awareness control algorithms; ETSI DMG [11], LIMERIC [31], and DC-BTR&P [43]. I highlighted the benefits and limitations of these approaches for road safety. POSACC proved to be effective for overcoming the limitations of my previous work, DC-BTR&P [43], by assigning a higher warning range to vehicles with higher dynamics. POSACC demonstrated its effectiveness to control the beacon transmission parameters in real-time and it also was able to limit the position error and improve communication reliability, while maintaining the warning distance, channel load, and end-to-end latency into the operative range of cooperative safety applications. Finally, POSACC outperformed the benchmark beaconing algorithms by providing the operational requirements of cooperative safety applications in a wider range of traffic situations.

I evaluated the impact of awareness control on V2V-based overtaking application in autonomous driving [46]. First, I proposed an analytical model for the overtaking with autonomous vehicles. Second, I designed an operation mode for the overtaking application considering a kinematics-based trajectory prediction model for tracking the new positions from received CAMs. Then, I evaluated the effectiveness of relevant awareness control approaches; ETSI DMG [11], IVTRC [35], IVTRC-Th [47], and POSACC [45], for supporting the V2V-based overtaking application. I also evaluated the fixed beaconing approach of 10 Hz specified by ETSI in [11]. I highlighted the benefits and limitations of these approaches for road safety. I assessed the incident detection capability of the overtaking application when it is running with messages gathered from the addressed approaches, taking into account motion state sensors' errors and packet losses due to channel fading. POSACC demonstrated its feasibility for rapidly adapting to changes in vehicle dynamics, achieving a stable CAM transmission rate, which increases its probability of detecting unsafe overtaking maneuvers. POSACC proved its effectiveness regarding the remaining addressed approaches for supporting the V2V-based overtaking application, achieving the higher IDR in different operating conditions.

6.2 Future Work

In addition to future work topics presented in the conclusion section of each main chapter, an interesting extension of this work includes the application of the proposed algorithms and mechanisms in emergent technologies, such as IEEE 802.11bd [93] and cellular vehicle-to-

everything (C-V2X) [94]. Supporters of DSRC [16] are looking to evolve some aspects of its protocols, to prepare for vehicle-to-everything (V2X) applications coming in the future. Accordingly, in 2018, IEEE 802.11 Working Group established a task group, TGbd, for the next generation V2X (NGV) to develop a new amendment IEEE 802.11bd [93] as the natural evolution of IEEE 802.11p [7]. The IEEE 802.11bd standard is supposed to provide a vehicular ad-hoc environment with performance enhancement compared to IEEE 802.11p in terms of throughput, latency, reliability, and communication range. On the other hand, long-term evolution-V2X (LTE-V2X) is an alternative wireless technology for V2X direct communications [95]. It adopted many of the higher layer standards of DSRC, while it employed LTE-V2X PC5 mode 4 (i.e., direct communication mode without the help of base stations) [94] as the protocols of PHY and MAC layers, which was first defined in 3GPP Rel-14 specifications in 2017. Although LTE-V2X is relatively new, it quickly emerged as the alternative technology of DSRC in some regions of the world. For example, in 2018, the Ministry of Industry and Information Technology in China assigned the 5.905 – 5.925 GHz frequency band to LTE-V2X to promote its development and pilot deployment. In the U.S., the Society of Automotive Engineers (SAE) is developing the minimum system requirements for LTE-V2X (SAE J3161/1) [96] to support many of the V2X applications defined for DSRC. In 3GPP Rel-15 standardization, several enhancements of LTE-V2X were specified to support higher data rate, reliability, and lower channel access latency. In 2020, 3GPP specified yet another 3GPP side-link technology for V2X based on New Radio (NR), referred to as NR-V2X PC5, as a part of Rel-16 features [94].

There are several technical differences between DSRC [16] and LTE-V2X [94] which impose a challenge for transmitting Basic Safety Messages [10], [97] in C-V2X-based systems. LTE-V2X PC5 mode 4 employs autonomous resource selection using semi-persistent scheduling (SPS) at the MAC layer to control the channel access. In PC5 mode 4, each node autonomously selects side-link resources and broadcasts packets using selected side-link resources. Therefore, the operation scenario of PC5 mode 4 is similar to one in DSRC in the sense that both protocols do not require the help of base stations, and the channel access mechanisms are fully distributed. However, the SPS resource selection of LTE-V2X PC5 mode 4 has several drawbacks for road safety. The first issue is the Persistent Packet Collision Problem, which raises from multiples vehicles selecting the same communication resource. If multiple vehicles select the same communication resource, transmissions will repeatedly collide. The second issue is the Persistent Half-Duplex Problem, where multiple vehicles transmit simultaneously, and even if different sub-channels are used they will not be able to hear each other while transmitting. The third issue is the Persistent Near-Far Problem, where the strength of the signal from a nearby vehicle will be too strong that it will affect the transmissions from cars that are further away. Therefore, these issues should be carefully addressed to successfully implement collision avoidance applications on C-V2X-based systems.

Appendix A

Publications

Journal (WoS):

- **S. Bolufé**, C. A. Azurdia-Meza, S. Céspedes, and S. Montejo-Sánchez, "Impact of Awareness Control on V2V-based Overtaking Application in Autonomous Driving," *IEEE Communications Letters*, vol. 25, no. 4, pp. 1373-1377, 2021.
- **S. Bolufé**, C. A. Azurdia-Meza, S. Céspedes, S. Montejo-Sánchez, R. D. Souza, and E. M. G. Fernández, "POSACC: Position-Accuracy based Adaptive Beaconing Algorithm for Cooperative Vehicular Safety Systems," *IEEE Access*, vol. 8, pp. 15484-15501, 2020.
- H. Kang, R. Becerra, **S. Bolufé**, C. A. Azurdia-Meza, S. Montejo-Sánchez, and D. Zabala-Blanco, "Neuroevolution-Based Adaptive Antenna Array Beamforming Scheme to Improve the V2V Communication Performance at Intersections," *Sensors 2021, 21(9), 2956*, 2021.
- E. Salazar, C. A. Azurdia-Meza, D. Zabala-Blanco, **S. Bolufé**, and I. Soto, "Semi-Supervised Extreme Learning Machine Channel Estimator and Equalizer for Vehicle to Vehicle Communications," *Electronics 2021, 10, 968*, 2021.

Conference:

- R. Becerra, **S. Bolufé**, H. Kang, and C. A. Azurdia-Meza, "Antenna Array Synthesis Through Particle Swarm Optimization for V2V Communications in Urban Intersections," in *IEEE Latin-American Conference on Communications (LATINCOM 2020)*, Santo Domingo, Dominican Republic, 2020.
- A. Marroquin, M. A. To, C. A. Azurdia-Meza, and **S. Bolufé**, "A General Overview of Vehicle-to-X (V2X) Beacon-Based Cooperative Vehicular Networks," in *IEEE 39th Central America and Panama Convention (IEEE CONCAPAN 2019)*, Guatemala City, Guatemala, 2019.
- P. A. Ortega, **S. Bolufé**, S. Céspedes, C. A. Azurdia-Meza, S. Montejo-Sánchez, and F. Maciel-Barboza, "Connectivity Improvement in Urban Intersections Obstructed by Buildings using RSUs," in *School on Systems and Networks (SSN 2018)*, Universidad Austral de Chile, Valdivia, Chile, 2018.

- J. Rubio-Loyola, H. Galeana-Zapien, F. Aguirre-Gracia, C. Aguilar-Fuster, **S. Bolufé**, C. A. Azurdia-Meza, and S. Montejo-Sánchez, "Towards Intelligent Tuning of Frequency and Transmission Power Adjustment in Beacon-based Ad-Hoc Networks," in *4th International Conference on Vehicle Technology and Intelligent Transport Systems (VEHITS 2018)*, Funchal, Madeira, Portugal, 2018.
- **S. Bolufé**, C. A. Azurdia-Meza, S. Céspedes, S. Montejo-Sánchez, R. D. Souza, E. M. G. Fernández, and C. Estevez, "Dynamic Beaconing using Probability Density Functions in Cooperative Vehicular Networks," in *4th International Conference on Vehicle Technology and Intelligent Transport Systems (VEHITS 2018)*, Funchal, Madeira, Portugal, 2018.
- **S. Bolufé**, S. Montejo-Sánchez, C. A. Azurdia-Meza, S. Céspedes, R. D. Souza, and E. M. G. Fernández, "Dynamic Control of Beacon Transmission Rate and Power with Position Error Constraint in Cooperative Vehicular Networks," in *33rd ACM/SIGAPP Symposium On Applied Computing (SAC'18)*, Pau, France, 2018.
- P. A. Ortega, S. Céspedes, **S. Bolufé**, and C. A. Azurdia-Meza, "Experimental Evaluation of Adaptive Beaconing for Vehicular Communications," in *6th International Workshop on ADVANCEs in ICT infrastructures and Services (ADVANCE 2018)*, Santiago, Chile, 2018.
- S. Montejo-Sánchez, C. A. Azurdia-Meza, **S. Bolufé**, S. Céspedes, I. Soto, and R. D. Souza, "Novel Channel Hopping Sequence Approaches to Rendezvous for VANETs," in *IEEE CHILECON 2017*, Pucón, Chile, 2017.
- **S. Bolufé**, S. Montejo-Sánchez, C. A. Azurdia-Meza, S. Céspedes, R. D. Souza, and E. M. G. Fernández, "Dynamic Control of Beacon Transmission Rate with Position Accuracy in Vehicular Networks," in *III Spring School on Networks (SSN 2017)*, Pucón, Chile, 2017.

Bibliography

[1] A. Maimaris and G. Papageorgiou, "A Review of Intelligent Transportation Systems from a Communications Technology Perspective," in *IEEE 19th International Conference on Intelligent Transportation Systems (ITSC)*, pp. 54–59, 2016.

[2] K. Bengler, K. Dietmayer, B. Farber, M. Maurer, C. Stiller, and H. Winner, "Three Decades of Driver Assistance Systems: Review and Future Perspectives," *IEEE Intelligent Transportation Systems Magazine*, vol. 6, no. 4, pp. 6–22, 2014.

[3] "Federal Communications Commission (FCC) allocates spectrum in 5.9 GHz range for intelligent transportation systems uses," *Report No. ET 99-5*, 1999.

[4] IEEE 1609 Working Group, "IEEE Standard for Wireless Access in Vehicular Environments (WAVE) – Multi-Channel Operation," *IEEE Std 1609.4-2016 (Revision of IEEE Std 1609.4-2010)*, 2016.

[5] IEEE 1609 Working Group, "IEEE Standard for Wireless Access in Vehicular Environments (WAVE) – Networking Services," *IEEE Std 1609.3-2016 (Revision of IEEE Std 1609.3-2010)*, 2016.

[6] IEEE 1609 Working Group, "IEEE Standard for Wireless Access in Vehicular Environments – Security Services for Applications and Management Messages," *IEEE Std 1609.2-2016 (Revision of IEEE Std 1609.2-2013)*, 2016.

[7] IEEE 802.11 Working Group, "Wireless LAN Medium Access Control (MAC) and Physical Layer (PHY) Specifications Amendment 6: Wireless Access in Vehicular Environments," *IEEE Std 802.11p*, 2010.

[8] IEEE 802.11 Working Group, "IEEE Standard for Information Technology - Part 11: Wireless LAN Medium Access Control (MAC) and Physical Layer (PHY) Specifications," *IEEE Std 802.11-2016 (Revision of IEEE Std 802.11-2012)*, 2016.

[9] IEEE 1609 Working Group, "IEEE Guide for Wireless Access in Vehicular Environments (WAVE) - Architecture," *IEEE Std 1609.0-2019 (Revision of IEEE Std 1609.0-2013)*, 2019.

[10] SAE, "Dedicated Short Range Communications (DSRC) Message Set Dictionary," *SAE Std J2735*, 2016.

[11] ETSI, "Intelligent Transport Systems (ITS); Vehicular Communications; Basic Set of Applications; Part 2: Specification of Cooperative Awareness Basic Service," *ETSI EN 302 637-2 V1.4.1*, 2019.

[12] ETSI, "Intelligent Transport Systems (ITS); V2X Applications; Part 3: Longitudinal Collision Risk Warning (LCRW) application requirements specification," *ETSI TS 101 539-3 V1.1.1*, 2013.

[13] ETSI, "Intelligent Transport Systems (ITS); V2X Applications; Part 2: Intersection Collision Risk Warning (ICRW) application requirements specification," *ETSI TS 101 539-2 V1.1.1*, 2018.

[14] CAMP VSCC, "Vehicle Safety Communications Project: Task 3 Final Report; Identify Intelligent Vehicle Safety Applications enabled by DSRC," *NHTSA, US DoT, Tech Rep DoT HS 809859*, 2005.

[15] R. K. Schmidt, T. Leinmüller, E. Schoch, F. Kargl, and G. Schäfer, "Exploration of Adaptive Beaconing for Efficient Intervehicle Safety Communication," *IEEE Network*, vol. 24, no. 1, pp. 14–19, 2010.

[16] J. B. Kenney, "Dedicated Short-Range Communications (DSRC) Standards in the United States," *Proceedings of the IEEE*, vol. 99, no. 7, pp. 1162–1182, 2011.

[17] COMeSafety, "Communication for eSafety: D31 European ITS Communication Architecture Overall Framework Proof of Concept Implementation," EU FP6 COMeSafety project (FP6-027377), Tech. Rep. COMeSafety Project Deliverable D31, 2008.

[18] J. Mišić, G. Badawy, and V. B. Mišić, "Performance Characterization for IEEE 802.11p Network With Single Channel Devices," *IEEE Transactions on Vehicular Technology*, vol. 60, no. 4, pp. 1775–1787, 2011.

[19] M. Torrent-Moreno, J. Mittag, P. Santi, and H. Hartenstein, "Vehicle-to-Vehicle Communication: Fair Transmit Power Control for Safety-Critical Information," *IEEE Transactions on Vehicular Technology*, vol. 58, no. 7, pp. 3684–3703, 2009.

[20] Y. Yao, X. Chen, L. Rao, X. Liu, and X. Zhou, "LORA: Loss Differentiation Rate Adaptation Scheme for Vehicle-to-Vehicle Safety Communications," *IEEE Transactions on Vehicular Technology*, vol. 66, no. 3, pp. 2499–2512, 2017.

[21] M. Raya and J.-P. Hubaux, "The Security of Vehicular Ad Hoc Networks," in *3rd ACM Workshop on Security of Ad Hoc and Sensor Networks (SASN '05)*, pp. 11–21, 2005.

[22] G. Boquet, I. Pisa, J. L. Vicario, A. Morell, and J. Serrano, "Analysis of Adaptive Beaconing Protocols for Intersection Assistance Systems," in *14th Annual Conference on Wireless On-demand Network Systems and Services (WONS)*, pp. 67–74, 2018.

[23] A. Weinfield, J. Kenney, and G. Bansal, "An Adaptive DSRC Message Transmission Rate Control Algorithm," in *18th World Congress on Intelligent Transport Systems*, pp. 1–12, 2011.

[24] S. Rezaei, R. Sengupta, H. Krishnan, and X. Guan, "Adaptive Communication Scheme for Cooperative Active Safety System," in *WoCo*, 2008.

[25] M. Van Eenennaam, W. K. Wolterink, G. Karagiannis, and G. Heijenk, "Exploring the Solution Space of Beaconing in VANETs," in *IEEE Vehicular Networking Conference (VNC)*, pp. 1–8, 2009.

[26] R. K. Schmidt, T. Köllmer, T. Leinmüller, B. Böddeker, and G. Schäfer, "Degradation of Transmission Range in VANETs caused by Interference," *Praxis der Informationsverarbeitung und Kommunikation (PIK)*, vol. 32, pp. 224–234, 2009.

[27] G. Bianchi, "Performance Analysis of the IEEE 802.11 Distributed Coordination Function," *IEEE Journal on Selected Areas in Communications*, vol. 18, no. 3, pp. 535–547, 2000.

[28] B. Shabir, M. A. Khan, A. U. Rahman, A. W. Malik, and A. Wahid, "Congestion Avoidance in Vehicular Networks: A Contemporary Survey," *IEEE Access*, vol. 7, pp. 173196–173215, 2019.

[29] S. A. A. Shah, E. Ahmed, F. Xia, A. Karim, M. Shiraz, and R. M. Noor, "Adaptive Beaconing Approaches for Vehicular Ad Hoc Networks: A Survey," *IEEE Systems Journal*, vol. 12, no. 2, pp. 1263–1277, 2018.

[30] T. Tielert, D. Jiang, Q. Chen, L. Delgrossi, and H. Hartenstein, "Design Methodology and Evaluation of Rate Adaptation Based Congestion Control for Vehicle Safety Communications," in *IEEE Vehicular Networking Conference (VNC)*, pp. 116–123, 2011.

[31] G. Bansal, J. B. Kenney, and C. E. Rohrs, "LIMERIC: A Linear Adaptive Message Rate Algorithm for DSRC Congestion Control," *IEEE Transactions on Vehicular Technology*, vol. 62, no. 9, pp. 4182–4197, 2013.

[32] E. Egea-Lopez and P. Pavon-Mariño, "Distributed and Fair Beaconing Rate Adaptation for Congestion Control in Vehicular Networks," *IEEE Transactions on Mobile Computing*, vol. 15, no. 12, pp. 3028–3041, 2016.

[33] ETSI, "Intelligent Transport Systems (ITS); Decentralized Congestion Control Mechanisms for Intelligent Transport Systems operating in the 5 GHz range; Access layer part;," *ETSI TS 102 687 V1.2.1*, 2018.

[34] B. Kloiber, J. Härri, and T. Strang, "Dice the TX power - Improving Awareness Quality in VANETs by random transmit power selection," in *IEEE Vehicular Networking Conference (VNC)*, pp. 56–63, 2012.

[35] C. Huang, Y. P. Fallah, R. Sengupta, and H. Krishnan, "Intervehicle Transmission Rate Control for Cooperative Active Safety System," *IEEE Transactions on Intelligent Transportation Systems*, vol. 12, no. 3, pp. 645–658, 2011.

[36] M. Sepulcre, J. Gozalvez, O. Altintas, and H. Kremo, "Integration of Congestion and Awareness Control in Vehicular Networks," *Ad Hoc Networks*, vol. 37, pp. 29–43, 2016.

[37] F. Goudarzi and H. Asgari, "Non-Cooperative Beacon Rate and Awareness Control for VANETs," *IEEE Access*, vol. 5, pp. 16858–16870, 2017.

[38] J. Aznar-Poveda, E. Egea-Lopez, A. Garcia-Sanchez, and P. Pavon-Mariño, "Time-to-Collision-Based Awareness and Congestion Control for Vehicular Communications," *IEEE Access*, vol. 7, pp. 154192–154208, 2019.

[39] P. M. d'Orey and M. Boban, "Empirical Evaluation of Cooperative Awareness in Vehicular Communications," in *IEEE 79th Vehicular Technology Conference (VTC Spring)*, pp. 1–5, 2014.

[40] T. Lorenzen and H. Tchouankem, "Evaluation of an Awareness Control Algorithm for VANETs based on ETSI EN 302 637-2 V1.3.2," in *IEEE International Conference on Communication Workshop (ICCW)*, pp. 2458–2464, 2015.

[41] J. Breu, A. Brakemeier, and M. Menth, "A quantitative study of Cooperative Awareness Messages in production VANETs," *EURASIP Journal on Wireless Communications and Networking*, vol. 98, pp. 1–18, 2014.

[42] M. Torrent-Moreno, M. Killat, and H. Hartenstein, "The Challenges of Robust Inter-Vehicle Communications," in *IEEE 62nd Vehicular Technology Conference (VTC-2005-Fall)*, pp. 319–323, 2005.

[43] S. Bolufé, S. Montejo-Sánchez, C. A. Azurdia-Meza, S. Céspedes, R. D. Souza, and E. M. G. Fernandez, "Dynamic Control of Beacon Transmission Rate and Power with Position Error Constraint in Cooperative Vehicular Networks," in *33rd Annual ACM Symposium on Applied Computing (SAC'18)*, pp. 2084–2091, 2018.

[44] S. Bolufé, C. A. Azurdia-Meza, S. Céspedes, S. Montejo-Sánchez, R. D. Souza, E. M. G. Fernandez, and C. Estevez, "Dynamic Beaconing using Probability Density Functions in Cooperative Vehicular Networks," in *4th International Conference on Vehicle Technology and Intelligent Transport Systems - RESIST*, pp. 636–642, 2018.

[45] S. Bolufé, C. A. Azurdia-Meza, S. Céspedes, S. Montejo-Sánchez, R. D. Souza, and E. M. G. Fernandez, "POSACC: Position-Accuracy Based Adaptive Beaconing Algorithm for Cooperative Vehicular Safety Systems," *IEEE Access*, vol. 8, pp. 15484–15501, 2020.

[46] S. Bolufé, C. A. Azurdia-Meza, S. Céspedes, and S. Montejo-Sánchez, "Impact of Awareness Control on V2V-Based Overtaking Application in Autonomous Driving," *IEEE Communications Letters*, vol. 25, no. 4, pp. 1373–1377, 2021.

[47] C.-L. Huang, Y. P. Fallah, R. Sengupta, and H. Krishnan, "Adaptive Intervehicle Communication Control for Cooperative Safety Systems," *IEEE network*, vol. 24, no. 1, pp. 6–13, 2010.

[48] S. Bolufé, S. Montejo-Sánchez, C. A. Azurdia-Meza, S. Céspedes, R. D. Souza, and E. M. G. Fernandez, "Dynamic Control of Beacon Transmission Rate with Position Accuracy in Vehicular Networks," in *III Spring School on Networks (SSN 2017)*, 2017.

[49] S. Montejo-Sánchez, C. Azurdia-Meza, S. Bolufé, S. Céspedes, I. Soto, and R. Demo Souza, "Novel Channel Hopping Sequence Approaches to Rendezvous for VANETs," in *2017 CHILEAN Conference on Electrical, Electronics Engineering, Information and Communication Technologies (CHILECON)*, 2017.

[50] P. A. Ortega, S. Céspedes, S. Bolufé, and C. A. Azurdia-Meza, "Experimental Evaluation of Adaptive Beaconing for Vehicular Communications," in *6th International Workshop on ADVANCEs in ICT infrastructures and Services (ADVANCE 2018)*, 2018.

[51] J. Rubio-Loyola, H. Galeana-Zapien, F. Aguirre-Gracia, C. Aguilar-Fuster, S. Bolufé, C. A. Azurdia-Meza, and S. Montejo-Sánchez, "Towards Intelligent Tuning of Frequency and Transmission Power Adjustment in Beacon-based Ad-Hoc Networks," in *4th International Conference on Vehicle Technology and Intelligent Transport Systems - RESIST*, 2018.

[52] P. A. Ortega, S. Bolufé, S. Céspedes, C. A. Azurdia-Meza, S. Montejo-Sánchez, and F. Maciel-Barboza, "Connectivity Improvement in Urban Intersections Obstructed by Buildings using RSUs," in *School on Systems and Networks (SSN 2018)*, 2018.

[53] A. Marroquin, M. A. To, C. A. Azurdia-Meza, and S. Bolufé, "A General Overview of Vehicle-to-X (V2X) Beacon-Based Cooperative Vehicular Networks," in *2019 IEEE 39th Central America and Panama Convention (IEEE CONCAPAN 2019)*, 2019.

[54] R. Becerra, S. Bolufé, H. Kang, and C. A. Azurdia-Meza, "Antenna Array Synthesis Through Particle Swarm Optimization for V2V Communications in Urban Intersections," in *2020 IEEE Latin-American Conference on Communications (LATINCOM 2020)*, 2020.

[55] E. Salazar, C. A. Azurdia-Meza, D. Zabala-Blanco, S. Bolufé, and I. Soto, "Semi-Supervised Extreme Learning Machine Channel Estimator and Equalizer for Vehicle to Vehicle Communications," *Electronics*, vol. 10, no. 8, 2021.

[56] H. Kang Kim, R. Becerra, S. Bolufé, C. A. Azurdia-Meza, S. Montejo-Sánchez, and D. Zabala-Blanco, "Neuroevolution-Based Adaptive Antenna Array Beamforming Scheme to Improve the V2V Communication Performance at Intersections," *Sensors*, vol. 21, no. 9, 2021.

[57] IEEE 1609 Working Group, "IEEE Draft Guide for Wireless Access in Vehicular Environments (WAVE) - Architecture," *IEEE P1609.0/D9*, 2017.

[58] ETSI, "Intelligent Transport Systems (ITS); Vehicular Communications; Basic Set of Applications; Part 2: Specification of Cooperative Awareness Basic Service," *ETSI EN 302 637-2 V1.3.2*, 2014.

[59] S. Zemouri, S. Djahel, and J. Murphy, "Smart Adaptation of Beacons Transmission Rate and Power for Enhanced Vehicular Awareness in VANETs," in *17th International IEEE Conference on Intelligent Transportation Systems (ITSC)*, pp. 739–746, 2014.

[60] B. Aygun, M. Boban, and A. M. Wyglinski, "ECPR: Environment-and Context-aware

Combined Power and Rate Distributed Congestion Control for Vehicular Communications," *Computer Communications*, vol. 93, pp. 3–16, 2016.

[61] N. An, M. Maile, D. Jiang, J. Mittag, and H. Hartenstein, "Balancing the Requirements for a Zero False Positive/Negative Forward Collision Warning," in *10th Conference on Wireless On-demand Network Systems and Services (WONS)*, pp. 191–195, 2013.

[62] T. Tielert, D. Jiang, H. Hartenstein, and L. Delgrossi, "Joint Power/Rate Congestion Control Optimizing Packet Reception in Vehicle Safety Communications," in *10th ACM International Workshop on Vehicular Inter-networking, Systems, and Applications (VANET'13)*, pp. 51–60, 2013.

[63] M. Sepulcre and J. Gozalvez, "On the Importance of Application Requirements in Cooperative Vehicular Communications," in *8th International Conference on Wireless On-Demand Network Systems and Services*, pp. 124–131, 2011.

[64] M. Sepulcre, J. Gozalvez, J. Härri, and H. Hartenstein, "Contextual Communications Congestion Control for Cooperative Vehicular Networks," *IEEE Transactions on Wireless Communications*, vol. 10, no. 2, pp. 385–389, 2011.

[65] M. Killat, F. Schmidt-Eisenlohr, H. Hartenstein, C. Rössel, P. Vortisch, S. Assenmacher, and F. Busch, "Enabling Efficient and Accurate Large-Scale Simulations of VANETs for Vehicular Traffic Management," in *4th ACM International Workshop on Vehicular Ad Hoc Networks (VANET 2007)*, pp. 29–38, 2007.

[66] *Vehicles in network simulation (Veins)*, Accessed on Jun. 1, 2017. [Online]. Available: https://veins.car2x.org/.

[67] D. Eckhoff and C. Sommer, "A Multi-Channel IEEE 1609.4 and 802.11p EDCA Model for the Veins Framework," in *5th ACM/ICST International Conference on Simulation Tools and Techniques for Communications, Networks and Systems (SIMUTools 2012)*, pp. 1–2, 2012.

[68] C. Sommer, S. Joerer, and F. Dressler, "On the Applicability of Two-Ray Path Loss Models for Vehicular Network Simulation," in *IEEE Vehicular Networking Conference (VNC)*, pp. 64–69, 2012.

[69] M. Boban and P. M. d'Orey, "Exploring the Practical Limits of Cooperative Awareness in Vehicular Communications," *IEEE Transactions on Vehicular Technology*, vol. 65, no. 6, pp. 3904–3916, 2016.

[70] C. Sommer, R. German, and F. Dressler, "Bidirectionally Coupled Network and Road Traffic Simulation for Improved IVC Analysis," *IEEE Transactions on Mobile Computing*, vol. 10, no. 1, pp. 3–15, 2011.

[71] E. Ahmed and H. Gharavi, "Cooperative Vehicular Networking: A Survey," *IEEE Transactions on Intelligent Transportation Systems*, vol. 19, no. 3, pp. 996–1014, 2018.

[72] U. Hernandez-Jayo and I. De-la-Iglesia, "Reliability of Cooperative Vehicular Applica-

tions on Real Scenarios Over an IEEE 802.11p Communications Architecture," in *International Conference on E-Business and Telecommunications (ICETE 2013)*, vol. 456, pp. 387–401, 2014.

[73] N. Haouari, S. Moussaoui, and S. Senouci, "Application Reliability Analysis of Density-Aware Congestion Control in VANETs," in *IEEE International Conference on Communications (ICC)*, pp. 1–6, 2018.

[74] ETSI, "Intelligent Transport Systems (ITS); ITS-G5 Access layer specification for Intelligent Transport Systems operating in the 5 GHz frequency band," *ETSI EN 302 663 V1.3.0*, 2019.

[75] ETSI, "Intelligent Transport Systems (ITS); Cross Layer DCC Management Entity for operation in the ITS G5A and ITS G5B medium; Validation set-up and results," *ETSI TR 101 613 V1.1.1*, 2015.

[76] ETSI, "Intelligent Transport Systems (ITS); Vehicular Communications; Basic Set of Applications; Part 3: Specifications of Decentralized Environmental Notification Basic Service," *ETSI EN 302 637-3 V1.3.1*, 2019.

[77] B. Kim, I. Kang, and H. Kim, "Resolving the Unfairness of Distributed Rate Control in the IEEE WAVE Safety Messaging," *IEEE Transactions on Vehicular Technology*, vol. 63, no. 5, pp. 2284–2297, 2014.

[78] N. Lyamin, A. Vinel, M. Jonsson, and B. Bellalta, "Cooperative Awareness in VANETs: On ETSI EN 302 637-2 Performance," *IEEE Transactions on Vehicular Technology*, vol. 67, no. 1, pp. 17–28, 2018.

[79] C. Chen, X. Liu, H. Chen, M. Li, and L. Zhao, "A Rear-End Collision Risk Evaluation and Control Scheme Using a Bayesian Network Model," *IEEE Transactions on Intelligent Transportation Systems*, vol. 20, no. 1, pp. 264–284, 2019.

[80] Y. Chen, K. Shen, and S. Wang, "Forward Collision Warning System considering both Time-to-Collision and Safety Braking Distance," in *IEEE 8th Conference on Industrial Electronics and Applications (ICIEA)*, pp. 972–977, 2013.

[81] O. Chakroun and S. Cherkaoui, "Enhancing Safety Messages Dissemination Over 802.11p/DSRC," in *38th Annual IEEE Conference on Local Computer Networks - Workshops*, pp. 179–187, 2013.

[82] M. A. Karabulut, A. F. M. S. Shah, and H. Ilhan, "Performance modeling and analysis of the IEEE 802.11 DCF for VANETs," in *9th International Congress on Ultra Modern Telecommunications and Control Systems and Workshops (ICUMT)*, pp. 346–351, 2017.

[83] X. Lei and S. H. Rhee, "Performance analysis and enhancement of IEEE 802.11p beaconing," *EURASIP Journal on Wireless Communications and Networking*, vol. 61, pp. 1–10, 2019.

[84] *Vehicles in network simulation (Veins)*, Accessed on Jun. 7, 2019. [Online]. Available: https://veins.car2x.org/.

[85] R. Stanica, E. Chaput, and A. Beylot, "Local Density Estimation for Contention Window Adaptation in Vehicular Networks," in *IEEE 22nd International Symposium on Personal, Indoor and Mobile Radio Communications*, pp. 730–734, 2011.

[86] E. Yurtsever, J. Lambert, A. Carballo, and K. Takeda, "A Survey of Autonomous Driving: Common Practices and Emerging Technologies," *IEEE Access*, vol. 8, pp. 58443–58469, 2020.

[87] I. Yaqoob, L. U. Khan, S. M. A. Kazmi, M. Imran, N. Guizani, and C. S. Hong, "Autonomous Driving Cars in Smart Cities: Recent Advances, Requirements, and Challenges," *IEEE Network*, vol. 34, no. 1, pp. 174–181, 2019.

[88] J. Wang, J. Liu, and N. Kato, "Networking and Communications in Autonomous Driving: A Survey," *IEEE Communications Surveys & Tutorials*, vol. 21, no. 2, pp. 1243–1274, 2018.

[89] E. Belyaev, P. Molchanov, A. Vinel, and Y. Koucheryavy, "The Use of Automotive Radars in Video-Based Overtaking Assistance Applications," *IEEE Transactions on Intelligent Transportation Systems*, vol. 14, no. 3, pp. 1035–1042, 2013.

[90] O. Popescu, S. Sha-Mohammad, H. Abdel-Wahab, D. C. Popescu, and S. El-Tawab, "Automatic Incident Detection in Intelligent Transportation Systems Using Aggregation of Traffic Parameters Collected Through V2I Communications," *IEEE Intelligent Transportation Systems Magazine*, vol. 9, no. 2, pp. 64–75, 2017.

[91] SAE J2945/1, "On-Board System Requirements for V2V Safety Communications," 2020.

[92] M. Sepulcre, J. Gozalvez, J. Härri, and H. Hartenstein, "Application-Based Congestion Control Policy for the Communication Channel in VANETs," *IEEE Communications Letters*, vol. 14, no. 10, pp. 951–953, 2010.

[93] IEEE 802.11 Next Generation V2X Study Group, "802.11 NGV Proposed PAR," *IEEE 802.11-18/0861r9*, 2018.

[94] 3GPP, "Overall description of Radio Access Network (RAN) aspects for Vehicle-to-everything (V2X) based on LTE and NR," *TR 37.985 V16.0.0*, 2020.

[95] T. Shimizu, B. Cheng, H. Lu, and J. Kenney, "Comparative Analysis of DSRC and LTE-V2X PC5 Mode 4 with SAE Congestion Control," in *IEEE VNC*, 2020.

[96] SAE J3161/1, "On-Board System Requirements for LTE V2X V2V Safety Communications," (under development) https://www.sae.org/standards/content/j3161/1/.

[97] S. Heo, W. Yoo, H. Jang, and J.-M. Chung, "H-V2X Mode 4 Adaptive Semipersistent Scheduling Control for Cooperative Internet of Vehicles," *IEEE Internet of Things Journal*, vol. 8, no. 13, pp. 10678–10692, 2021.